TECHNISCHE UNIVERSITÄT
CHEMNITZ

Faculty of Economics and
Business Administration

Dynamics between trading volume, volatility and open interest in agricultural futures markets: A Bayesian time-varying coefficient approach

Robert L. Czudaj

Chemnitz Economic Papers, No. 030, May 2019

Chemnitz University of Technology
Faculty of Economics and Business Administration
Thüringer Weg 7
09107 Chemnitz, Germany

Phone +49 (0)371 531 26000
Fax +49 (0371) 531 26019
https://www.tu-chemnitz.de/wirtschaft/index.php.en
wirtschaft@tu-chemnitz.de

Dynamics between trading volume, volatility and open interest in agricultural futures markets: A Bayesian time-varying coefficient approach

Robert L. Czudaj[1]

Chemnitz University of Technology, Department of Economics and Business Administration, Chair for Empirical Economics, D-09126 Chemnitz

Abstract

The dynamics between trading volume and volatility for seven agricultural futures markets are examined by drawing on the large literature for equity markets and by allowing for heterogeneity of investors beliefs proxied by open interest. In addition, time-varying effects on the transmission mechanism of shocks are also accounted for by implementing a Bayesian VAR model, which allows for time-variation stemming from both the coefficients and the variance covariance structure of the model's disturbances. This is important since it accounts for changes in the number of trades and the size of trades across different periods, which can have different effects on the volatility-volume relation. The results show that the Granger causality and the reaction to shocks varies substantially over time. This highlights the importance to allow for time-variation when modeling the relationship between volatility, trading volume and open interest for agricultural futures markets. In general, the findings indicate that volatility of agricultural futures markets is driven by previous period's trading volume and open interest. However, the reversed relationship from lagged volatility to trading volume and open interest is limited to certain periods of time.

Keywords: Agricultural futures markets, open interest, time-varying Bayesian VAR, trading volume, volatility

JEL classification: C32, G13, Q14

[1]e-mail: robert-lukas.czudaj@wirtschaft.tu-chemnitz.de, phone: (0049)-371-531-31323, fax: (0049)-371-531-831323.

1. Introduction

In recent years a huge rise in volatility of agricultural commodity markets has been observed, especially between 2007 and 2008, which had dramatic consequences on food prices in developing countries. A number of reasons has been provided for this development: the rapid economic growth in emerging economies like China and India (Gilbert, 2010a), bio fuel programs in the US and the European Union (Abbott et al., 2008; Mitchel, 2008), a weakening of the US dollar, periods of underinvestment in agriculture (World Bank, 2007), large variation in harvests and inventory levels and speculative effects (Masters, 2008; Cooke and Robles, 2009; Gilbert, 2010b; Gutierrez, 2013). To get further insights on the potential reasons for the large increase in volatility on agricultural commodity markets, this paper focuses on the relationship between return volatility, trading volume and open interest on seven important agricultural futures markets.

Especially, the link between agricultural futures trading volume and return volatility is crucial for several reasons. First, we try to establish empirical regularities concerning the effect of trading volume on the volatility in these markets in order to get more insights on the financialization and speculation arguments raised in previous studies. Second, our findings might provide important implications and helpful guidance for market regulators, which decide on the effectiveness and efficiency of market restrictions such as daily price movement and position limits. Third, our findings might also be important for policymakers in order to discover market manipulations and to assess the effectiveness of (or the need for) central bank intervention. Finally, our results might also provide practical implications for investors on agricultural futures markets to construct more efficient hedge ratios or risk measures (e.g. value at risk) and better investment strategies (Mougoué and Aggarwal, 2011).

The existing literature offers a great number of studies providing theoretical and empirical foundations for a causal relationship between the variation in asset prices and their trading volume. One line of reasoning known as the mixture of distributions hypothesis (MDH) is that the relationship between asset prices and trading volume exists because of a joint dependence on a common latent variable (Clark, 1973; Epps and Epps, 1976; Tauchen and Pitts, 1983; Harris, 1987; Andersen, 1996). This hypothesis implies a positive contemporaneous effect from trading volume to the volatility of asset returns, in which price changes are sampled from a mixture of normal distributions with volume per transaction or number of transactions acting as a mixing variable (Bessembinder and Seguin, 1993). The second explanation is based on the concept of sequential arrival of information

(SAI) and implies that news are propagated to market participants sequentially one after another resulting in a sequence of transitional equilibria prior to the final equilibrium (Copeland, 1976; Morse, 1981; Jennings et al., 1981; Jennings and Barry, 1983; Smirlock and Starks, 1988). Therefore, the sequential arrival of new information drives both trading volume and return volatility. Admati and Pfleiderer (1988) provide a third explanation showing that traders with trade timing discretion tend to trade when previous period's trading volume is large. Therefore, the effect of trading volume on return volatility depends on the recent level of trading volume.

An important issue when analyzing the relationship between trading volume and volatility of financial assets is the heterogeneity of investors beliefs. The arrival of new information changes the beliefs of the investors and a larger heterogeneity of beliefs tends to increase the trading volume (Kim and Verrecchia, 1991). The dispersion of investors expectations intensifies a positive correlation between trading volume and contemporaneous as well as future volatility (Shalen, 1993). To account for this fact we also include the previous day's open interest as a proxy for the heterogeneity of beliefs following Bessembinder et al. (1996). Therefore, this paper contributes to the literature by analyzing the relationship between trading volume, volatility and open interest for agricultural futures markets. While the literature on the link between trading volume, volatility and open interest is vast and manifold when referring to equity markets (e.g. Andersen, 1996; Bollerslev and Jubinski, 1999; Chan and Fong, 2000; Liesenfeld, 2001; Lee and Rui, 2002; Fleming et al., 2006; Ning and Tse, 2009; Fleming and Kirby, 2011; Jena et al., 2018), it is silent on the corresponding relation for agricultural commodity markets. Solely Bessembinder and Seguin (1993) include two agricultural futures markets (for cotton and wheat) into their analysis and find positive trading volume effects and negative open interest effects on the volatility for both markets. In addition, Malliaris and Urrutia (1998) examine the determinants of trading volume on agricultural futures markets and argue that volatility has explanatory power for the trading volume.

Moreover, a crucial aspect neglected in previous studies is the allowance for the potential of time-variation in the relationship between volatility, trading volume and open interest. The changing character of (agricultural) commodity markets observed over the recent years suggests a time-varying relationship between the variables of interest. Time-variation might arise from changes in the number of trades and the size of trades across different periods, which can have different effects on the volatility-volume relationship as observed on equity markets (Chan and Fong, 2000). Especially, the SAI may imply a time-varying propagation mechanism of shocks. Rational and

forward looking investors incorporate recent news in their expectations and this induces day-by-day modifications in the transmission mechanism of shocks between the three variables of interest. Therefore, it is important to account for time-variation in the transmission of shocks between trading volume, volatility and open interest in agricultural futures markets. We thus apply a flexible framework which accounts for time-varying parameters in order to measure changes in the corresponding relationship. Hence, we implement a Bayesian time-varying parameter vector autoregression model with stochastic volatility (B-TVP-VAR-SV) according to Primiceri (2005), where the time-variation stems from both the coefficients and the variance covariance structure of the model's disturbances. The latter captures potential heteroscedasticity of the errors and is modeled by a multivariate stochastic volatility approach. This is important if we want to distinguish between variation in the typical size of the exogenous innovations and variation in the transmission mechanism (Czudaj, 2019). The application of a time-varying coefficient model is much more suitable in this case compared to a discrete structural break approach since changes on financial markets are often smooth rather than discrete due to the role of aggregation over a large number of investors with different expectations and risk aversion. Moreover, the drifting coefficients allow for the potential of non-linearity in the relationship between trading volume, volatility and open interest for agricultural futures markets, which has previously been identified e.g. by Bessembinder and Seguin (1993).

The remainder of the paper is structured as follows. Section 2 describes our data set and our empirical framework while Section 3 discusses our empirical results. Section 4 concludes.

2. Data and methodology

2.1. Data

We use data for a daily sample period running from January 3, 2000 to October 17, 2018 on closing prices, trading volume and previous day's open interest of first nearby futures contracts for seven agricultural commodities traded either at the Intercontinental Exchange (ICE) or the Chicago Board of Trade (CBOT), namely ICE Coffee, CBOT Corn, ICE Cotton, CBOT Soybean Oil, CBOT Soybeans, ICE Sugar No. 11, and CBOT Wheat. The start of the sample period in the year 2000 is motivated by the main focus of our study, which lies on the financialization period of agricultural commodities that started shortly after the turn of the Millennium. The data provided

by Stevens Analytics has been download from Quandl (`https://www.quandl.com/`) and continuous non-overlapping end-to-end concatenations of the nearby futures price series have been constructed by rolling over on the last trading day of the expiring or front contract. Then, we have computed daily futures returns using continuous closing prices as follows

$$r_t = 100 \ln(p_t/p_{t-1}), \tag{1}$$

where p_t represents the futures price on day t, and we have reported the corresponding descriptive statistics in Table 1 together with the statistics for trading volume and open interest. These are in line with stylized facts often observed for financial asset returns as follows. First, means and especially medians of daily returns are close to zero in most cases. Second, downswings of financial assets are often steeper than upswings which is manifested by negatively skewed return distributions such as observed for four out of seven agricultural futures returns. Third, most returns have heavy tails which is expressed by excess kurtosis (> 3) compared to the Gaussian. This feature is most pronounced for corn and cotton futures returns. Solely futures returns for soybean oil and wheat show neither excess kurtosis nor negative skewness. Finally, most futures returns do not show serial correlation which means that the null of no serial correlation of order 1 cannot be rejected for all returns except for corn and cotton based on the weighted Ljung-Box test. However, the second moments clearly exhibit serial correlation, i.e. the same null can be rejected for squared returns at the 5% level in all cases. Therefore, high volatility periods exhibit some degree of persistence and this leads to volatility clustering often observed for financial returns. These stylized facts will be addressed when estimating the volatility of agricultural futures returns in the next subsection.

*** Insert Table 1 about here ***

One reason to focus on futures instead of spot markets is the fact that we are able to consider previous day's open interest as a proxy for the dispersion of beliefs which would not be possible when focusing on the spot market. Although open interest is not a perfect proxy for heterogeneity of investors' beliefs, it reflects the cross-sectional variation in investors' net demand for positions

including the variation attributable to heterogeneity of beliefs (Bessembinder et al., 1996).[2] However, as a next step, it is necessary to remove the seasonal pattern present in the time series of trading volume and open interest since in contrast to other commodities, agricultural commodities are typically characterized by an annual crop cycle. This results in seasonal patterns that are already documented in the literature (see e.g. Fama and French, 1987; Sørensen, 2002; Geman and Nguyen, 2005; Hevia et al., 2018) and also appear in the raw series for trading volume and open interest as can be seen in Figures 1 and 2. Therefore, seasonal fluctuations have been removed by using the procedure proposed by Cleveland et al. (1990), which is able to eliminate multiple seasonal components. Such complicated seasonal patterns often occur in data with higher frequencies. For example, daily data might include a weekly pattern and also an annual pattern. The corresponding seasonally adjusted time series are illustrated in Figures A.1 and A.2 in Appendix A.2. Especially for soybeans and wheat, the level of trading volume decreased substantially during the great recession period around 2007 and 2009 and the volatility of agricultural futures trading volume continuously increased from 2000 to 2018. The descriptive statistics provided in Table 1 show that the markets are very different in size. The corn futures market is the largest in trading volume and open interest while the coffee futures market is the smallest. This is also confirmed by their standard deviations and makes it necessary to analyze the relationship between trading volume, volatility and open interest for several agricultural futures markets since the corresponding dynamics might be very different.

*** Insert Figures 1 and 2 about here ***

[2] In this context it is also worth mentioning that the previous literature has also considered the effect of the order imbalance (i.e. the difference between the number of buyer-initiated trades and the number of seller-initiated trades over a day) on the relationship between volatility and trading volume when analyzing equity markets (Chan and Fong, 2000; Ning and Tse, 2009). However, the main reason for the exclusion of order imbalance is the availability of adequate data. Data for buyer- and seller-initiated trades, which could be used to construct order imbalance measures, is only available from the Commodity Futures Trading Commission (CFTC) in weekly frequency and also not for the whole sample period under observation for all commodity futures markets considered.

2.2. GARCH modeling

Our empirical approach laid out in detail in the following basically consists of two steps: (1) In the first step, we fit different GARCH models using the returns of agricultural futures markets and rely on the Schwarz Bayesian information criterion (SBC) as the criterion to select the best fitting model. Then we use the estimated time-varying standard deviation of this best fitting model as our proxy for the volatility in agricultural futures markets. (2) In the second step (see Section 2.3), we plug the volatility into our B-TVP-VAR-SV models together with trading volume and open interest and the SBC is also used as the criterion to select the lag length of these VAR models.[3]

To adequately approximate the volatility of agricultural futures returns, we refer to the stylized facts discussed in Section 2.1 and thus we fit several GARCH models described in the following. As already mentioned above we choose the best fitted model referring to the SBC and rely on the fitted standard deviation series of the corresponding model as our time-varying volatility measure. As presented in Table 1 and also provided e.g. by Myers and Hanson (1993) daily returns of agricultural futures have a mean close to zero. Therefore these are modeled as follows

$$r_t = \sigma_t \varepsilon_t, \tag{2}$$

where σ_t is a time-varying volatility function and ε_t denotes an *i.i.d.* innovation independent of σ_t. Beside the two standard choices, the standard normal (i.e. $N(0,1)$) and Student's t distribution with shape ν (i.e. t_ν), we also consider two distributional assumptions for ε_t which allow for the fact that daily returns are often skewed as reported in Table 1. Hence, we also use the skew standard normal with skewness κ (i.e. $sN(0,1)_\kappa$) and the skew t with shape ν and skewness κ (i.e. $t_{\nu,\kappa}$) relying on the procedure for introducing skewness into symmetric distributions based on Fernández and Steel (1998).[4] In addition, we also apply the generalized error distribution with shape ν (i.e.

[3] The main reason for relying on this two-step approach lies within our application. The main aim of the present paper is to examine the relationship between trading volume and volatility for agricultural futures markets by controlling for previous day's open interest. Therefore, in the first step we estimate the volatility of these markets by fitting GARCH models and in the second step we plug it into our B-TVP-VAR-SV models together with trading volume and open interest. If we would alternatively use a TVP-VAR-GARCH model instead we would link the levels of all three variables (i.e. returns, trading volume and open interest) together with the volatilities of all three variables (e.g. the volatility of the trading volume). This would shift the focus of the paper and would depart from the literature on the volatility-trading volume nexus for financial markets. Therefore, we do not use a TVP-VAR-GARCH model but instead rely on stochastic volatility to model the variance covariance matrix of the innovations (see Section 2.3), which has also been widely used in the previous literature on time-varying VAR models (see e.g. Canova and Gambetti, 2009; Koop et al., 2011; Ellis et al., 2014).

[4] Fernández and Steel (1998) propose introducing skewness into unimodal and symmetric distributions by adding

GED_ν) such as used by Mougoué and Aggarwal (2011) in a comparable situation.

First of all, σ_t is estimated by a simple GARCH(1,1) model as follows[5]

$$\sigma_t^2 = \omega + \alpha r_{t-1}^2 + \beta \sigma_{t-1}^2 \quad \text{with} \quad \omega > 0, \quad \alpha \geq 0, \quad \beta \geq 0 \quad \text{and} \quad \alpha + \beta < 1. \tag{3}$$

However, traders often react more strongly to negative than to positive news and therefore the volatility function of financial assets is often considered to be asymmetric with respect to positive and negative shocks. Thus we also conduct three different asymmetric GARCH approaches: the exponential GARCH (EGARCH) model proposed by Nelson (1991)

$$h_t = \omega + \alpha \varepsilon_{t-1} + \beta h_{t-1} + \gamma(|\varepsilon_{t-1}| - E(|\varepsilon_{t-1}|)), \tag{4}$$

where $\sigma_t = \exp(h_t)$ with no sign restrictions for the parameters and $E(.)$ denotes the expectations operator, an asymmetric power GARCH (AP-GARCH) introduced by Ding et al. (1993)

$$\sigma_t^\delta = \omega + \alpha(|r_{t-1}| - \theta r_{t-1})^\delta + \beta \sigma_{t-1}^\delta \quad \text{with} \quad \omega > 0, \quad \alpha \geq 0, \quad \beta \geq 0, \quad \theta \in (-1, 1) \quad \text{and} \quad \delta \in (0, 2], \tag{5}$$

and the GJR-GARCH model suggested by Glosten et al. (1993)

$$\sigma_t^2 = \omega + \alpha r_{t-1}^2 + \beta \sigma_{t-1}^2 + \phi I(r_{t-1} < 0) \quad \text{with} \quad \omega > 0, \quad \alpha \geq 0, \quad \beta \geq 0 \quad \text{and} \quad \alpha + \beta + \frac{\phi}{2} < 1, \tag{6}$$

where $I(.)$ denotes an indicator function.

The estimated coefficients for the best fitting models out of the four GARCH approaches and the five distributional assumptions for each of the seven agricultural futures returns are provided in Table 2 together with several diagnostic statistics (the corresponding results for all individual models considered are provided in Appendix A.3 to save space). The great majority of coefficient estimates (especially for the βs) is significantly different from zero at least at the 5% level. The weighted version of the Ljung-Box (WLB) test proposed by Fisher and Gallagher (2012) confirms that the applied GARCH models depict the serial correlation in the second moments of the futures returns

inverse scale factors in the positive and negative real half lines.

[5] GARCH models of higher orders turned out to be inferior according to the model fit and have therefore not been considered to model daily returns volatility in the following.

discussed above since the squared residuals of our GARCH models are free of serial correlation in each case except for the coffee futures market. Furthermore, to show that our GARCH models are also able to capture a potential asymmetry in the reaction to positive and negative shocks, we have conducted the sign bias (SB) test introduced by Engle and Ng (1993), which tests the null of no effect to lagged positive and/or negative shocks.[6] Except for the coffee and the wheat futures market, a potential asymmetry either does not exist or has been captured well by the chosen models.

*** Insert Table 2 about here ***

As already mentioned in the beginning of this subsection, we use the fitted time series of the standard deviation $\hat{\sigma}_t$ of the model that minimizes the SBC provided in Table 2 as our time-varying volatility measure.[7] The chosen $\hat{\sigma}_t$, $t = 1, \ldots, T$, has been plotted in Figure 3 for all agricultural futures markets under observation. It becomes evident that the volatility of agricultural futures returns changes strongly over time and in most cases has its largest peaks during the great recession period from December 2007 to June 2009. This period also includes the world food price crisis. Although showing strong volatility in the great recession period, the futures markets for cotton and sugar exhibit their strongest volatility around 2011. Interestingly, the volatility of futures returns for coffee – the smallest market in trading volume – appears to be a special case and has its largest peak in 2001 and another spike around 2014.

*** Insert Figure 3 about here ***

[6] We have estimated an auxiliary regression

$$\hat{z}_t^2 = c_0 + c_1 I(\hat{\varepsilon}_{t-1} < 0) + c_2 I(\hat{\varepsilon}_{t-1} < 0)\hat{\varepsilon}_{t-1} + c_3 I(\hat{\varepsilon}_{t-1} \geq 0) + u_t,$$

where $\hat{z}_t^2$ represents squared standardized residuals and $\hat{\varepsilon}_{t-1}$ one-day lagged residuals for each GARCH model, and have tested the joint null H_0: $c_1 = c_2 = c_3 = 0$ according to Engle and Ng (1993).

[7] As an alternative we have also considered the Akaike information criterion (AIC). The models minimizing the AIC solely differ for soybean oil and soybeans futures; however their fitted volatility series is strongly correlated with the volatility series chosen according to the SBC. Hence, we see this as indication that this choice does not alter our results presented in Section 3.

2.3. Time-varying Bayesian VAR framework

According to Clark (1973), Epps and Epps (1976) and Tauchen and Pitts (1983) trading volume and volatility are jointly endogenous variables. Therefore, we use an approach that is not restricted by any assumptions about the relationship between the variables of interest and threats all of them endogenously. Moreover, to account for time-variation in the relationship between trading volume, volatility and open interest on agricultural futures markets, we conduct the Bayesian time-varying parameter vector autoregression approach with stochastic volatility (B-TVP-VAR-SV) in the spirit of Primiceri (2005), which allows both the coefficients and the variance covariance matrix to change over time. The major benefit of this framework is that it allows the data to determine whether the time-variation stems from changes in the size of the shock – the *impulse* – or from changes in the propagation mechanism – the *response*. The model is specified as given below

$$Y_t = X_t' B_t + A_t^{-1} \Sigma_t \epsilon_t \quad \text{with} \quad X_t' = I_3 \otimes [1, Y_{t-1}, \ldots, Y_{t-p}] \quad \text{and} \quad B_t = \{B_{j,t}\}_{j=0}^{p}, \tag{7}$$

$$B_t = B_{t-1} + \upsilon_t, \quad a_t = a_{t-1} + \xi_t \quad \text{and} \quad \log \varsigma_t = \log \varsigma_{t-1} + \eta_t, \tag{8}$$

where Y_t is a three-dimensional vector including open interest, trading volume and volatility (in this ordering) for each agricultural futures market separately.[8] A_t is a lower triangular matrix with ones on the main diagonal and a_t is a vector stacking all free elements of A_t row-wise. Σ_t is a diagonal matrix with positive elements $\varsigma_t = \text{diag}(\Sigma_t)$, ϵ_t is a trivariate standard normally distributed innovation (i.e. $N(0, I_3)$) and $\{B_{j,t}\}_{j=0}^{p}$ are coefficient matrices for p lags in the VAR that are allowed to vary over time.

[8] We believe that the chosen ordering is the most reasonable choice since open interest refers to the previous day and is the sum of all open positions in the corresponding futures market. Therefore, it is reasonable that open interest effects trading volume and volatility contemporaneously but not vice versa. Since the return volatility is computed based on closing prices, it is also plausible that it is affected by trading volume contemporaneously but trading volume might be affected by return volatility with a lag. All three time series have been standardized to eliminate differences in the levels of the three variables. It is also worth noting that we have estimated B-TVP-VAR-SV models for each agricultural futures market separately instead of putting all markets into one large model. The main reason for this is that the latter would shift the focus of the paper since we focus on the relationship between return volatility, trading volume and open interest for agricultural futures markets instead of analyzing (volatility) spillovers between the different markets (which most likely also exist). The latter issue refers to a different strand of the literature (see e.g. Beckmann and Czudaj, 2014; Gardebroek et al., 2016; Sanjuán-López and Dawson, 2017) and is therefore beyond the scope of this paper.

The lag length of the VAR models $p = 2$ is selected by minimization of the SBC.[9] Allowing the matrix A_t to vary over time is important since a constant A_t would imply that a shock to one variable has a time-invariant effect on the other variables. Moreover, accounting for the possibility of heteroscedasticity by a time-varying Σ_t avoids fictitious dynamics that might arise from overlooking heteroscedasticity (Cogley and Sargent, 2005). B_t and a_t are modeled by simple random walks while ς_t follows a geometric random walk which belongs to the class of stochastic volatility models.[10] The disturbances of the model $\{\epsilon_t, \upsilon_t, \xi_t, \eta_t\}$ are assumed to be jointly normally distributed using the diagonality assumption on the variance covariance matrix $V = \text{var}\left[(\epsilon_t, \upsilon_t, \xi_t, \eta_t)'\right] = \text{diag}\left(I_3, Q, S, W\right)$, where Q, S and W are positive definite matrices. See Primiceri (2005) for details.

The B-TVP-VAR-SV models given by Eqs. (7) and (8) are estimated by a Markov Chain Monte Carlo (MCMC) algorithm using 50,000 iterations excluding the burn-in period of 5,000. More precisely, we use Gibbs sampling to sample from the joint posterior distribution of $\{B^T, A^T, \Sigma^T, V\}$, where B^T denotes the entire path of the coefficients $\{B_t\}_{t=1}^T$, Σ^T gives the entire path of the variance covariance matrices and A^T is the entire path of the lower triangular matrices. Appendix A.1 provides details on the Gibbs sampling algorithm in line with Del Negro and Primiceri (2015).[11] We have also checked the convergence of the Markov chains for all parameters included in our B-TVP-VAR-SV model relying on different diagnostics. Since each parameter is estimated in a time-varying fashion, we simulate the Markov chains for all parameters for each point in time. Therefore, we have provided autocorrelation functions (ACFs) for the first, fifth, tenth and twentieth lag for the VAR coefficients of all markets over time (see Appendix A.5) and also p-values for the Geweke (1992) diagnostic over time testing the null hypothesis of equal means in the first 10% and the last 50% of the Markov chain (see Appendix A.6). The ACFs show low correlation (mostly below 0.25), which gets even lower for higher lags, and therefore indicate good mixing. The Geweke (1992) tests confirm this finding since the null of equal means cannot be rejected for the vast majority of time

[9] Solely for the soybeans futures market SBC is minimized for $p = 3$ instead of $p = 2$. However, in order to achieve comparability between the different futures markets, he have decided to use the same lag length (i.e. $p = 2$) for all models.

[10] This constitutes an alternative to GARCH-type innovations and is in line with the related literature (see e.g. Canova and Gambetti, 2009; Koop et al., 2011; Ellis et al., 2014).

[11] It is also worth mentioning that $\hat{B}_{OLS}$, $\hat{V}(\hat{B}_{OLS})$, $\hat{A}_{OLS}$, $\hat{V}(\hat{A}_{OLS})$ have been estimated by OLS within a training sample period using the first 80 days (i.e. the period running from January 3, 2000 to April 26, 2000) to initialize the priors (see Appendix A.1 for details).

periods for all markets (5% false rejections are by chance due to the chosen significance level) and therefore show that the two parts of the chain are from the same distribution.

3. Empirical results

In the next two subsections we provide time-varying Granger causality tests and a time-varying impulse response analysis based on the model given by Eqs. (7) and (8) to get insights on the dynamics between trading volume, volatility and open interest on agricultural futures markets.

3.1. Time-varying Granger causality testing

In this section we provide a rolling fixed window version of the Granger causality test with a fixed window size of $k = 80$ days (for similar analyses see e.g. Thoma, 1994; Swanson, 1998; Shi et al., 2018) to examine if the variables of interest have predictive ability for each other. The rolling fixed window test starts with an initial sample period of 80 days (i.e. January 3, 2000 to April 26, 2000) and is based on the asymptotically χ^2-distributed Granger causality test statistic of type Wald $GC_{1,\dots,k}$. Then the sample period is moved by adding the next day and at the same time deleting the first observation to compute $GC_{2,\dots,k+1}$. This results in a time series of Granger causality test statistics $\{GC_{t,\dots,t+k-1}, \quad t = 1, \dots, T-k+1\}$, for which we have computed p-values for testing the null of no Granger causality between trading volume, volatility and open interest on agricultural futures markets.[12]

Figure 4 illustrates the corresponding p-values (in the range between 0 and 1) for the rolling fixed window version of the Granger causality test between the volatility of agricultural futures returns, their trading volume and their open interest. We have tested four different hypotheses. First, the null that trading volume does not Granger-cause volatility has been clearly rejected at each conventional level for each agricultural futures market for most parts of the sample period (see Panel (a) in Figure 4), especially for the sugar and the wheat futures market. However, this strong predictability seems to have disappeared during the period of the great recession between December 2007 to June 2009. Second, we also find several periods, for which the null that open

[12] Although the rolling window version of the Granger causality test is more suitable to detect structural changes in forecasting power compared to the forward expanding window version of the test, for which the initial sample period is extended by one day in each step, we have also provided the findings for the forward expanding window version of the test in Appendix A.4 to check for robustness.

interest does not Granger-cause volatility can also be rejected for all markets (see Panel (b) in Figure 4), especially for the corn and the wheat futures market. This shows that volatility is significantly affected by both previous period's trading volume and previous period's open interest which acts as a proxy for the dispersion of investors beliefs. The other two hypotheses test the reversed null, i.e. the effect of previous volatility either on trading volume or on open interest, and provide less pronounced results. We find some evidence for Granger causality running from volatility to trading volume but solely in certain very short periods of time (see Panel (c) in Figure 4). Most pronounced periods of trading volume being affected by lagged volatility can be found for corn, sugar and wheat. The impact of previous period's volatility on the heterogeneity of investors beliefs proxied by open interest is even weaker except for soybean oil futures around 2014 (see Panel (d) in Figure 4). All these conclusion are roughly supported for most of the considered futures markets by the results of the forward expanding window version of the Granger causality test reported in Appendix A.4.[13]

Overall, we find that volatility of agricultural futures markets can clearly be forecasted by the lags of both trading volume and open interest. However, the reversed forecasting ability from lagged volatility to trading volume and open interest is limited to certain periods of time. This indicates that it is crucial to allow for time-variation when modeling this relationship.

*** Insert Figure 4 about here ***

3.2. Time-varying impulse response analysis

As a next step, we provide a time-varying impulse response analysis focusing on the four scenarios examined in the previous subsection. Thus, we analyze the effect of a one-unit shock of one element of ϵ_t provided in Eq. (7) on one of the three variables included in Y_t over a horizon of 60 days. The corresponding response depends on the time-varying parameter estimates for B_t, A_t and Σ_t

[13]It should be noted that Granger causality refers to predictability of the past of one variable (X) for another (Y) but does not imply that there is indeed causation from X to Y in a more general sense. Therefore, this concept should not be confused with a common causality definition. In our setting it is possible that trading activity contains assessment information of an expected volatility shock and adjusts to a different level of expected volatility shock. In this sense, it is the expected volatility shock that drives trading but not vice versa. Therefore, one should be cautious to interpret this result referring to causality in a more general sense since in modern markets information are often impounded into the price very quickly.

at a given day t. Thus the responses have been calculated for each day t included in our data set except for the first 80 days used as a training sample to initialize our priors (see Appendix A.1). This results in time-varying impulse response functions depending on t that have been plotted in Figures 5 to 11 as three-dimensional graphs for each of the four scenarios for all seven agricultural futures markets.[14] The figures illustrate the reactions as medians of their corresponding posterior distributions at a specific day t and a specific horizon but do not include confidence bands due to clarity of visualization. However, to make inference on the reactions for certain periods of time and to illustrate the time-varying significance of the responses, we have also reported the four impulse responses for three specific points in time (namely 2000-05-01, 2008-09-15 and 2018-10-17)[15] together with their 68% and 95% confidence intervals in Appendix A.9.

Overall, the reaction to each shock varies substantially over time but it converges to zero for most of the time periods when the horizon increases. The former again highlights the importance to account for time-variation when modeling the relationship between volatility, trading volume and open interest for agricultural futures markets. The latter can be seen as indication that the VAR models are stationary at most points in time, although the persistence of shocks also differs over time. In addition, it turns out that the time-varying pattern is affected by market-specific characteristics. As already discussed in Section 2.1 the markets differ substantially in size and thus their reaction to shocks also varies to some extent. This confirms the findings by Chan and Fong (2000) for equity markets regarding the importance of the size of trades for the volatility-trading volume relationship. In the following two subsections we distinguish between effects to and effects stemming from volatility for each market.

*** Insert Figures 5 to 11 about here ***

[14] To enhance clarity Appendix A.7 provides rotated versions of the corresponding time-varying impulse response functions and Appendix A.8 illustrates these as contour plots.

[15] We have decided to use (1) the first trading day in our sample period, for which the impulse response can be obtained considering that the first 80 days are lost due to the initialization of the priors and another 2 days are lost because we estimate the VAR model with 2 lags, (2) the date of the collapse of Lehman Brothers as the most important event in our sample period and (3) the last trading day in the sample period.

3.3. Effect of trading volume and open interest shocks on volatility

The bottom part in Figures 5 to 11 shows the time-varying reaction of volatility to a shock of either trading volume (left plot) or open interest (right plot) for each agricultural futures market. Generally, we see that a trading volume shock leads to a statistically significant increase of the volatility (see also Panel (c) of the plots provided in Appendix A.9). This finding is not surprising since the more trades are done, the more prices and returns will vary. This also confirms the literature on equity markets: for instance, Chan and Fong (2000) find that daily stock return volatility is positively affected by trading volume and that both the number of trades and the size of trades play significant roles in the volatility-volume relation.[16] We therefore do not restrict our analysis on agricultural futures markets to a constant coefficient approach but allow the relationship between volatility and trading volume to vary over time. This enables us to account for changes in the number of trades and the size of trades across different periods and we also find a significantly positive effect of trading volume on volatility.

As expected the magnitude of the positive reaction to this shock differs substantially over time and across the seven markets. Very strong reactions can for example be observed during the great recession period between 2007 and 2009 for soybean oil, soybeans, sugar and wheat, in the period around 2011/12 characterized by a strong increase of trading volume in agricultural futures markets (especially for cotton, soybeans and wheat; see Figure 1) as well as in the latest period for cotton and sugar. As already mentioned in Section 2.1 the coffee market differs considerably from the others in size of trades and shows the most pronounced volatility responses to trading volume shocks with a peak reaction in 2015. This indicates that changes in trading volume induce day-by-day modifications in the transmission mechanism of shocks. Moreover, this also confirms the concept of sequential arrival of information mentioned in the Introduction.

The inclusion of open interest as a proxy for heterogeneity of investors beliefs can be seen as a control variable controlling for the effect of trading volume on volatility discussed above. The response of volatility to open interest shocks differs strongly over time and across the seven futures markets, is generally less significant than the reaction to trading volume shocks and does not solely show positive but also negative reactions. The latter confirms the result by Bessembinder and

[16] Ning and Tse (2009) also find a positive trading volume effect on stock market volatility while controlling for potential asymmetries stemming from trading volume and open interest.

Seguin (1993) mentioned in the Introduction. Generally, we find periods of positive, mostly short-run, effects and also periods of longer lasting negative effects. This basically verifies the important role of open interest and the heterogeneity of investors beliefs within the relationship between volatility and trading volume. The corresponding impulse response graphs provided in Figures 5 to 11 (bottom right) show several market specific volatility reactions to open interest shocks. E.g. for coffee and corn, we find strong positive reactions in the early 2000s until the beginning of the great recession period and very short-lived positive effects at the end of our sample period, which are directly followed by longer lasting negative effects. The positive reactions in the first part of the sample period might be due to the financialization of commodity markets that started in the early 2000s since an increase in open interest indicates a rise of futures contracts, which means that there is more money flowing into that market and this also increases the volatility. This implies that the current price trend continues. However, periods of negative volatility reactions after an open interest shock indicate that the current trend may level off and are also in line with the literature. The finding that a higher level of open interest reduces volatility is consistent with the idea that variations in open interest reflect changes in market depth (Bessembinder and Seguin, 1993).

Cotton futures roughly show a similar pattern as discussed above for coffee and corn futures. For soybean oil, soybeans and wheat futures, we find strong positive effects in the second part of the sample period and strong negative reactions during the great recession period around 2007 and 2009. The reaction of volatility to an open interest shock appears to be a special case for sugar futures since we solely observe a strong positive reaction at the end of the sample period, which is characterized by a strong increase in open interest for most of the commodities.

3.4. Effect of volatility shocks on trading volume and open interest

The upper part in Figures 5 to 11 shows the time-varying reaction of either trading volume (left plot) or open interest (right plot) to a volatility shock for each agricultural futures market. The impact of a volatility shock to trading volume is generally much lower in magnitude compared to the reversed impulse response for all considered markets, which can be seen by comparing the color scales for the upper plots in Figures 5 to 11 with the bottom ones. This verifies our Granger causality test results discussed in Section 3.1 that volatility is much more effected by trading volume than vice versa.

The effect of trading volume to a volatility shock varies considerably in sign, over time and

across markets but also turns out to be significant for a few periods of time. Periods of pronounced positive reactions include the years around 2000 as well as 2018 for coffee, the period of the great recession for soybean oil and soybeans and shortly after for cotton. Strong negative reactions are observed during the great recession period for corn and cotton as well as in the latest period for cotton and soybeans. A negative short-run effect can also be observed for sugar and wheat futures recurrently throughout the entire sample period. This implies that an increase in volatility sometimes restrains investors to trade. For most of the markets the time-varying reaction of open interest to a volatility shock exhibits a very similar pattern compared to the reaction of the trading volume, which shows that an increase in volatility can also have positive and negative effects on the dispersion of investors beliefs.

3.5. Forecasting exercise

As a final step of our analysis, we also examine if the considered variables are useful to explain each other within an out-of-sample context. Therefore, we have re-estimated our B-TVP-VAR-SV model for each agricultural commodity market using data until the last trading day in June 2018 (i.e. June 29, 2018) and we have used the subsequent period (i.e. July 2, 2018 to October 17, 2018) including 76 trading days to evaluate our forecasts for volatility, trading volume and open interest. We have compared the forecasting performance of our model with an univariate ARMA(2,2) model solely relying on past information of each corresponding series without taking into account information of the other two series. This helps us to examine how much information is added when including past information for the other series. Conventional forecast evaluation diagnostics including the RMSE, the MAE and the Diebold-Mariano test statistic are reported in Table 3. These clearly show that our B-TVP-VAR-SV model outperforms a simple ARMA(2,2) model. The only exception is the cotton futures market, for which we get mixed findings. However, it is also worth noting that we do not claim that our proposed model used in this study is the best model in terms of out-of-sample forecasts for the considered variables (i.e. volatility, trading volume and open interest) but the main focus of this study lies on the analysis of the time-varying relationship between the three considered variables and in this section we also show that our model provides at least some predictability compared to a simple univariate model.

*** Insert Table 3 about here ***

4. Conclusion

This study contributes to the literature on the trading volume and volatility nexus (1) by focusing on agricultural futures markets, (2) by controlling for heterogeneity of investors beliefs proxied by open interest and (3) by allowing for time-variation due to the potential of a changing pattern in the transmission mechanism of shocks. We make use of a flexible Bayesian VAR approach which allows for daily shifts stemming from both the coefficients and the variance covariance structure of the model's disturbances. Our results based on time-varying Granger causality testing and a time-varying impulse response analysis show that the predictability as well as the reaction to shocks varies substantially over time. This highlights the importance to account for time-variation when modeling the relationship between volatility, trading volume and open interest for agricultural futures markets. In general, we find that volatility of agricultural futures markets is driven by previous period's trading volume and open interest. However, the reversed relationship from lagged volatility to trading volume and open interest is limited to certain periods of time.

Our findings indicate that changes in trading volume and investors expectations induce day-by-day modifications in the transmission mechanism of shocks and confirm the concept of sequential arrival of information introduced by Copeland (1976) among others. Therefore, our results have direct implications for investors pursuing forward looking trading decisions based on the volatility (e.g. by calculating the value-at-risk). In addition, our findings have also important implications for market regulators, who decide on the implementation of market restrictions such as daily price movement and position limits. According to our results they might be able to lower the volatility on agricultural futures markets partly caused by speculation to keep commodity prices more stable.

An interesting avenue for further research provided by our study and related to the debate about the financialization of commodity markets (see e.g. Kim, 2015) would be to examine which type of market participants (e.g. hedgers, speculators or financial traders) is responsible for agricultural futures market volatility. The Commodity Futures Trading Commission provides detailed position data for agricultural futures markets available at a weekly frequency which might be helpful for answering this question. In this vein the construction and consideration of order imbalance measures might also provide further insights.

References

Abbott PC, Hurt C, Tyner WE. What's driving food prices? Farm Foundation Issue Reports 2008;No. 37951.

Admati AR, Pfleiderer P. A theory of intraday patterns: Volume and price variability. Review of Financial Studies 1988;1(1):3–40.

Andersen T. Return volatility and trading volume: An information flow interpretation of stochastic volatility. Journal of Finance 1996;51(1):169–204.

Beckmann J, Czudaj R. Volatility transmission in agricultural futures markets. Economic Modelling 2014;36(C):541–6.

Bessembinder H, Chan K, Seguin PJ. An empirical examination of information, differences of opinion, and trading activity. Journal of Financial Economics 1996;40(1):105–34.

Bessembinder H, Seguin PJ. Price volatility, trading volume, and market depth: Evidence from futures markets. Journal of Financial and Quantitative Analysis 1993;28(1):21–39.

Bollerslev T, Jubinski D. Equity trading volume and volatility: Latent information arrivals and common long-run dependencies. Journal of Business & Economic Statistics 1999;17(1):9–21.

Canova F, Gambetti L. Structural changes in the US economy: Is there a role for monetary policy? Journal of Economic Dynamics and Control 2009;33(2):477–90.

Carter CK, Kohn R. On Gibbs sampling for state space models. Biometrika 1994;81(3):541–53.

Chan K, Fong WM. Trade size, order imbalance, and the volatility-volume relation. Journal of Financial Economics 2000;57(2):247–73.

Clark P. A subordinated stochastic process model with finite variance for speculative prices. Econometrica 1973;41(1):135–55.

Cleveland RB, Cleveland WS, McRae JE, Terpenning I. STL: A seasonal-trend decomposition procedure based on Loess. Journal of Official Statistics 1990;6(1):3–73.

Cogley T, Sargent TJ. Drifts and volatilities: Monetary policies and outcomes in the post WWII US. Review of Economic Dynamics 2005;8(2):262–302.

Cooke B, Robles M. Recent food price movements: A time series analysis. International Food Policy Research Institute (IFPRI) Discussion Papers 2009;No. 00942.

Copeland TE. A model of asset trading under the assumption of sequential information arrival. Journal of Finance 1976;31(4):1149–68.

Czudaj RL. Crude oil futures trading and uncertainty. Energy Economics 2019;80:793–811.

Del Negro M, Primiceri GE. Time varying structural vector autoregressions and monetary policy: A Corrigendum. Review of Economic Studies 2015;82(4):1342–5.

Ding Z, Granger C, Engle R. A long memory property of stock market returns and a new model. Journal of Empirical Finance 1993;1(1):83–106.

Ellis C, Mumtaz H, Zabczyk P. What lies beneath? A time-varying FAVAR model for the UK transmission mechanism. Economic Journal 2014;124(576):668–99.

Engle R, Ng VK. Measuring and testing the impact of news on volatility. Journal of Finance 1993;48(5):1749–78.

Epps TW, Epps ML. The stochastic dependence of security price changes and transaction volumes: Implications for the mixture-of-distributions hypothesis. Econometrica 1976;44(2):305–21.

Fama EF, French KR. Commodity futures prices: Some evidence on forecast power, premiums, and the theory of storage. Journal of Business 1987;60(1):55–73.

Fernández C, Steel MFJ. On Bayesian modeling of fat tails and skewness. Journal of the American Statistical Association 1998;93(441):359–71.

Fisher TJ, Gallagher CM. New weighted portmanteau statistics for time series goodness of fit testing. Journal of the American Statistical Association 2012;107(498):777–87.

Fleming J, Kirby C. Long memory in volatility and trading volume. Journal of Banking & Finance 2011;35(7):1714–26.

Fleming J, Kirby C, Ostdiek B. Stochastic volatility, trading volume, and the daily flow of information. Journal of Business 2006;79(3):1551–90.

Gardebroek C, Hernandez MA, Robles M. Market interdependence and volatility transmission among major crops. Agricultural Economics 2016;47(2):141–55.

Geman H, Nguyen VN. Soybean inventory and forward curve dynamics. Management Science 2005;51(7):1076–91.

Geweke J. Evaluating the accuracy of sampling-based approaches to calculating posterior moments. In: Bernardo JM, Berger J, Dawid AP, Smith JFM, editors. Bayesian Statistics 4. Oxford: Oxford University Press; 1992. p. 169–93.

Gilbert CL. How to understand high food prices. Journal of Agricultural Economics 2010a;61(2):398–425.

Gilbert CL. Speculative influences on commodity futures prices 2006-2008. United Nations Conference on Trade and Development (UNCTAD) Discussion Papers 2010b;No. 197.

Glosten LR, Jagannathan R, Runkle DE. On the relation between the expected value and the volatility of the nominal excess return on stocks. Journal of Finance 1993;48(5):1779–801.

Gutierrez L. Speculative bubbles in agricultural commodity markets. European Review of Agricultural Economics 2013;40(2):217–38.

Harris L. Transaction data tests of the mixture of distributions hypothesis. Journal of Financial and Quantitative Analysis 1987;22(2):127–41.

Hevia C, Petrella I, Sola M. Risk premia and seasonality in commodity futures. Journal of Applied Econometrics 2018;forthcoming.

Jena SK, Tiwari AK, Roubaud D, Shahbaz M. Index futures volatility and trading activity: Measuring causality at a multiple horizon. Finance Research Letters 2018;24:247–55.

Jennings RH, Barry CB. Information dissemination and portfolio choice. Journal of Financial and Quantitative Analysis 1983;18(01):1–19.

Jennings RH, Starks LT, Fellingham JC. An equilibrium model of asset trading with sequential information arrival. Journal of Finance 1981;36(1):143–61.

Kim A. Does futures speculation destabilize commodity markets? Journal of Futures Markets 2015;35(8):696–714.

Kim O, Verrecchia RE. Trading volume and price reactions to public announcements. Journal of Accounting Research 1991;29(2):302–21.

Kim S, Shephard N, Chib S. Stochastic volatility: Likelihood inference and comparison with ARCH models. Review of Economic Studies 1998;65(3):361–93.

Koop G, Leon-Gonzalez R, Strachan RW. Bayesian inference in a time varying cointegration model. Journal of Econometrics 2011;165(2):210–20.

Lee BS, Rui O. The dynamic relationship between stock returns and trading volume: Domestic and cross-country evidence. Journal of Banking & Finance 2002;26(1):51–78.

Liesenfeld R. A generalized bivariate mixture model for stock price volatility and trading volume. Journal of Econometrics 2001;104(1):141–78.

Malliaris AG, Urrutia JL. Volume and price relationships: Hypotheses and testing for agricultural futures. Journal of Futures Markets 1998;18(1):53–72.

Masters MW. Written Testimony before the Committee on Homeland Security and Governmental Affairs. United States Senate May 20 http://hsgacsenategov/public/_files/052008Masterspdf (accessed August 22, 2017) 2008;.

Mitchel D. A Note On Rising Food Prices. The World Bank, 2008. URL: https://elibrary.worldbank.org/doi/abs/10.1596/1813-9450-4682. doi:10.1596/1813-9450-4682. arXiv:https://elibrary.worldbank.org/doi/pdf/10.1596/1813-9450-4682.

Morse D. Price and trading volume reaction surrounding earnings announcements – A closer examination. Journal of Accounting Research 1981;19(2):374–83.

Mougoué M, Aggarwal R. Trading volume and exchange rate volatility: Evidence for the sequential arrival of information hypothesis. Journal of Banking & Finance 2011;35(10):2690–703.

Myers RJ, Hanson SD. Pricing commodity options when the underlying futures price exhibits time-varying volatility. American Journal of Agricultural Economics 1993;75(1):121–30.

Nelson DB. Conditional heteroskedasticity in asset returns: A new approach. Econometrica 1991;59(2):347–70.

Ning Z, Tse Y. Order imbalance in the FTSE index futures market: Electronic versus open outcry trading. Journal of Business Finance & Accounting 2009;36(1-2):230–52.

Palm F. GARCH models of volatility. Handbook of Statistics 1996;14:209–40.

Primiceri GE. Time varying structural vector autoregressions and monetary policy. Review of Economic Studies 2005;72(3):821–52.

Sanjuán-López AI, Dawson PJ. Volatility effects of index trading and spillovers on US agricultural futures markets: A multivariate GARCH approach. Journal of Agricultural Economics 2017;68(3):822–38.

Shalen CT. Volume, volatility, and the dispersion of beliefs. Review of Financial Studies 1993;6(2):405–34.

Shi S, Phillips PCB, Hurn S. Change detection and the causal impact of the yield curve. Journal of Time Series Analysis 2018;39(6):966–87.

Smirlock M, Starks L. An empirical analysis of the stock price-volume relationship. Journal of Banking & Finance 1988;12(1):31–41.

Sørensen C. Modeling seasonality in agricultural commodity futures. Journal of Futures Markets 2002;22(5):393–426.

Swanson NR. Money and output viewed through a rolling window. Journal of Monetary Economics 1998;41(3):455–74.

Tauchen G, Pitts M. The price variability-volume relationship on speculative markets. Econometrica 1983;51(2):485–505.

Thoma MA. Subsample instability and asymmetries in money-income causality. Journal of Econometrics 1994;64(1):279–306.

White H. Maximum likelihood estimation of misspecified models. Econometrica 1982;50(1):1–25.

World Bank . World Development Report 2008: Agriculture for Development. Washington, DC: World Bank, 2007.

Tables and Figures

Table 1: **Descriptive statistics of returns, volume and open interest**

		Mean	SD	Median	Min	Max	Skewness	Kurtosis	WLB	p-value	WLB^2	p-value
	Coffee	-0.0006	2.1165	0.0000	-12.8467	16.6313	0.2215	3.4064	1.9642	0.1611	179.7968	0.0000
	Corn	0.0128	1.8066	0.0000	-24.5286	9.8013	-0.3391	9.4438	5.4189	0.0199	9.6893	0.0019
	Cotton	0.0091	1.9132	0.0000	-27.1398	16.7101	-0.4764	12.2637	7.4632	0.0063	6.9716	0.0083
Returns	**Soybean oil**	0.0130	1.4825	-0.0243	-7.2390	8.0804	0.1337	2.0668	0.0174	0.8951	52.9267	0.0000
	Soybeans	0.0138	1.5693	0.0512	-14.0831	7.5430	-0.6524	5.1889	0.0381	0.8452	15.6397	0.0001
	Sugar	0.0165	2.1114	0.0000	-12.3658	13.0305	-0.0778	2.6512	0.0247	0.8751	54.5834	0.0000
	Wheat	0.0155	2.0049	-0.0609	-10.0167	12.9293	0.2820	2.3072	0.3495	0.5544	75.3837	0.0000
	Coffee	7673.2767	8332.1527	6245.0000	0.0000	54263.0000	1.2211	1.7322	3458.5529	0.0000	2742.3589	0.0000
	Corn	97551.1892	64988.5581	87347.0000	0.0000	538170.0000	1.0585	1.8273	3027.9407	0.0000	1921.2205	0.0000
	Cotton	7801.5021	7870.3068	6412.5000	0.0000	66047.0000	1.1980	1.8859	2999.4255	0.0000	1763.8568	0.0000
Volume	**Soybean oil**	31356.7555	22269.9239	24471.0000	0.0000	172089.0000	0.8504	0.2970	3524.0600	0.0000	2504.0864	0.0000
	Soybeans	57012.5701	44650.7551	42470.0000	0.0000	327585.0000	1.0178	0.9393	3414.5540	0.0000	2426.4228	0.0000
	Sugar	41717.6902	24833.2996	39243.5000	0.0000	232949.0000	0.9056	1.7166	2706.2769	0.0000	1884.1141	0.0000
	Wheat	36466.2403	27880.6981	30123.0000	0.0000	231689.0000	1.0747	1.4704	3314.0658	0.0000	2620.5587	0.0000
	Coffee	35695.0051	37409.7258	26508.0000	0.0000	183611.0000	0.7645	-0.2447	4206.6905	0.0000	4243.7765	0.0000
	Corn	380817.7326	216429.3076	353642.0000	190.0000	1004304.0000	0.3043	-0.8913	4208.1946	0.0000	4386.2513	0.0000
	Cotton	51120.8498	49583.3746	36021.0000	0.0000	183932.0000	0.5659	-0.9929	4339.8058	0.0000	4376.8636	0.0000
Open interest	**Soybean oil**	110058.1956	57883.8741	103576.0000	15178.0000	275766.0000	0.4138	-0.8293	4622.6094	0.0000	4634.3730	0.0000
	Soybeans	152522.4346	110078.3514	126365.0000	1302.0000	445389.0000	0.5668	-0.7905	4256.1338	0.0000	4369.5811	0.0000
	Sugar	275061.6802	129824.4010	277113.0000	0.0000	548737.0000	-0.0802	-1.0672	4675.7727	0.0000	4679.4396	0.0000
	Wheat	139203.5400	81256.6174	140469.5000	2084.0000	313711.0000	0.0443	-1.2673	4185.1755	0.0000	4358.3431	0.0000

Note: The table reports descriptive statistics for agricultural futures daily closing returns (in %) calculated according to Eq. (1) as well as the daily volume traded and the previous day's open interest for a sample period running from January 3, 2000 to October 17, 2018. SD denotes standard deviation. WLB represents the test statistic of the weighted Ljung-Box test provided by Fisher and Gallagher (2012) for the null of no serial correlation of order 1. The following column provides the corresponding p-value. WLB^2 stands for the same test applied with squared returns.

Table 2: **Summary of best GARCH models**

	Coffee	**Corn**	**Cotton**	**Soybean oil**	**Soybeans**	**Sugar**	**Wheat**
	EGARCH	AP-GARCH	EGARCH	AP-GARCH	EGARCH	EGARCH	AP-GARCH
	$N(0,1)$	GED_ν	t_ν	$st_{\nu,\kappa}$	$N(0,1)$	$N(0,1)$	$st_{\nu,\kappa}$
ω	0.0258	0.0150	0.0106	0.0070	0.0056	0.0075	0.0061
p-value	0.0000	0.0000	0.0000	0.0000	0.0000	0.0000	0.0000
α	0.0237	0.0885	0.0517	0.0111	0.0293	-0.0010	0.0121
p-value	0.0036	0.0000	0.0000	0.0312	0.0000	0.8234	0.0359
β	0.9828	0.9247	0.9542	0.9908	0.9901	0.9952	0.9933
p-value	0.0000	0.0000	0.0000	0.0000	0.0000	0.0000	0.0000
γ	0.1711			0.1155	0.1449	0.0889	0.0941
p-value	0.0000			0.0000	0.0000	0.0000	0.0000
θ		0.0035	-0.0403				
p-value		0.9389	0.5252				
δ		0.8884	0.8288				
p-value		0.0000	0.0000				
ϕ							
p-value							
ν	4.5455	4.8278	5.4961	10.1745	7.1430	5.6715	6.3850
p-value	0.0000	0.0000	0.0000	0.0000	0.0000	0.0000	0.0000
κ		1.0518		1.0699			1.0746
p-value		0.0000		0.0000			0.0000
SBC	4.2090	3.4398	3.6166	3.6280	3.4626	4.3665	3.7935
AIC	4.2058	3.4353	3.6127	3.6241	3.4594	4.3632	3.7896
WLB	3.2436	29.7594	5.5653	17.2555	1.7496	1.3655	10.1866
p-value	0.0717	0.0000	0.0183	0.0000	0.1859	0.2426	0.0014
WLB^2	44.0251	3.6924	0.0009	0.0526	1.0940	2.9799	1.9779
p-value	0.0000	0.0547	0.9758	0.8187	0.2956	0.0843	0.1596
SB	27.1390	2.9797	1.8574	2.1045	6.8710	2.6952	10.1941
p-value	0.0000	0.3948	0.6025	0.5510	0.0761	0.4410	0.0170

Note: The table reports coefficient estimates and goodness-of-fit statistics using several different GARCH models. We have used four different GARCH specifications: GARCH refers to Eq. (3), EGARCH to Eq. (4), AP-GARCH to Eq. (5) and GJR-GARCH to Eq. (6). For all these models we have considered five different distributional assumptions for ε_t: the standard normal (i.e. $N(0,1)$) and Student's t with shape ν (i.e. t_ν), the skew standard normal with skewness κ (i.e. $sN(0,1)_\kappa$), the skew t with shape ν and skewness κ (i.e. $t_{\nu,\kappa}$), and the generalized error distribution with shape ν (i.e. GED_ν). The upper part of the table provides all parameter estimates together with their p-values using robust standard errors according to White (1982) (see Eq. (3) to (6) for the definition of the parameters). The bottom part of the table reports the Schwarz Bayesian information criterion (SBC), the Akaike information criterion (AIC), the weighted Ljung-Box test statistic (WLB) provided by Fisher and Gallagher (2012) for the null of no serial correlation of order 1 in the standardized residuals and the corresponding p-value, the weighted Ljung-Box test statistic (WLB^2) and p-value using squared standardized residuals and the sign bias test statistic (SB) and p-value for the null of no leverage effects in the standardized residuals (i.e. positive and/or negative effects to shocks) following Engle and Ng (1993). The best model has been selected by minimizing the SBC.

Table 3: **Forecast evaluation**

		B-TVP-VAR-SV		ARMA			
		RMSE	**MAE**	**RMSE**	**MAE**	**DM-stat**	***p*-value**
Coffee	**Open interest**	3.6717	3.0752	3.8071	3.1878	-5.0667	0.0000
	Volume	3.0644	2.2389	3.2224	2.3836	-4.8797	0.0000
	Volatility	1.6784	1.5511	1.9152	1.7650	-7.4937	0.0000
Corn	**Open interest**	4.0309	3.7479	57.8152	51.5823	-10.2672	0.0000
	Volume	3.4456	2.9853	57.6463	51.3303	-9.8744	0.0000
	Volatility	3.1829	2.8327	57.4555	51.2306	-8.7413	0.0000
Cotton	**Open interest**	1.1333	0.6042	1.2033	0.7762	-1.1094	0.2708
	Volume	0.6853	0.3436	0.7797	0.4681	-1.0511	0.2966
	Volatility	0.3393	0.2887	0.2338	0.1766	-9.4249	0.0000
Soybean oil	**Open interest**	1.6727	1.3780	2.8567	2.3762	-3.9840	0.0002
	Volume	1.1642	0.8950	2.8188	2.2926	-9.7522	0.0000
	Volatility	0.6136	0.5367	3.3661	2.6908	-10.2923	0.0000
Soybeans	**Open interest**	2.0408	1.3505	42.4642	37.0301	-9.6020	0.0000
	Volume	1.5507	1.3847	42.1033	37.1457	-9.5254	0.0000
	Volatility	1.2232	0.9826	42.4146	37.4265	-12.8329	0.0000
Sugar	**Open interest**	1.9638	1.6764	12.4765	10.1986	-8.1224	0.0000
	Volume	1.4652	1.2382	11.4224	10.2015	-9.3942	0.0000
	Volatility	0.6127	0.5052	11.6813	10.3095	-12.3530	0.0000
Wheat	**Open interest**	3.2627	3.0091	43.4188	38.8473	-10.3466	0.0000
	Volume	3.4429	2.9120	43.4889	38.9799	-10.5309	0.0000
	Volatility	4.0048	3.7423	44.2086	39.8529	-12.7080	0.0000

Note: The table reports forecast evaluation diagnostics based on the Bayesian time-varying parameter vector autoregression model with stochastic volatility (B-TVP-VAR-SV) and an autoregressive moving average (ARMA) model. RMSE denotes root mean square error, MAE stands for mean absolute error, DM-stat gives the Diebold-Mariano test statistic and the last column provides the corresponding p-value for testing the null of equal forecast accuracy of the two considered models. Data until the last trading day in June 2018 (i.e. June 29, 2018) has been used to estimate both models and the subsequent period (i.e. July 2, 2018 to October 17, 2018) including 76 trading days has been used to evaluate the forecast performance.

Figure 1: **Agricultural futures trading volume**

The plots show the non-seasonally adjusted trading volume of seven agricultural futures markets for a sample period running from January 3, 2000 to October 17, 2018. The cyan areas highlight the US recession periods from March 2001 to November 2001 and December 2007 to June 2009 according to the classification of the National Bureau of Economic Research.

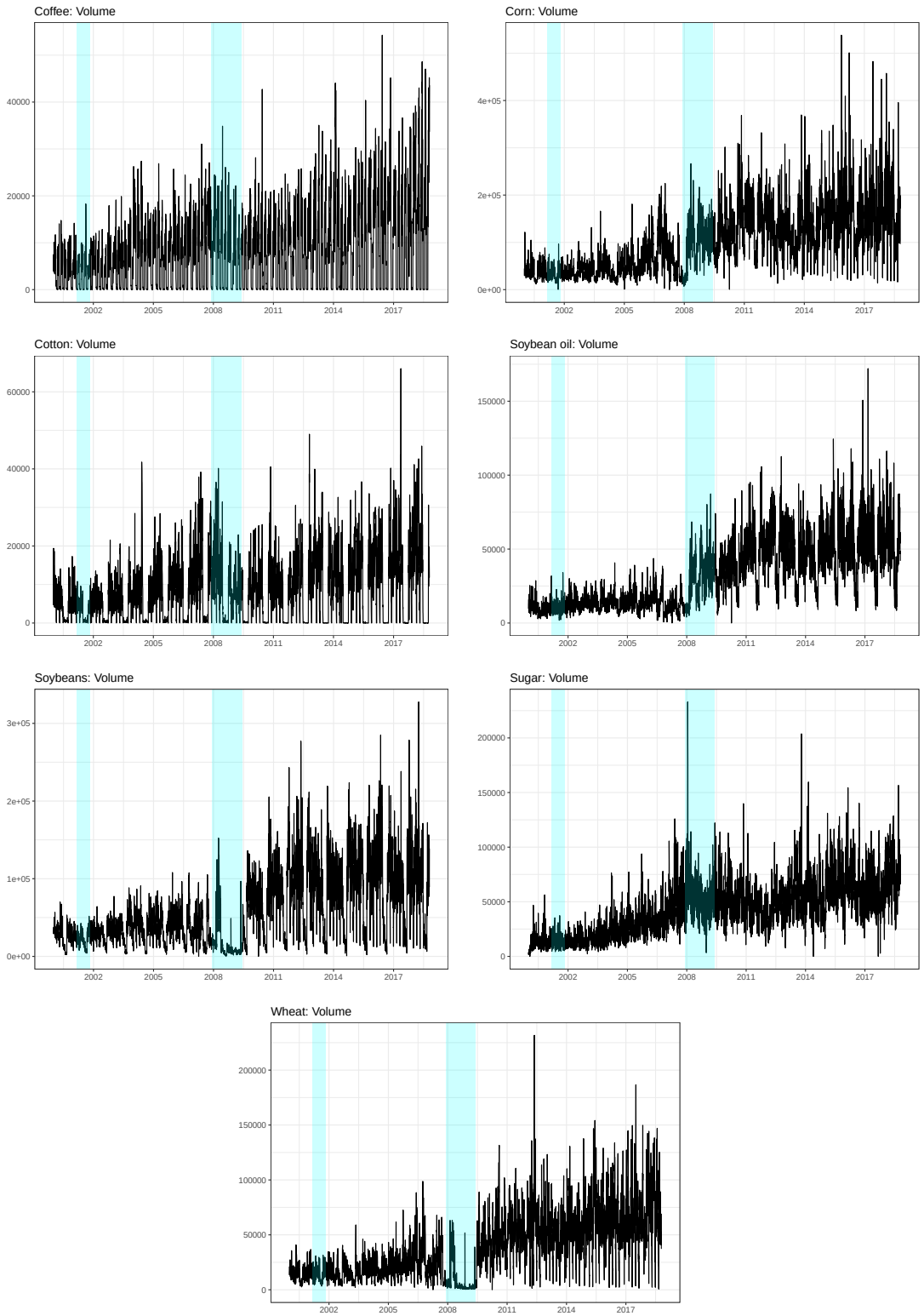

Figure 2: **Agricultural futures open interest**

The plots show the non-seasonally adjusted previous day open interest of seven agricultural futures markets for a sample period running from January 3, 2000 to October 17, 2018. The cyan areas highlight the US recession periods from March 2001 to November 2001 and December 2007 to June 2009 according to the classification of the National Bureau of Economic Research.

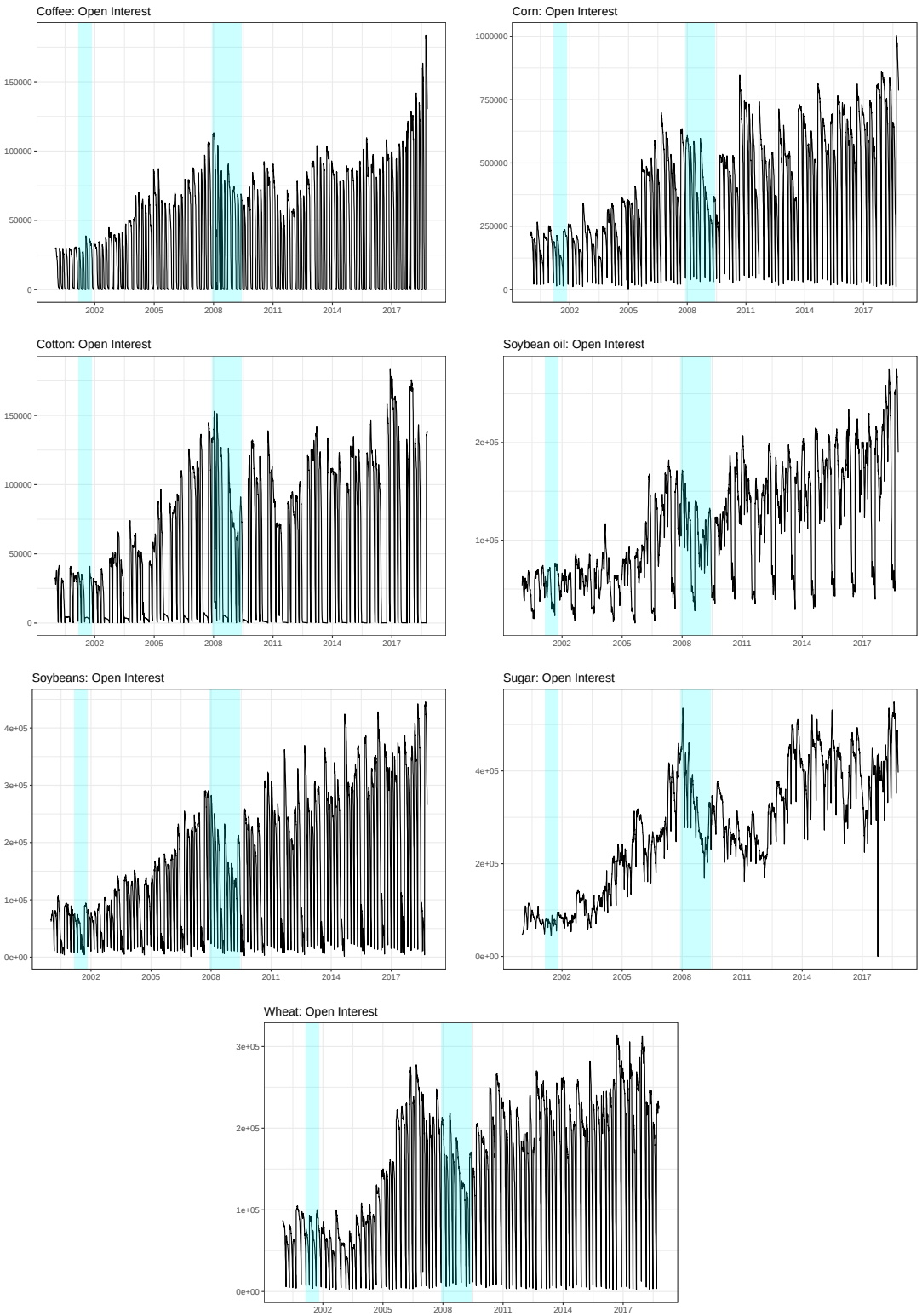

Figure 3: **Agricultural futures volatility**

The plots show the volatility of the returns of seven agricultural futures markets for a sample period running from January 3, 2000 to October 17, 2018. The volatility has been estimated by taking the standard deviation of fitted GARCH models presented in Table 2. The cyan areas highlight the US recession periods from March 2001 to November 2001 and December 2007 to June 2009 according to the classification of the National Bureau of Economic Research.

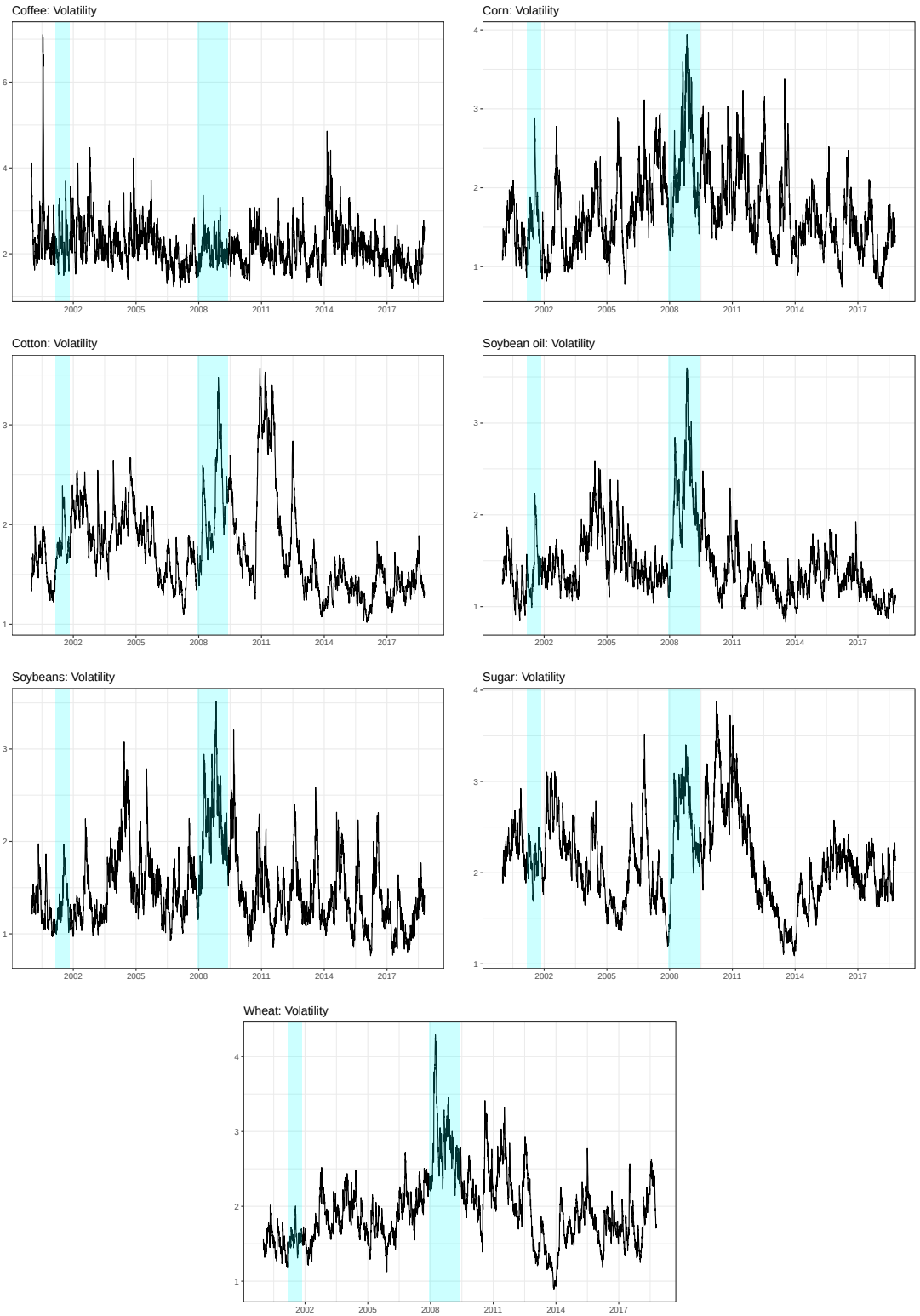

Figure 4: **Time-varying Granger causality between agricultural futures volatility, trading volume and open interest**

The plots show the p-values for a rolling fixed window version of the Granger causality test between the volatility of the returns of seven agricultural futures markets, their trading volume and their previous day's open interest for a sample period running from January 3, 2000 to October 17, 2018. The test is applied with a fixed window size of 80 days starting with a sample period running from January 3, 2000 to April 26, 2000 and moving forward by one day in each step while deleting the earliest observation. The cyan areas highlight the US recession periods according to the classification of the National Bureau of Economic Research. The vertical axis covers values from 0 to 1 and the red dashed line represents the 10% significance level.

Panel (a): Null hypothesis: Trading volume does not Granger-cause volatility

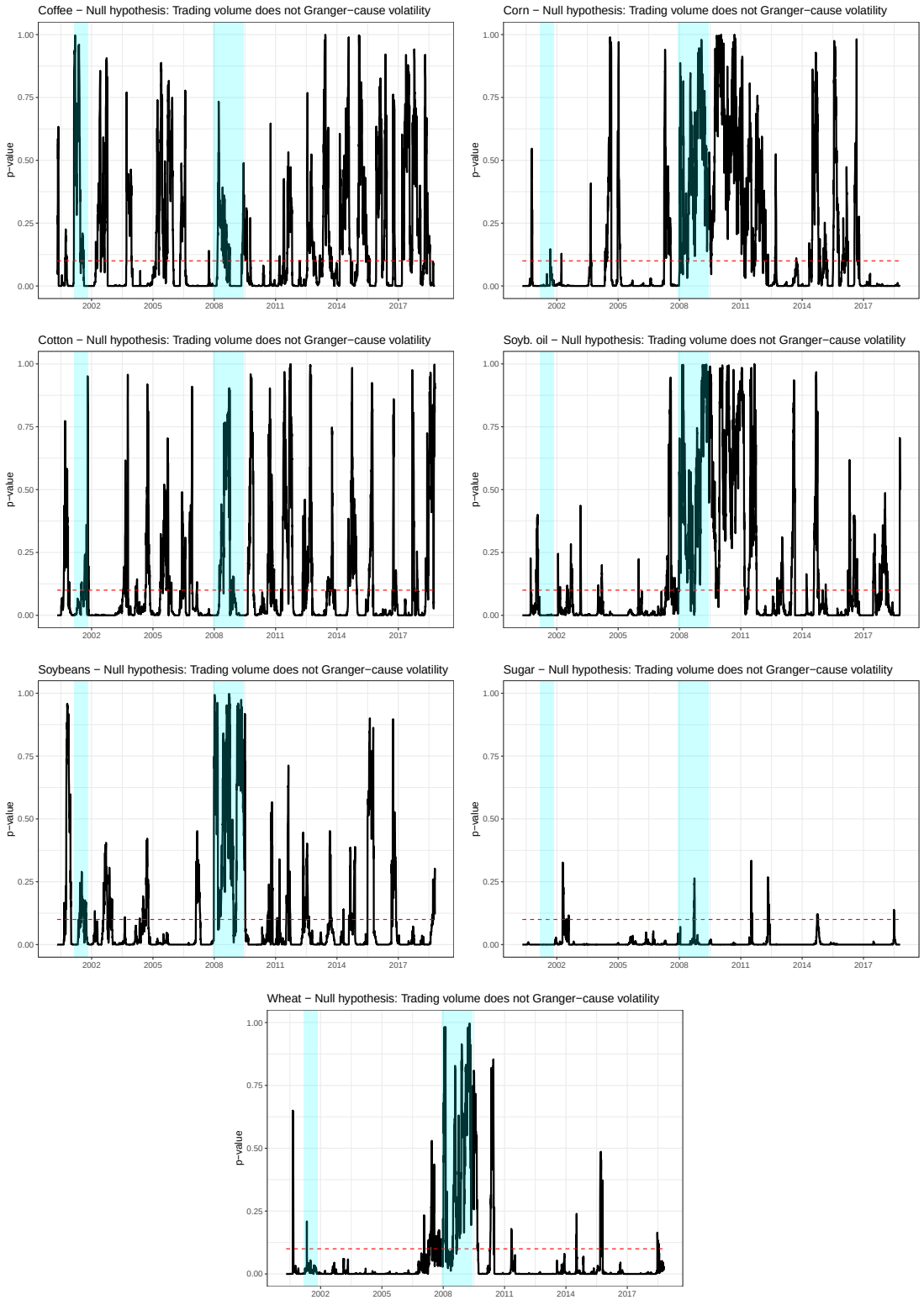

Panel (b): Null hypothesis: Open interest does not Granger-cause volatility

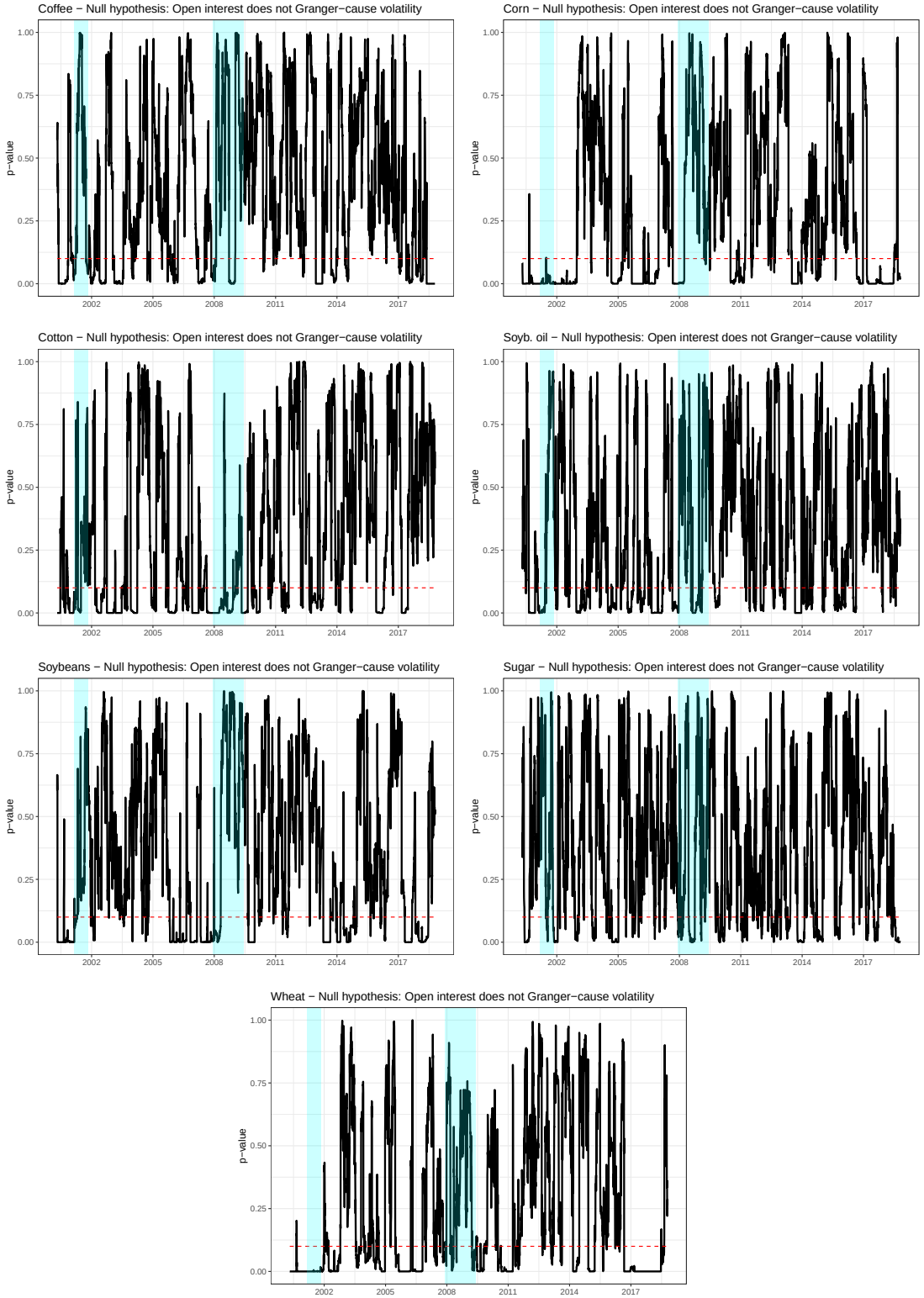

Panel (c): Null hypothesis: Volatility does not Granger-cause trading volume

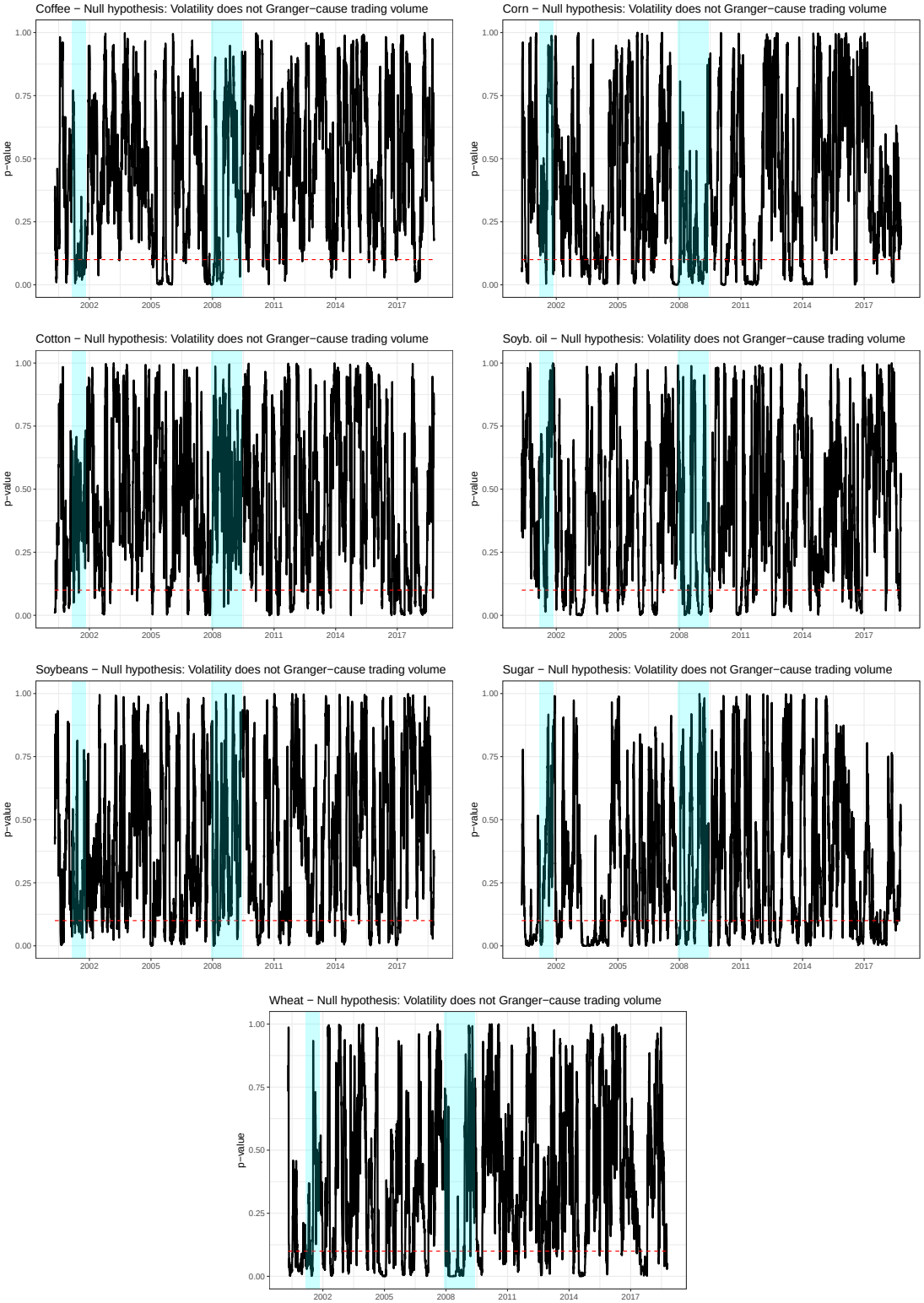

Panel (d): Null hypothesis: Volatility does not Granger-cause open interest

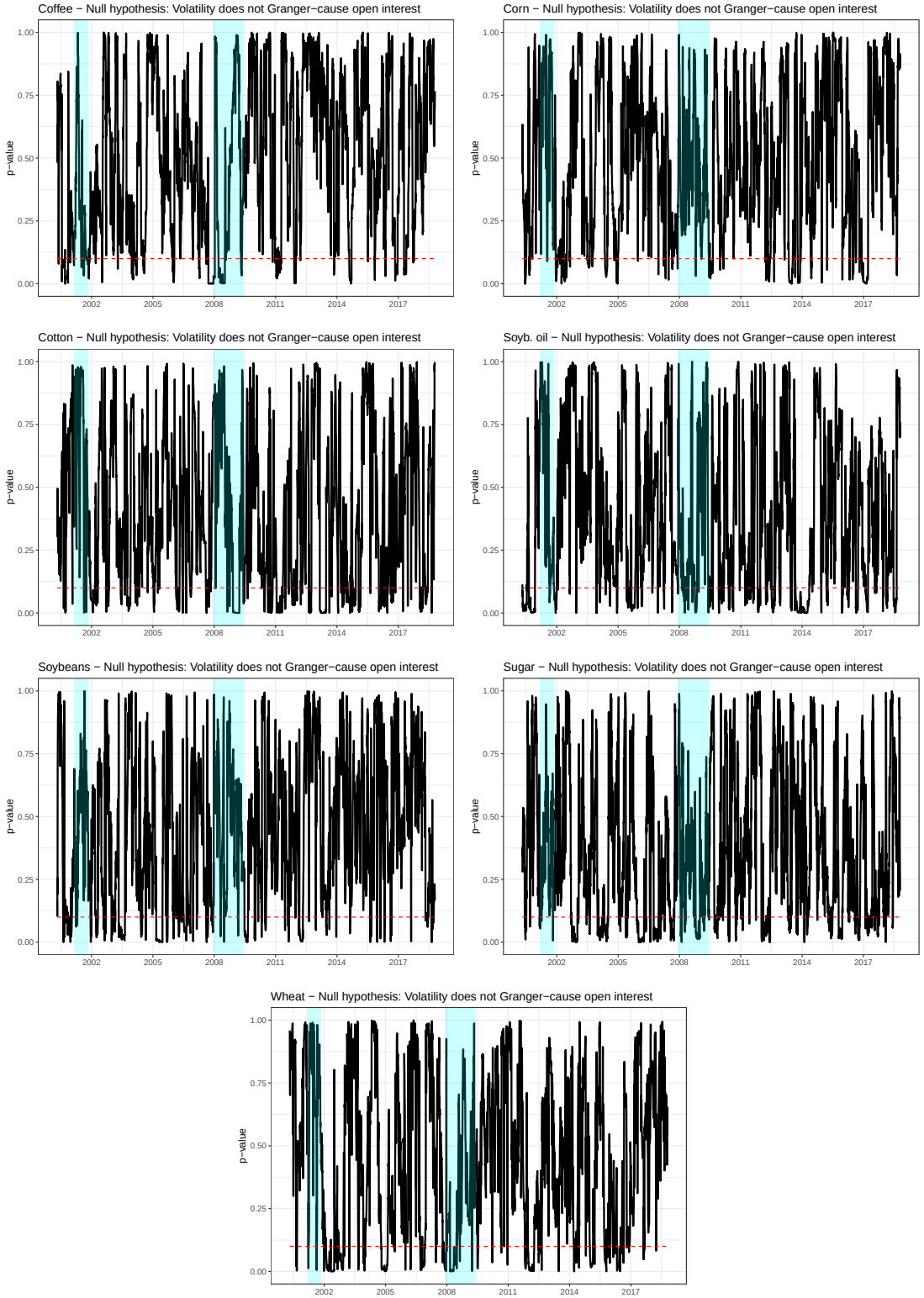

Figure 5: **Time-varying impulse responses for coffee**

The plots show the time-varying reactions of one-unit shocks between the volatility of returns, the trading volume and the previous day's open interest. The corresponding reactions have been calculated for a sample period running from January 3, 2000 to October 17, 2018 on a daily basis while data for the first 80 days (until April 26, 2000) has been used as a training sample to initialize the coefficient priors. The individual plots provide the response of the corresponding shock on the vertical axis ("Response"), the individual dates spanning our sample period on the bottom left axis ("Time") and the horizon from 0 to 60 over which the response is examined at the bottom right axis ("Horizon"). The magnitude of the responses to shocks are visualized by the color scale on the right of each individual plot.

Response of trading volume to a shock in volatility

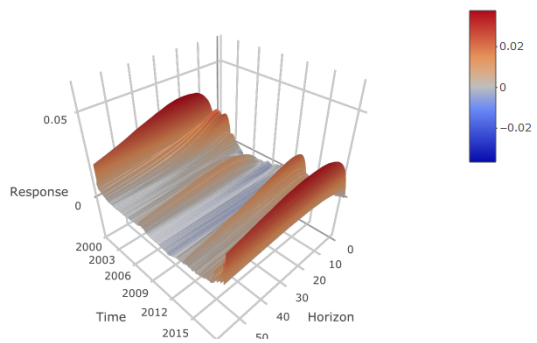

Response of open interest to a shock in volatility

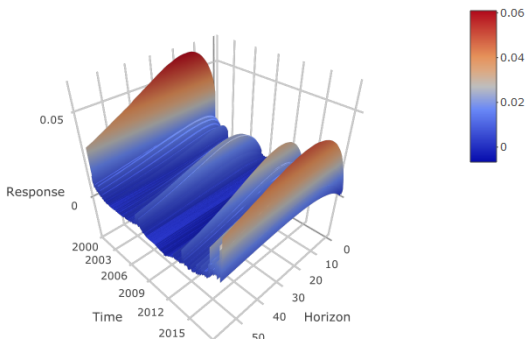

Response of volatility to a shock in trading volume

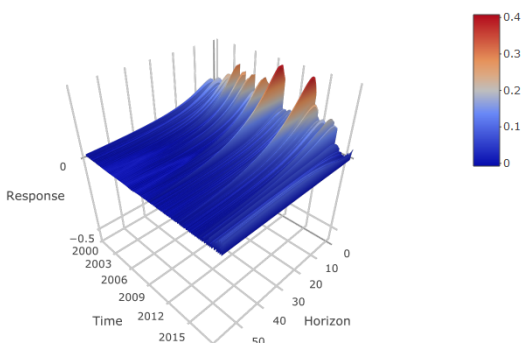

Response of volatility to a shock in open interest

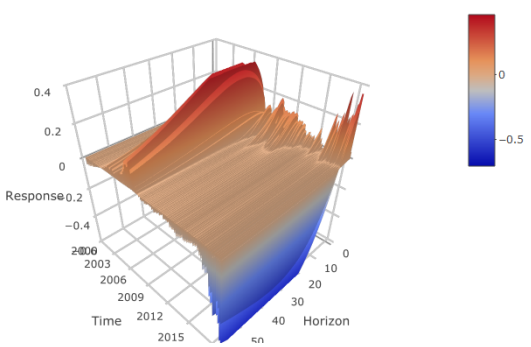

Figure 6: **Time-varying impulse responses for corn**

The plots show the time-varying reactions of one-unit shocks between the volatility of returns, the trading volume and the previous day's open interest. The corresponding reactions have been calculated for a sample period running from January 3, 2000 to October 17, 2018 on a daily basis while data for the first 80 days (until April 26, 2000) has been used as a training sample to initialize the coefficient priors. The individual plots provide the response of the corresponding shock on the vertical axis ("Response"), the individual dates spanning our sample period on the bottom left axis ("Time") and the horizon from 0 to 60 over which the response is examined at the bottom right axis ("Horizon"). The magnitude of the responses to shocks are visualized by the color scale on the right of each individual plot.

Response of trading volume to a shock in volatility

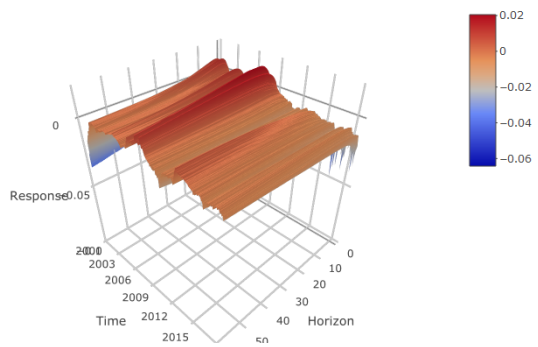

Response of open interest to a shock in volatility

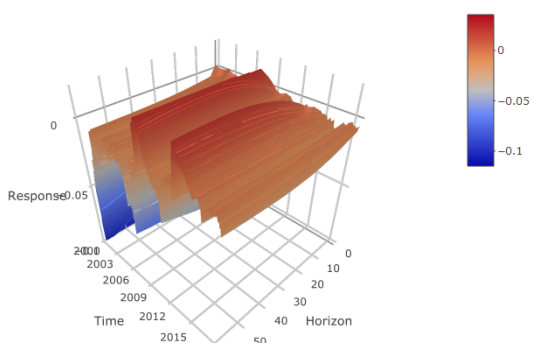

Response of volatility to a shock in trading volume

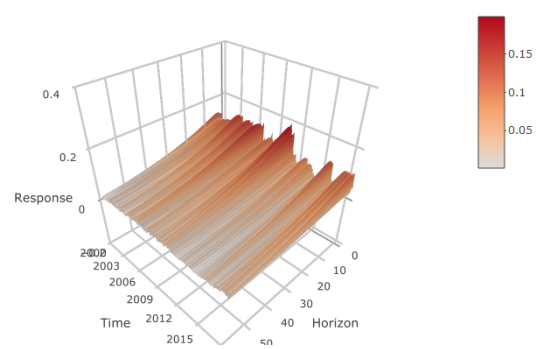

Response of volatility to a shock in open interest

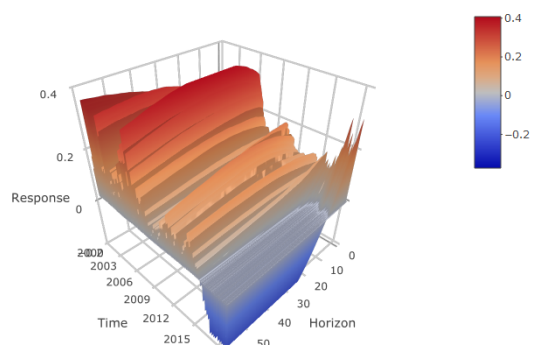

Figure 7: **Time-varying impulse responses for cotton**

The plots show the time-varying reactions of one-unit shocks between the volatility of returns, the trading volume and the previous day's open interest. The corresponding reactions have been calculated for a sample period running from January 3, 2000 to October 17, 2018 on a daily basis while data for the first 80 days (until April 26, 2000) has been used as a training sample to initialize the coefficient priors. The individual plots provide the response of the corresponding shock on the vertical axis ("Response"), the individual dates spanning our sample period on the bottom left axis ("Time") and the horizon from 0 to 60 over which the response is examined at the bottom right axis ("Horizon"). The magnitude of the responses to shocks are visualized by the color scale on the right of each individual plot.

Response of trading volume to a shock in volatility

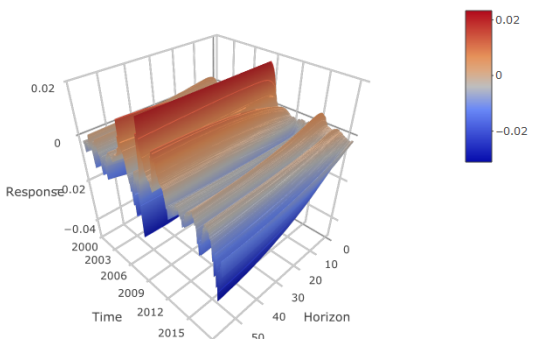

Response of open interest to a shock in volatility

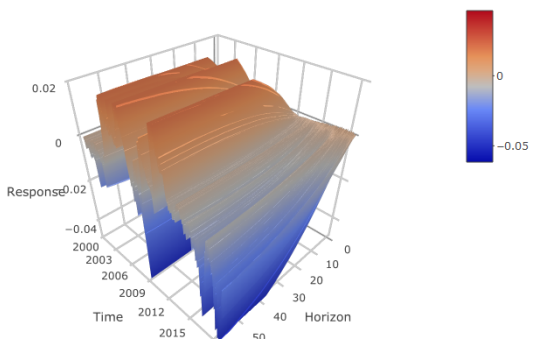

Response of volatility to a shock in trading volume

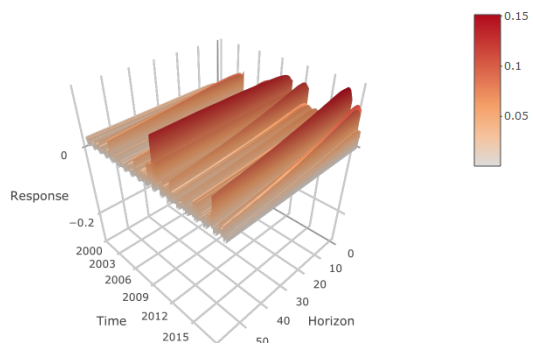

Response of volatility to a shock in open interest

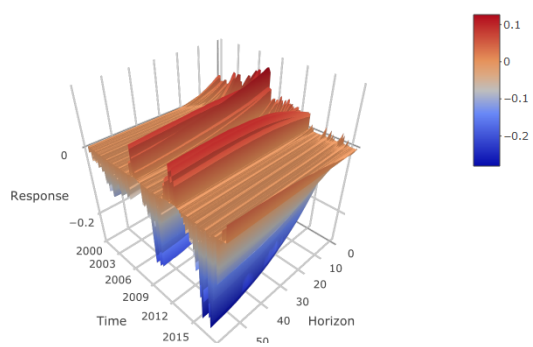

Figure 8: **Time-varying impulse responses for soybean oil**

The plots show the time-varying reactions of one-unit shocks between the volatility of returns, the trading volume and the previous day's open interest. The corresponding reactions have been calculated for a sample period running from January 3, 2000 to October 17, 2018 on a daily basis while data for the first 80 days (until April 26, 2000) has been used as a training sample to initialize the coefficient priors. The individual plots provide the response of the corresponding shock on the vertical axis ("Response"), the individual dates spanning our sample period on the bottom left axis ("Time") and the horizon from 0 to 60 over which the response is examined at the bottom right axis ("Horizon"). The magnitude of the responses to shocks are visualized by the color scale on the right of each individual plot.

Response of trading volume to a shock in volatility

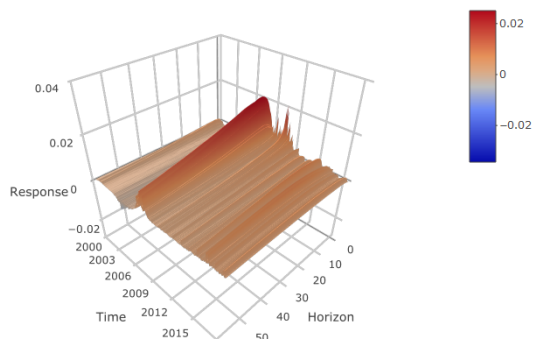

Response of open interest to a shock in volatility

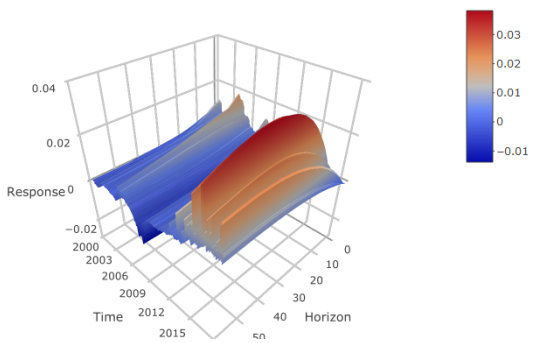

Response of volatility to a shock in trading volume

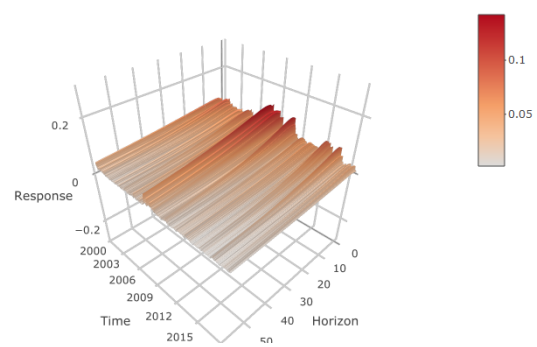

Response of volatility to a shock in open interest

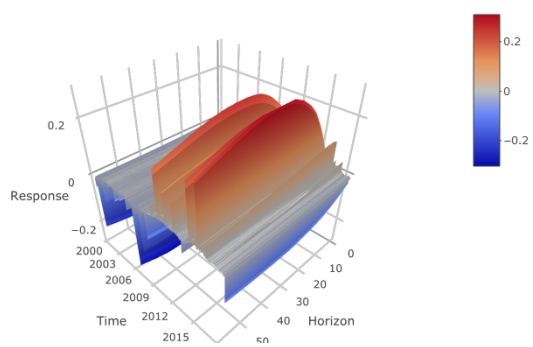

Figure 9: **Time-varying impulse responses for soybeans**

The plots show the time-varying reactions of one-unit shocks between the volatility of returns, the trading volume and the previous day's open interest. The corresponding reactions have been calculated for a sample period running from January 3, 2000 to October 17, 2018 on a daily basis while data for the first 80 days (until April 26, 2000) has been used as a training sample to initialize the coefficient priors. The individual plots provide the response of the corresponding shock on the vertical axis ("Response"), the individual dates spanning our sample period on the bottom left axis ("Time") and the horizon from 0 to 60 over which the response is examined at the bottom right axis ("Horizon"). The magnitude of the responses to shocks are visualized by the color scale on the right of each individual plot.

Response of trading volume to a shock in volatility

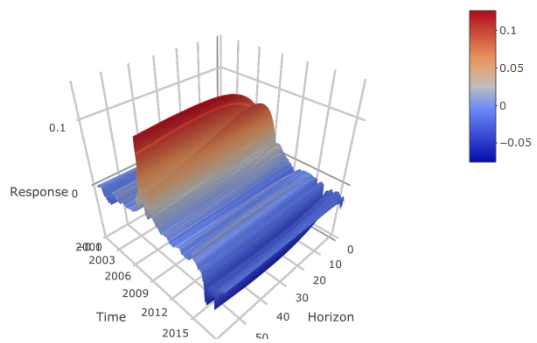

Response of open interest to a shock in volatility

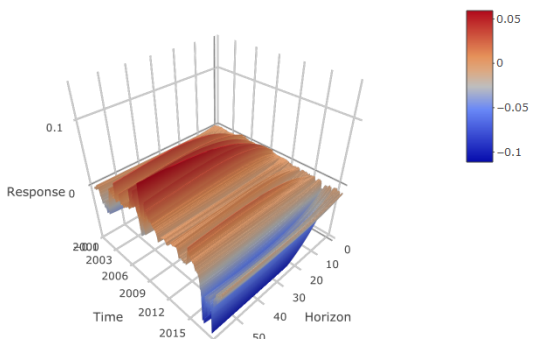

Response of volatility to a shock in trading volume

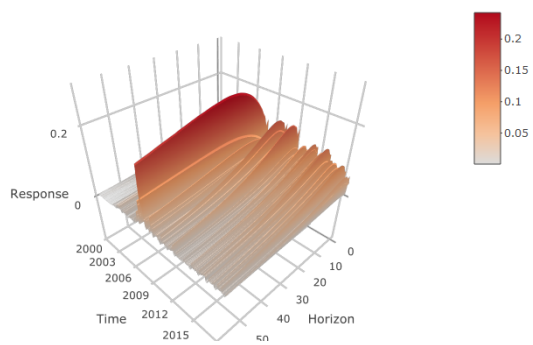

Response of volatility to a shock in open interest

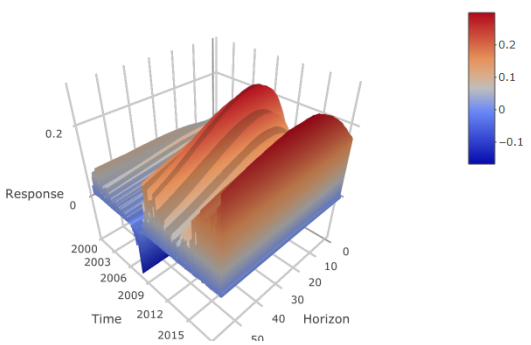

Figure 10: **Time-varying impulse responses for sugar**

The plots show the time-varying reactions of one-unit shocks between the volatility of returns, the trading volume and the previous day's open interest. The corresponding reactions have been calculated for a sample period running from January 3, 2000 to October 17, 2018 on a daily basis while data for the first 80 days (until April 26, 2000) has been used as a training sample to initialize the coefficient priors. The individual plots provide the response of the corresponding shock on the vertical axis ("Response"), the individual dates spanning our sample period on the bottom left axis ("Time") and the horizon from 0 to 60 over which the response is examined at the bottom right axis ("Horizon"). The magnitude of the responses to shocks are visualized by the color scale on the right of each individual plot.

Response of trading volume to a shock in volatility

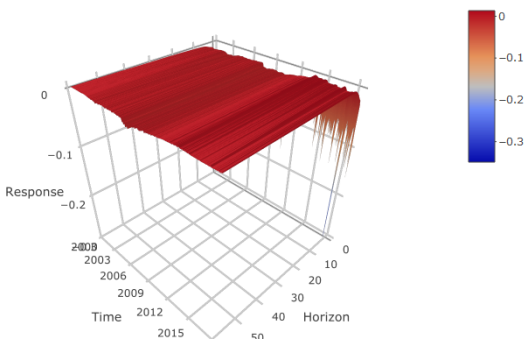

Response of open interest to a shock in volatility

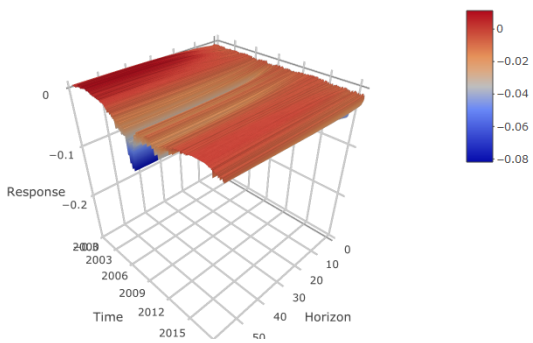

Response of volatility to a shock in trading volume

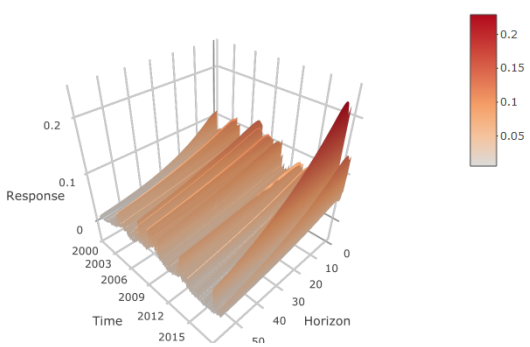

Response of volatility to a shock in open interest

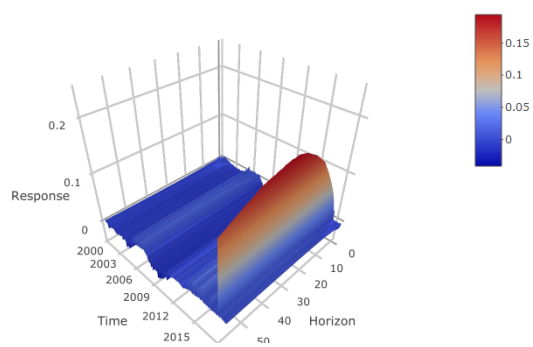

Figure 11: **Time-varying impulse responses for wheat**

The plots show the time-varying reactions of one-unit shocks between the volatility of returns, the trading volume and the previous day's open interest. The corresponding reactions have been calculated for a sample period running from January 3, 2000 to October 17, 2018 on a daily basis while data for the first 80 days (until April 26, 2000) has been used as a training sample to initialize the coefficient priors. The individual plots provide the response of the corresponding shock on the vertical axis ("Response"), the individual dates spanning our sample period on the bottom left axis ("Time") and the horizon from 0 to 60 over which the response is examined at the bottom right axis ("Horizon"). The magnitude of the responses to shocks are visualized by the color scale on the right of each individual plot.

Response of trading volume to a shock in volatility

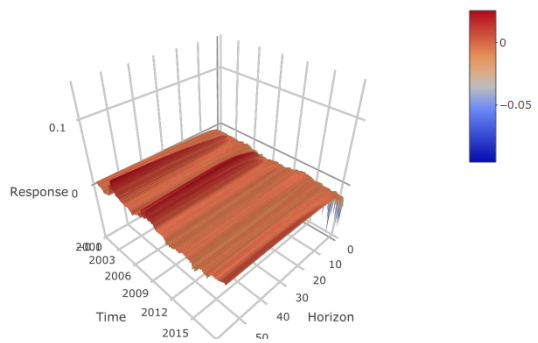

Response of open interest to a shock in volatility

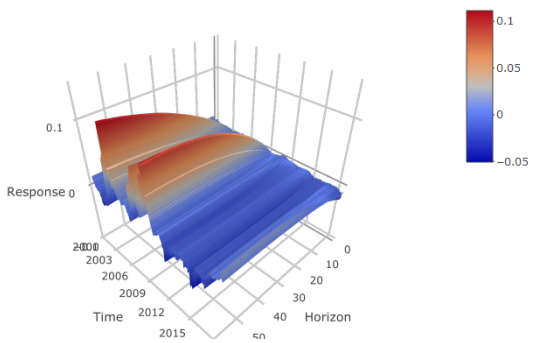

Response of volatility to a shock in trading volume

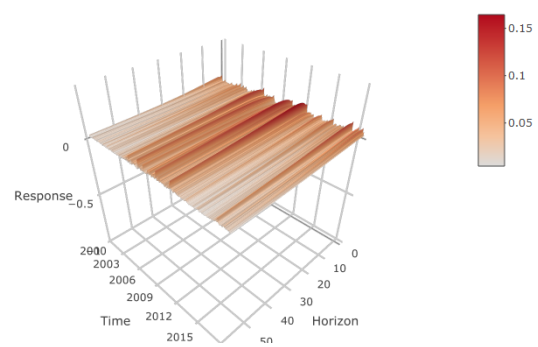

Response of volatility to a shock in open interest

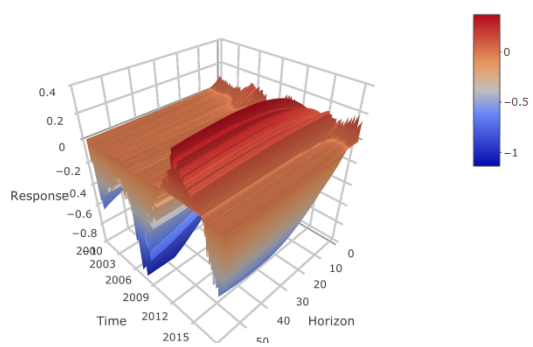

A. Appendix

A.1 MCMC algorithm

The model given by Eqs. (7) and (8) is estimated by a Bayesian MCMC algorithm using uninformative priors given below

$$p(B_0) = N(\hat{B}_{OLS}, k_B \cdot \hat{V}(\hat{B}_{OLS})) \quad \text{with} \quad k_B = 4, \tag{9}$$

$$p(A_0) = N(\hat{A}_{OLS}, k_A \cdot \hat{V}(\hat{A}_{OLS})) \quad \text{with} \quad k_A = 4, \tag{10}$$

$$p(\log \varsigma_0) = N(\log \hat{\varsigma}_{OLS}, k_\varsigma \cdot I_3) \quad \text{with} \quad k_\varsigma = 1, \tag{11}$$

$$p(Q) = IW(k_Q^2 \cdot pQ \cdot \hat{V}(\hat{B}_{OLS}), pQ) \quad \text{with} \quad k_Q = 0.01, pQ = 80, \tag{12}$$

$$p(W) = IW(k_W^2 \cdot pW \cdot I_3, pW) \quad \text{with} \quad k_W = 0.01, pW = 4, \tag{13}$$

$$p(S_j) = IW(k_S^2 \cdot pS_j \cdot \hat{V}(\hat{A}_{j,OLS}), pS_j) \quad \text{with} \quad k_S = 0.01, pS_j = 1 + j, \quad j = 1, 2 \tag{14}$$

where $N(.)$ stands for the normal and $IW(.)$ for the inverse Wishart distribution. To initialize the priors, $\hat{B}_{OLS}$, $\hat{V}(\hat{B}_{OLS})$, $\hat{A}_{OLS}$, $\hat{V}(\hat{A}_{OLS})$ have been estimated by OLS within a training sample period using the first 80 days.

We apply the Gibbs sampling algorithm by Del Negro and Primiceri (2015) with 50,000 draws excluding a burn-in sample of 5,000 as follows:

1. Initialize A^T, Σ^T, s^T and V^T,
2. Sample B^T from $p(B^T|\vartheta^{-B^T}, \Sigma^T)$ by applying the Carter and Kohn (1994) algorithm,
3. Sample Q from the inverse Wishart posterior $p(Q|B^T)$,
4. Sample A^T from $p(A^T|\vartheta^{-A^T}, \Sigma^T)$ by applying the Carter and Kohn (1994) algorithm,

5. Sample S from the inverse Wishart posterior $p(S|\vartheta^{-S}, \Sigma^T)$,

6. Sample s^T from $p(s^T|\Sigma^T, \vartheta)$ by applying the Kim et al. (1998) algorithm,

7. Sample Σ^T from $p(\Sigma^T|\vartheta, s^T)$ by applying the Carter and Kohn (1994) algorithm,

8. Sample W from the inverse Wishart posterior $p(W|\Sigma^T)$,

9. Go back to step 2,

where s^T denotes the entire path of auxiliary discrete variables necessary to conduct inference on the volatilities given in Σ^T (Del Negro and Primiceri, 2015). ϑ is defined as $\vartheta = [B^T, A^T, V]$ and ϑ^{-B^T} means $\vartheta \setminus B^T$.

Figure A.1: **Agricultural futures trading volume**

The plots show the seasonally adjusted trading volume of seven agricultural futures markets for a sample period running from January 3, 2000 to October 17, 2018. The cyan areas highlight the US recession periods from March 2001 to November 2001 and December 2007 to June 2009 according to the classification of the National Bureau of Economic Research.

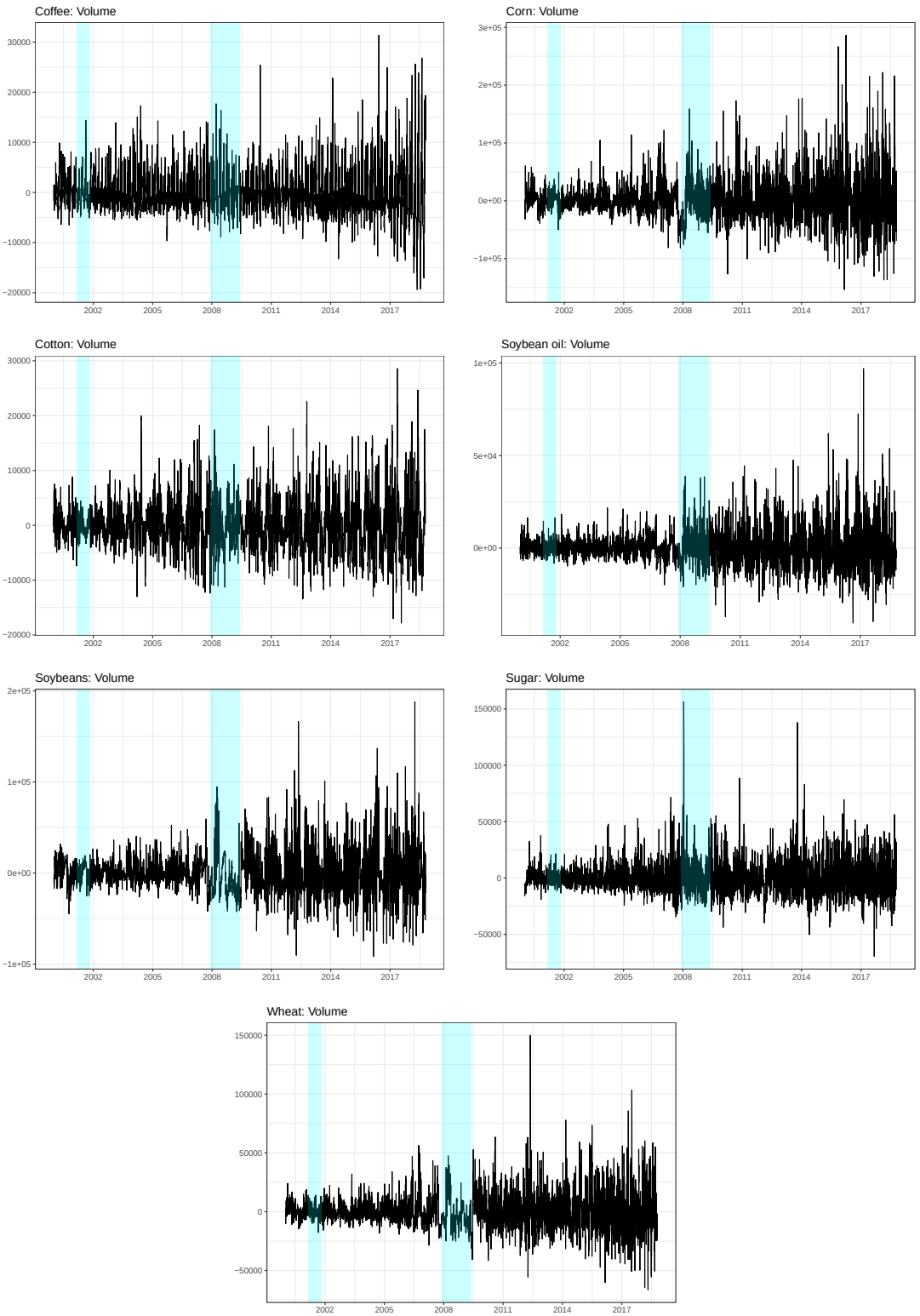

Figure A.2: **Agricultural futures open interest**

The plots show the seasonally adjusted previous day open interest of seven agricultural futures markets for a sample period running from January 3, 2000 to October 17, 2018. The cyan areas highlight the US recession periods from March 2001 to November 2001 and December 2007 to June 2009 according to the classification of the National Bureau of Economic Research.

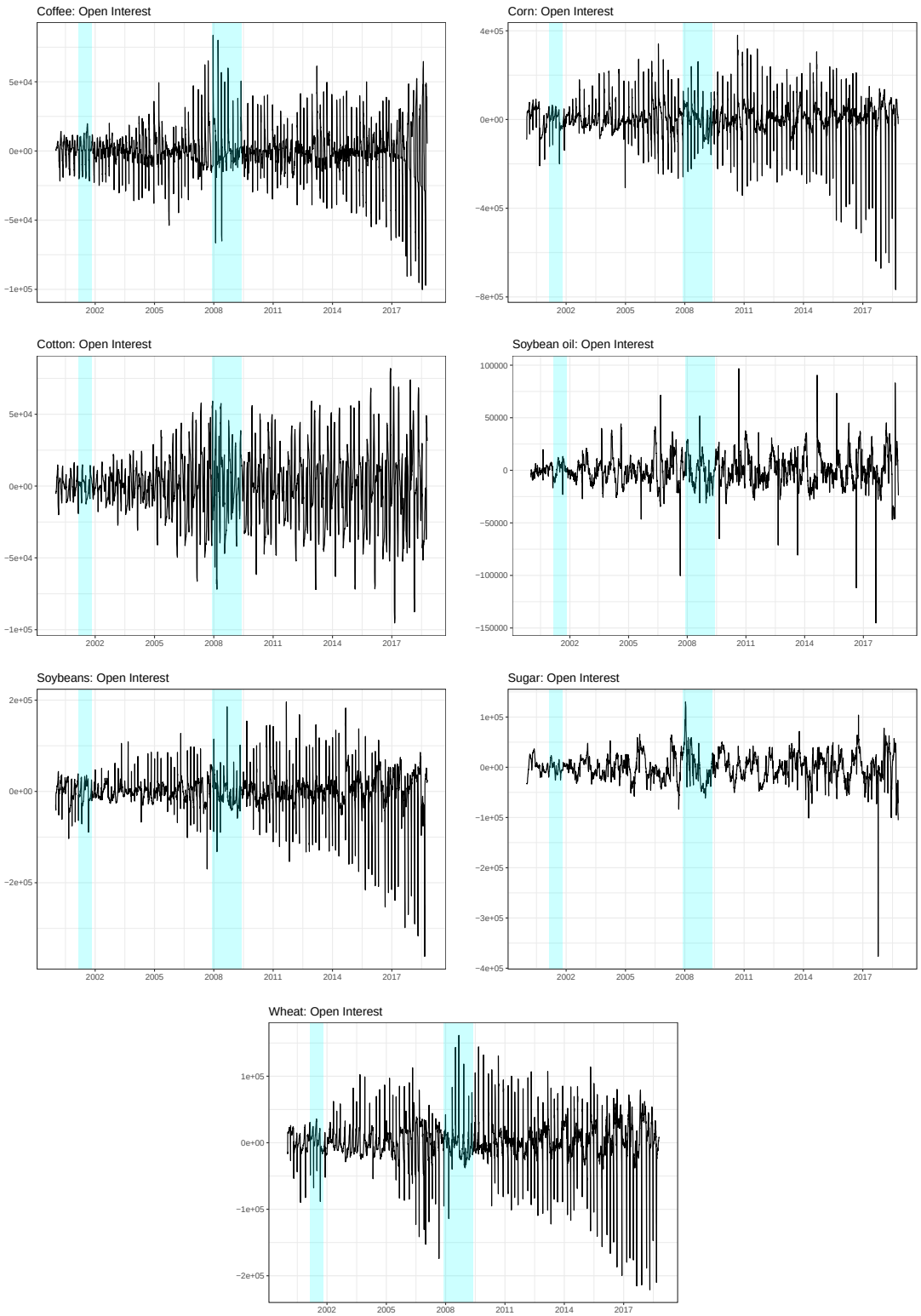

A.3 Estimated GARCH models

Table A.1: **GARCH models for coffee**

	GARCH					EGARCH					AP-GARCH					GJR-GARCH				
	$N(0,1)$	t_ν	$sN(0,1)_\kappa$	$st_{\nu,\kappa}$	GED_ν	$N(0,1)$	t_ν	$sN(0,1)_\kappa$	$st_{\nu,\kappa}$	GED_ν	$N(0,1)$	t_ν	$sN(0,1)_\kappa$	$st_{\nu,\kappa}$	GED_ν	$N(0,1)$	t_ν	$sN(0,1)_\kappa$	$st_{\nu,\kappa}$	GED_ν
ω	0.1305	0.0663	0.0861	0.1261	0.0656	**0.0258**	0.0325	0.0651	0.1319	0.0665	0.0871	0.1281	0.0661	0.0260	0.0328	0.0657	0.0812	0.0318	0.0456	0.0808
p-value	0.0500	0.0000	0.0456	0.0496	0.0190	**0.0000**	0.0003	0.0241	0.0472	0.0000	0.0454	0.0455	0.0165	0.0000	0.0004	0.0200	0.0033	0.0000	0.1976	0.0040
α	0.1004	0.0336	0.1056	0.1183	0.0813	**0.0237**	0.0881	0.0985	0.1010	0.0343	0.1061	0.1201	0.0815	0.0239	0.0883	0.0990	0.0836	0.0269	0.0928	0.1013
p-value	0.0003	0.0040	0.0000	0.0002	0.0000	**0.0036**	0.0000	0.0000	0.0002	0.0028	0.0000	0.0002	0.0000	0.0033	0.0000	0.0000	0.0000	0.0017	0.0028	0.0000
β	0.8808	0.9655	0.8905	0.8850	0.9130	**0.9828**	0.9228	0.9130	0.8799	0.9654	0.8898	0.8838	0.9128	0.9827	0.9225	0.9127	0.9042	0.9780	0.9126	0.9046
p-value	0.0000	0.0000	0.0000	0.0000	0.0000	**0.0000**	0.0000	0.0000	0.0000	0.0000	0.0000	0.0000	0.0000	0.0000	0.0000	0.0000	0.0000	0.0000	0.0000	0.0000
γ		0.2101				**0.1711**				0.2108				0.1715				0.1804		
p-value		0.0000				**0.0000**				0.0000				0.0000				0.0000		
θ			-0.1359				-0.1336				-0.1383				-0.1345				-0.1380	
p-value			0.0043				0.0076				0.0029				0.0071				0.0136	
δ			1.4527				1.1202				1.4600				1.1230				1.2177	
p-value			0.0000				0.0000				0.0000				0.0000				0.0000	
ϕ				-0.0433				-0.0336				-0.0448				-0.0340				-0.0355
p-value				0.0205				0.0101				0.0169				0.0094				0.0058
ν					4.5104	**4.5455**	4.5449	4.5314					4.5077	4.5420	4.5427	4.5287	1.1790	1.1807	1.1826	1.1819
p-value					0.0000	**0.0000**	0.0000	0.0000					0.0000	0.0000	0.0000	0.0000	0.0000	0.0000	0.0000	0.0000
κ									0.9843	0.9838	0.9826	0.9799	0.9842	0.9857	0.9855	0.9830				
p-value									0.0000	0.0000	0.0000	0.0000	0.0000	0.0000	0.0000	0.0000				
SBC	4.3257	4.3231	4.3216	4.3239	4.2163	**4.2090**	4.2105	4.2158	4.3263	4.3237	4.3221	4.3244	4.2169	4.2097	4.2111	4.2165	4.2253	4.2200	4.2211	4.2248
AIC	4.3238	4.3205	4.3183	4.3213	4.2137	**4.2058**	4.2066	4.2126	4.3237	4.3204	4.3182	4.3211	4.2137	4.2058	4.2066	4.2126	4.2227	4.2168	4.2172	4.2216
WLB	4.4529	3.5061	3.4985	3.4933	4.0848	**3.2436**	3.3268	3.2447	4.4671	3.5002	3.4912	3.4928	4.0869	3.2406	3.3226	3.2410	4.1756	3.3141	3.3722	3.3068
p-value	0.0348	0.0611	0.0614	0.0616	0.0433	**0.0717**	0.0682	0.0717	0.0346	0.0614	0.0617	0.0616	0.0432	0.0718	0.0683	0.0718	0.0410	0.0687	0.0663	0.0690
WLB^2	20.1154	25.0485	28.0925	17.8417	32.7187	**44.0251**	60.1128	26.7568	19.7820	24.6904	27.4534	17.3328	32.6241	43.7973	59.6809	26.5869	28.9643	37.0088	47.3885	23.8677
p-value	0.0000	0.0000	0.0000	0.0000	0.0000	**0.0000**	0.0000	0.0000	0.0000	0.0000	0.0000	0.0000	0.0000	0.0000	0.0000	0.0000	0.0000	0.0000	0.0000	0.0000
SB	19.3319	17.7895	18.8252	14.4870	25.4816	**27.1390**	32.4695	18.0107	19.0705	17.4779	18.3716	14.0576	25.4561	27.0127	32.2698	17.8981	24.1601	23.7627	27.1957	17.0978
p-value	0.0002	0.0005	0.0003	0.0023	0.0000	**0.0000**	0.0000	0.0004	0.0003	0.0006	0.0004	0.0028	0.0000	0.0000	0.0000	0.0005	0.0000	0.0000	0.0000	0.0007
$APGof$	570.6369	585.0279	562.4225	567.4884	66.0008	**69.7436**	71.9016	72.9416	543.3829	556.1396	524.1453	536.5199	40.3813	54.8360	51.7512	47.1594	98.1649	116.9781	104.8581	108.0845
p-value	0.0000	0.0000	0.0000	0.0000	0.0044	**0.0018**	0.0010	0.0008	0.0000	0.0000	0.0000	0.0000	0.4091	0.0476	0.0831	0.1734	0.0000	0.0000	0.0000	0.0000

Note: The table reports coefficient estimates and goodness-of-fit statistics using several different GARCH models. We have used four different GARCH specifications: GARCH refers to Eq. (3), EGARCH to Eq. (4), AP-GARCH to Eq. (5) and GJR-GARCH to Eq. (6). For all these models we have considered five different distributional assumptions for ε_t: the standard normal (i.e. $N(0,1)$) and Student's t with shape ν (i.e. t_ν), the skew standard normal with skewness κ (i.e. $sN(0,1)_\kappa$), the skew t with shape ν and skewness κ (i.e. $t_{\nu,\kappa}$), and the generalized error distribution with shape ν (i.e. GED_ν). The upper part of the table provides all parameter estimates together with their p-values using robust standard errors according to White (1982) (see Eq. (3) to (6) for the definition of the parameters). The bottom part of the table reports the Schwarz Bayesian information criterion (SBC), the Akaike information criterion (AIC), the weighted Ljung-Box test statistic (WLB) provided by Fisher and Gallagher (2012) for the null of no serial correlation of order 1 in the standardized residuals and the corresponding p-value, the weighted Ljung-Box test statistic (WLB^2) and p-value using squared standardized residuals, the sign bias test statistic (SB) and p-value for the null of no leverage effects in the standardized residuals (i.e. positive and/or negative effects to shocks) following Engle and Ng (1993), and the adjusted version of Pearson's χ^2 goodness-of-fit test statistic ($APGof$) provided by Palm (1996) and p-value for the null that the empirical distribution of the standardized residuals matches the chosen theoretical density. The best model within each model class associated with the lowest value for the SBC is underlined and the best model across all models is reported in bold.

Table A.2: **GARCH models for corn**

	GARCH					EGARCH					AP-GARCH					GJR-GARCH				
	$N(0,1)$	t_ν	$sN(0,1)_\kappa$	$st_{\nu,\kappa}$	GED_ν	$N(0,1)$	t_ν	$sN(0,1)_\kappa$	$st_{\nu,\kappa}$	GED_ν	$N(0,1)$	t_ν	$sN(0,1)_\kappa$	$st_{\nu,\kappa}$	GED_ν	$N(0,1)$	t_ν	$sN(0,1)_\kappa$	$st_{\nu,\kappa}$	GED_ν
ω	0.0458	0.0315	0.0417	0.0469	0.0173	0.0062	0.0151	0.0187	0.0466	0.0316	0.0413	0.0464	0.0171	0.0062	**0.0150**	0.0186	0.0277	0.0111	0.0233	0.0297
p-value	0.2672	0.0000	0.0433	0.8645	0.1116	0.0000	0.0000	0.0513	0.3249	0.0000	0.0483	0.9138	0.0998	0.0000	**0.0000**	0.0406	0.7918	0.0000	0.0000	0.2835
α	0.0585	-0.0236	0.0880	0.0441	0.0733	-0.0001	0.0881	0.0656	0.0606	-0.0236	0.0888	0.0448	0.0734	-0.0016	**0.0885**	0.0650	0.0664	-0.0099	0.0847	0.0557
p-value	0.1419	0.0883	0.0030	0.8371	0.0008	0.9826	0.0000	0.0000	0.1956	0.0995	0.0035	0.8966	0.0005	0.8110	**0.0000**	0.0000	0.6753	0.1880	0.0000	0.0797
β	0.9253	0.9735	0.9069	0.9197	0.9251	0.9896	0.9249	0.9221	0.9232	0.9736	0.9067	0.9193	0.9250	0.9896	**0.9247**	0.9218	0.9248	0.9840	0.9211	0.9197
p-value	0.0000	0.0000	0.0000	0.0136	0.0000	0.0000	0.0000	0.0000	0.0000	0.0000	0.0000	0.1186	0.0000	0.0000	**0.0000**	0.0000	0.0000	0.0000	0.0000	0.0000
γ		0.1469				0.1560				0.1490				0.1567				0.1485		
p-value		0.0000				0.0000				0.0000				0.0000				0.0000		
θ			0.1478				-0.0071				0.1443				**0.0035**				0.0619	
p-value			0.0993				0.8764				0.1092				**0.9389**				0.2350	
δ			0.8712				0.8819				0.8785				**0.8884**				0.8696	
p-value			0.0000				0.0000				0.0000				**0.0000**				0.0000	
ϕ				0.0432				0.0220				0.0437				0.0239				0.0327
p-value				0.7902				0.1334				0.8620				0.0989				0.2472
ν					4.6640	4.7922	4.8008	4.6816					4.6874	4.8218	**4.8278**	4.7126	1.1727	1.1875	1.1898	1.1769
p-value					0.0000	0.0000	0.0000	0.0000					0.0000	0.0000	**0.0000**	0.0000	0.0000	0.0000	0.0000	0.0000
κ									1.0262	1.0269	1.0258	1.0275	1.0509	1.0530	**1.0518**	**1.0532**				
p-value									0.0000	0.0000	0.0000	0.0000	0.0000	0.0000	**0.0000**	0.0000				
SBC	3.6116	3.5941	3.5923	3.6081	3.4540	3.4410	3.4404	3.4542	3.6118	3.5943	3.5925	3.6082	3.4534	3.4403	**3.4398**	3.4534	3.4840	3.4726	3.4719	3.4834
AIC	3.6097	3.5915	3.5890	3.6055	3.4514	3.4378	3.4365	3.4510	3.6092	3.5910	3.5886	3.6050	3.4501	3.4365	**3.4353**	3.4495	3.4814	3.4694	3.4680	3.4802
WLB	23.7485	24.2121	24.9368	22.5051	27.4057	29.0459	29.8347	26.3697	23.7604	24.2750	25.0041	22.5578	27.4492	28.9802	**29.7594**	26.3070	25.7480	26.9048	27.6808	24.4441
p-value	0.0000	0.0000	0.0000	0.0000	0.0000	0.0000	0.0000	0.0000	0.0000	0.0000	0.0000	0.0000	0.0000	0.0000	**0.0000**	0.0000	0.0000	0.0000	0.0000	0.0000
WLB^2	3.2582	4.5985	4.8036	2.8564	1.8335	3.2585	3.7335	1.5602	3.0435	4.4658	4.6698	2.7641	1.8196	3.2316	**3.6924**	1.5324	2.2384	3.6982	4.2095	1.8471
p-value	0.0711	0.0320	0.0284	0.0910	0.1757	0.0711	0.0533	0.2116	0.0811	0.0346	0.0307	0.0964	0.1774	0.0722	**0.0547**	0.2158	0.1346	0.0545	0.0402	0.1741
SB	10.4295	13.5901	10.4113	12.4726	2.9396	3.5896	2.9198	3.9600	9.6572	13.0429	9.9850	12.0778	2.8961	3.6350	**2.9797**	4.0460	4.9440	6.8807	5.6180	6.4896
p-value	0.0152	0.0035	0.0154	0.0059	0.4010	0.3093	0.4042	0.2658	0.0217	0.0045	0.0187	0.0071	0.4079	0.3037	**0.3948**	0.2565	0.1759	0.0758	0.1318	0.0901
$APGof$	878.6501	802.7057	799.8169	868.6062	380.7904	378.8364	375.2588	381.4651	736.0179	681.3702	680.9626	715.5013	261.2894	247.8155	**250.8870**	257.9719	548.6414	551.1436	554.5384	547.7206
p-value	0.0000	0.0000	0.0000	0.0000	0.0000	0.0000	0.0000	0.0000	0.0000	0.0000	0.0000	0.0000	0.0000	0.0000	**0.0000**	0.0000	0.0000	0.0000	0.0000	0.0000

Note: The table reports coefficient estimates and goodness-of-fit statistics using several different GARCH models. We have used four different GARCH specifications: GARCH refers to Eq. (3), EGARCH to Eq. (4), AP-GARCH to Eq. (5) and GJR-GARCH to Eq. (6). For all these models we have considered five different distributional assumptions for ε_t: the standard normal (i.e. $N(0,1)$) and Student's t with shape ν (i.e. t_ν), the skew standard normal with skewness κ (i.e. $sN(0,1)_\kappa$), the skew t with shape ν and skewness κ (i.e. $t_{\nu,\kappa}$), and the generalized error distribution with shape ν (i.e. GED_ν). The upper part of the table provides all parameter estimates together with their p-values using robust standard errors according to White (1982) (see Eq. (3) to (6) for the definition of the parameters). The bottom part of the table reports the Schwarz Bayesian information criterion (SBC), the Akaike information criterion (AIC), the weighted Ljung-Box test statistic (WLB) provided by Fisher and Gallagher (2012) for the null of no serial correlation of order 1 in the standardized residuals and the corresponding p-value, the weighted Ljung-Box test statistic (WLB^2) and p-value using squared standardized residuals, the sign bias test statistic (SB) and p-value for the null of no leverage effects in the standardized residuals (i.e. positive and/or negative effects to shocks) following Engle and Ng (1993), and the adjusted version of Pearson's χ^2 goodness-of-fit test statistic ($APGof$) provided by Palm (1996) and p-value for the null that the empirical distribution of the standardized residuals matches the chosen theoretical density. The best model within each model class associated with the lowest value for the SBC is underlined and the best model across all models is reported in bold.

Table A.3: **GARCH models for cotton**

	GARCH					EGARCH					AP-GARCH					GJR-GARCH				
	$N(0,1)$	t_ν	$sN(0,1)_\kappa$	$st_{\nu,\kappa}$	GED_ν	$N(0,1)$	t_ν	$sN(0,1)_\kappa$	$st_{\nu,\kappa}$	GED_ν	$N(0,1)$	t_ν	$sN(0,1)_\kappa$	$st_{\nu,\kappa}$	GED_ν	$N(0,1)$	t_ν	$sN(0,1)_\kappa$	$st_{\nu,\kappa}$	GED_ν
ω	0.0155	0.0067	0.0069	0.0137	0.0217	0.0036	**0.0106**	0.0175	0.0162	0.0068	0.0071	0.0143	0.0215	0.0036	0.0105	0.0175	0.0033	0.0063	0.0033	0.0033
p-value	0.0003	0.0000	0.0013	0.0005	0.3100	0.0000	**0.0000**	0.0000	0.0001	0.0000	0.0005	0.0001	0.2713	0.0000	0.0000	0.0000	0.0000	0.0000	0.0000	0.0000
α	0.0391	0.0161	0.0406	0.0430	0.0460	0.0161	**0.0517**	0.0482	0.0394	0.0159	0.0408	0.0432	0.0460	0.0161	0.0517	0.0482	0.0500	0.0182	0.0500	0.0500
p-value	0.0000	0.0092	0.0000	0.0000	0.1426	0.0087	**0.0000**	0.0000	0.0000	0.0088	0.0000	0.0000	0.1103	0.0084	0.0000	0.0000	0.0000	0.0184	0.0000	0.0000
β	0.9563	0.9959	0.9653	0.9590	0.9467	0.9951	**0.9542**	0.9533	0.9557	0.9958	0.9650	0.9585	0.9468	0.9952	0.9543	0.9532	0.9000	0.9930	0.9000	0.9000
p-value	0.0000	0.0000	0.0000	0.0000	0.0000	0.0000	**0.0000**	0.0000	0.0000	0.0000	0.0000	0.0000	0.0000	0.0000	0.0000	0.0000	0.0000	0.0000	0.0000	0.0000
γ		0.0615				0.0657				0.0616				0.0657				0.0655		
p-value		0.0000				0.0000				0.0000				0.0000				0.0000		
θ			-0.1154				**-0.0403**				-0.1118				-0.0387				0.0500	
p-value			0.2660				**0.5252**				0.2613				0.5420				0.0000	
δ			0.8402				**0.8288**				0.8426				0.8286				2.0000	
p-value			0.0000				**0.0000**				0.0000				0.0000				0.0000	
ϕ				-0.0120				-0.0150				-0.0119				-0.0147				0.0500
p-value				0.2802				0.2206				0.2876				0.2322				0.0000
ν					5.4117	5.4792	**5.4961**	5.4024					5.4088	5.4759	5.4923	5.4008	2.0000	1.0997	2.0000	2.0000
p-value					0.0000	0.0000	**0.0000**	0.0000					0.0000	0.0000	0.0000	0.0000	0.0001	0.0000	0.0000	0.0000
κ									0.9772	0.9847	0.9859	0.9777	1.0167	1.0148	1.0181	1.0160				
p-value									0.0000	0.0000	0.0000	0.0000	0.0000	0.0000	0.0000	0.0000				
SBC	3.7323	3.7137	3.7107	3.7327	3.6313	3.6191	**3.6166**	3.6317	3.7327	3.7143	3.7114	3.7331	3.6320	3.6198	3.6172	3.6324	5.2623	3.6589	5.1998	5.5526
AIC	3.7304	3.7111	3.7075	3.7301	3.6287	3.6159	**3.6127**	3.6285	3.7301	3.7111	3.7075	3.7298	3.6287	3.6159	3.6127	3.6285	5.2597	3.6557	5.1960	5.5494
WLB	4.1583	4.9131	5.8808	4.2232	4.3898	4.8250	**5.5653**	4.4194	4.2008	4.9257	5.8816	4.2622	4.3757	4.8196	5.5536	4.4057	3.0929	5.5347	2.9827	2.6825
p-value	0.0414	0.0267	0.0153	0.0399	0.0362	0.0280	**0.0183**	0.0355	0.0404	0.0265	0.0153	0.0390	0.0365	0.0281	0.0184	0.0358	0.0786	0.0186	0.0842	0.1015
WLB^2	0.0013	0.0012	0.0007	0.0013	0.0014	0.0013	**0.0009**	0.0014	0.0013	0.0012	0.0007	0.0013	0.0014	0.0013	0.0009	0.0014	0.0009	0.0014	0.0009	0.0008
p-value	0.9711	0.9723	0.9790	0.9711	0.9698	0.9715	**0.9758**	0.9701	0.9709	0.9722	0.9788	0.9709	0.9699	0.9715	0.9758	0.9701	0.9758	0.9702	0.9764	0.9780
SB	1.8510	1.7227	1.7819	1.8352	1.8918	1.7361	**1.8574**	1.8577	1.8528	1.7228	1.7832	1.8366	1.8917	1.7362	1.8576	1.8586	2.0792	1.7102	2.0793	2.0753
p-value	0.6039	0.6319	0.6189	0.6073	0.5952	0.6289	**0.6025**	0.6025	0.6035	0.6319	0.6186	0.6070	0.5952	0.6289	0.6025	0.6023	0.5561	0.6347	0.5561	0.5569
$APGof$	387.1714	358.9797	359.5375	378.5084	60.2876	39.6363	**43.7595**	61.5867	391.7606	359.3680	364.5997	386.6419	54.0605	41.0907	39.0079	54.4346	2891.2328	214.8512	2873.8716	719.6893
p-value	0.0000	0.0000	0.0000	0.0000	0.0159	0.4415	**0.2765**	0.0120	0.0000	0.0000	0.0000	0.0000	0.0550	0.3791	0.4695	0.0513	0.0000	0.0000	0.0000	0.0000

Note: The table reports coefficient estimates and goodness-of-fit statistics using several different GARCH models. We have used four different GARCH specifications: GARCH refers to Eq. (3), EGARCH to Eq. (4), AP-GARCH to Eq. (5) and GJR-GARCH to Eq. (6). For all these models we have considered five different distributional assumptions for ε_t: the standard normal (i.e. $N(0,1)$) and Student's t with shape ν (i.e. t_ν), the skew standard normal with skewness κ (i.e. $sN(0,1)_\kappa$), the skew t with shape ν and skewness κ (i.e. $t_{\nu,\kappa}$), and the generalized error distribution with shape ν (i.e. GED_ν). The upper part of the table provides all parameter estimates together with their p-values using robust standard errors according to White (1982) (see Eq. (3) to (6) for the definition of the parameters). The bottom part of the table reports the Schwarz Bayesian information criterion (SBC), the Akaike information criterion (AIC), the weighted Ljung-Box test statistic (WLB) provided by Fisher and Gallagher (2012) for the null of no serial correlation of order 1 in the standardized residuals and the corresponding p-value, the weighted Ljung-Box test statistic (WLB^2) and p-value using squared standardized residuals, the sign bias test statistic (SB) and p-value for the null of no leverage effects in the standardized residuals (i.e. positive and/or negative effects to shocks) following Engle and Ng (1993), and the adjusted version of Pearson's χ^2 goodness-of-fit test statistic ($APGof$) provided by Palm (1996) and p-value for the null that the empirical distribution of the standardized residuals matches the chosen theoretical density. The best model within each model class associated with the lowest value for the SBC is underlined and the best model across all models is reported in bold.

Table A.4: **GARCH models for soybean oil**

	GARCH					EGARCH					AP-GARCH					GJR-GARCH				
	$N(0,1)$	t_ν	$sN(0,1)_\kappa$	$st_{\nu,\kappa}$	GED_ν	$N(0,1)$	t_ν	$sN(0,1)_\kappa$	$st_{\nu,\kappa}$	GED_ν	$N(0,1)$	t_ν	$sN(0,1)_\kappa$	$st_{\nu,\kappa}$	GED_ν	$N(0,1)$	t_ν	$sN(0,1)_\kappa$	$st_{\nu,\kappa}$	GED_ν
ω	0.0267	0.0113	0.0236	0.0259	0.0246	0.0074	0.0200	0.0238	0.0243	0.0104	0.0216	0.0237	0.0232	**0.0070**	0.0190	0.0225	0.0256	0.0080	0.0217	0.0249
p-value	0.9668	0.0000	0.0238	0.9493	0.5044	0.0000	0.0001	0.4392	0.7677	0.0000	0.0708	0.7590	0.6278	**0.0000**	0.0002	0.5711	0.3377	0.0000	0.0001	0.3092
α	0.0510	0.0084	0.0553	0.0545	0.0555	0.0123	0.0617	0.0606	0.0500	0.0073	0.0544	0.0529	0.0547	**0.0111**	0.0609	0.0592	0.0532	0.0103	0.0588	0.0574
p-value	0.9409	0.0897	0.0000	0.9006	0.2042	0.0171	0.0000	0.1070	0.5897	0.1365	0.0000	0.5342	0.3504	**0.0312**	0.0000	0.2293	0.0758	0.0370	0.0000	0.0392
β	0.9384	0.9887	0.9398	0.9394	0.9354	0.9902	0.9381	0.9366	0.9403	0.9896	0.9416	0.9413	0.9366	**0.9908**	0.9392	0.9377	0.9368	0.9895	0.9388	0.9379
p-value	0.3158	0.0000	0.0000	0.1161	0.0000	0.0000	0.0000	0.0000	0.0000	0.0000	0.0000	0.0000	0.0000	**0.0000**	0.0000	0.0000	0.0000	0.0000	0.0000	0.0000
γ		0.1087				0.1168				0.1069				**0.1155**				0.1127		
p-value		0.0000				0.0000				0.0000				**0.0000**				0.0000		
θ			-0.0548				-0.0836				-0.0474				-0.0751				-0.0688	
p-value			0.1552				0.0315				0.2299				0.0521				0.0661	
δ			1.6424				1.4433				1.6389				1.4465				1.5255	
p-value			0.0000				0.0000				0.0000				0.0000				0.0000	
ϕ				-0.0088				-0.0125				-0.0074				-0.0110				-0.0105
p-value				0.4147				0.0782				0.3701				0.1127				0.1136
ν					10.5935	10.0857	10.2767	10.5627					10.6924	**10.1745**	10.3614	10.6523	1.6030	1.5929	1.5991	1.6030
p-value					0.0000	0.0000	0.0000	0.0000					0.0000	**0.0000**	0.0000	0.0000	0.0000	0.0000	0.0000	0.0000
κ									1.0673	1.0685	1.0668	1.0663	1.0699	**1.0699**	1.0690	1.0687				
p-value									0.0000	0.0000	0.0000	0.0000	0.0000	**0.0000**	0.0000	0.0000				
SBC	3.6455	3.6468	3.6463	3.6461	3.6297	3.6294	3.6296	3.6301	3.6439	3.6451	3.6447	3.6445	3.6283	**3.6280**	3.6282	3.6288	3.6334	3.6337	3.6338	3.6339
AIC	3.6436	3.6442	3.6430	3.6435	3.6271	3.6261	3.6257	3.6269	3.6413	3.6419	3.6408	3.6413	3.6250	**3.6241**	3.6237	3.6249	3.6308	3.6305	3.6299	3.6307
WLB	17.8888	17.2123	17.6333	17.9052	18.0904	17.3287	17.7145	18.1242	17.8174	17.1005	17.5487	17.8257	18.0427	**17.2555**	17.6568	18.0672	17.9902	17.2628	17.6600	18.0129
p-value	0.0000	0.0000	0.0000	0.0000	0.0000	0.0000	0.0000	0.0000	0.0000	0.0000	0.0000	0.0000	0.0000	**0.0000**	0.0000	0.0000	0.0000	0.0000	0.0000	0.0000
WLB^2	0.5347	0.0009	0.3104	0.5672	1.1990	0.0852	0.4585	1.2690	0.4457	0.0129	0.2299	0.4677	1.0925	**0.0526**	0.3882	1.1494	0.8574	0.0207	0.3928	0.9040
p-value	0.4646	0.9762	0.5774	0.4514	0.2735	0.7704	0.4983	0.2599	0.5044	0.9095	0.6316	0.4940	0.2959	**0.8187**	0.5332	0.2837	0.3545	0.8856	0.5308	0.3417
SB	1.7158	1.5538	1.4540	1.4456	1.9899	2.0500	2.1382	1.6117	1.7145	1.6174	1.4901	1.4527	2.0059	**2.1045**	2.1479	1.6235	1.7334	1.6086	1.6437	1.4042
p-value	0.6334	0.6699	0.6929	0.6949	0.5745	0.5621	0.5442	0.6567	0.6337	0.6554	0.6846	0.6932	0.5712	**0.5510**	0.5423	0.6541	0.6295	0.6574	0.6495	0.7045
$APGof$	187.7055	182.2530	187.4803	186.3406	124.2880	137.6342	128.4741	123.0146	100.9233	101.6269	102.1193	98.1584	20.9022	**30.1257**	25.5386	22.1123	148.9050	158.9868	155.8420	152.2398
p-value	0.0000	0.0000	0.0000	0.0000	0.0000	0.0000	0.0000	0.0000	0.0000	0.0000	0.0000	0.0000	0.9922	**0.8452**	0.9524	0.9865	0.0000	0.0000	0.0000	0.0000

Note: The table reports coefficient estimates and goodness-of-fit statistics using several different GARCH models. We have used four different GARCH specifications: GARCH refers to Eq. (3), EGARCH to Eq. (4), AP-GARCH to Eq. (5) and GJR-GARCH to Eq. (6). For all these models we have considered five different distributional assumptions for ε_t: the standard normal (i.e. $N(0,1)$) and Student's t with shape ν (i.e. t_ν), the skew standard normal with skewness κ (i.e. $sN(0,1)_\kappa$), the skew t with shape ν and skewness κ (i.e. $t_{\nu,\kappa}$), and the generalized error distribution with shape ν (i.e. GED_ν). The upper part of the table provides all parameter estimates together with their p-values using robust standard errors according to White (1982) (see Eq. (3) to (6) for the definition of the parameters). The bottom part of the table reports the Schwarz Bayesian information criterion (SBC), the Akaike information criterion (AIC), the weighted Ljung-Box test statistic (WLB) provided by Fisher and Gallagher (2012) for the null of no serial correlation of order 1 in the standardized residuals and the corresponding p-value, the weighted Ljung-Box test statistic (WLB^2) and p-value using squared standardized residuals, the sign bias test statistic (SB) and p-value for the null of no leverage effects in the standardized residuals (i.e. positive and/or negative effects to shocks) following Engle and Ng (1993), and the adjusted version of Pearson's χ^2 goodness-of-fit test statistic ($APGof$) provided by Palm (1996) and p-value for the null that the empirical distribution of the standardized residuals matches the chosen theoretical density. The best model within each model class associated with the lowest value for the SBC is underlined and the best model across all models is reported in bold.

Table A.5: **GARCH models for soybeans**

	GARCH					EGARCH					AP-GARCH					GJR-GARCH				
	$N(0,1)$	t_ν	$sN(0,1)_\kappa$	$st_{\nu,\kappa}$	GED_ν	$N(0,1)$	t_ν	$sN(0,1)_\kappa$	$st_{\nu,\kappa}$	GED_ν	$N(0,1)$	t_ν	$sN(0,1)_\kappa$	$st_{\nu,\kappa}$	GED_ν	$N(0,1)$	t_ν	$sN(0,1)_\kappa$	$st_{\nu,\kappa}$	GED_ν
ω	0.0247	0.0147	0.0204	0.0215	0.0197	**0.0056**	0.0142	0.0149	0.0258	0.0152	0.0214	0.0226	0.0202	0.0059	0.0147	0.0154	0.0221	0.0071	0.0171	0.0180
p-value	0.0006	0.0000	0.2600	0.0013	0.0038	**0.0000**	0.0027	0.0587	0.0004	0.0000	0.3289	0.0013	0.0038	0.0000	0.0017	0.0620	0.0041	0.0000	0.0100	0.0343
α	0.0648	0.0225	0.0758	0.0783	0.0677	**0.0293**	0.0761	0.0841	0.0647	0.0236	0.0759	0.0789	0.0679	0.0302	0.0763	0.0848	0.0657	0.0260	0.0759	0.0810
p-value	0.0000	0.0009	0.0058	0.0000	0.0000	**0.0000**	0.0000	0.0000	0.0000	0.0004	0.0207	0.0000	0.0000	0.0000	0.0000	0.0000	0.0000	0.0000	0.0000	0.0000
β	0.9261	0.9858	0.9277	0.9297	0.9260	**0.9901**	0.9319	0.9335	0.9256	0.9851	0.9270	0.9292	0.9256	0.9898	0.9314	0.9331	0.9262	0.9881	0.9298	0.9317
p-value	0.0000	0.0000	0.0000	0.0000	0.0000	**0.0000**	0.0000	0.0000	0.0000	0.0000	0.0000	0.0000	0.0000	0.0000	0.0000	0.0000	0.0000	0.0000	0.0000	0.0000
γ		0.1471				**0.1449**				0.1469				0.1452				0.1453		
p-value		0.0000				**0.0000**				0.0000				0.0000				0.0000		
θ			-0.1430				-0.1952				-0.1516				-0.2011				-0.1717	
p-value			0.0941				0.0001				0.1190				0.0000				0.0006	
δ			1.3032				1.1936				1.2781				1.1843				1.2261	
p-value			0.0104				0.0000				0.0263				0.0000				0.0000	
ϕ				-0.0306				-0.0430				-0.0320				-0.0440				-0.0371
p-value				0.0009				0.0000				0.0004				0.0000				0.0000
ν					7.0960	**7.1430**	7.1019	7.1496					7.0529	7.1051	7.0602	7.1009	1.4210	1.4269	1.4246	1.4231
p-value					0.0000	**0.0000**	0.0000	0.0000					0.0000	0.0000	0.0000	0.0000	0.0000	0.0000	0.0000	0.0000
κ									0.9677	0.9583	0.9591	0.9633	0.9703	0.9641	0.9640	0.9659				
p-value									0.0000	0.0000	0.0000	0.0000	0.0000	0.0000	0.0000	0.0000				
SBC	3.5158	3.5098	3.5118	3.5141	3.4695	**3.4626**	3.4639	3.4668	3.5159	3.5094	3.5114	3.5139	3.4698	3.4627	3.4640	3.4669	3.4790	3.4734	3.4749	3.4772
AIC	3.5139	3.5073	3.5086	3.5115	3.4669	**3.4594**	3.4600	3.4635	3.5133	3.5062	3.5076	3.5107	3.4666	3.4589	3.4595	3.4631	3.4765	3.4702	3.4710	3.4739
WLB	1.6530	1.7725	1.7424	1.7392	1.6577	**1.7496**	1.7657	1.7917	1.6557	1.7920	1.7558	1.7453	1.6589	1.7637	1.7760	1.7967	1.6523	1.7578	1.7531	1.7630
p-value	0.1986	0.1831	0.1868	0.1872	0.1979	**0.1859**	0.1839	0.1807	0.1982	0.1807	0.1851	0.1865	0.1977	0.1842	0.1826	0.1801	0.1986	0.1849	0.1855	0.1843
WLB^2	1.7028	1.3768	1.0915	1.4076	2.2359	**1.0940**	0.6966	1.1672	1.6862	1.3408	1.0228	1.3635	2.2477	1.0993	0.6787	1.1604	1.9444	1.2341	0.8669	1.2869
p-value	0.1919	0.2406	0.2961	0.2355	0.1348	**0.2956**	0.4039	0.2800	0.1941	0.2469	0.3119	0.2429	0.1338	0.2944	0.4100	0.2814	0.1632	0.2666	0.3518	0.2566
SB	1.7496	5.4057	5.4671	5.0942	2.1681	**6.8710**	7.1521	6.7279	1.7569	5.6240	5.7086	5.3581	2.1361	7.0164	7.3159	6.8755	1.8467	6.1034	6.3348	5.9466
p-value	0.6260	0.1444	0.1406	0.1650	0.5383	**0.0761**	0.0672	0.0811	0.6244	0.1314	0.1267	0.1474	0.5447	0.0714	0.0625	0.0760	0.6048	0.1067	0.0964	0.1142
$APGof$	258.4997	255.7573	249.2670	242.9385	100.3561	**103.5555**	97.2551	112.4014	197.7526	183.0141	184.2868	190.2427	43.6733	31.6139	36.1071	47.1892	154.4160	163.9440	156.5466	155.5552
p-value	0.0000	0.0000	0.0000	0.0000	0.0000	**0.0000**	0.0000	0.0000	0.0000	0.0000	0.0000	0.0000	0.2795	0.7936	0.6026	0.1727	0.0000	0.0000	0.0000	0.0000

Note: The table reports coefficient estimates and goodness-of-fit statistics using several different GARCH models. We have used four different GARCH specifications: GARCH refers to Eq. (3), EGARCH to Eq. (4), AP-GARCH to Eq. (5) and GJR-GARCH to Eq. (6). For all these models we have considered five different distributional assumptions for ε_t: the standard normal (i.e. $N(0,1)$) and Student's t with shape ν (i.e. t_ν), the skew standard normal with skewness κ (i.e. $sN(0,1)_\kappa$), the skew t with shape ν and skewness κ (i.e. $t_{\nu,\kappa}$), and the generalized error distribution with shape ν (i.e. GED_ν). The upper part of the table provides all parameter estimates together with their p-values using robust standard errors according to White (1982) (see Eq. (3) to (6) for the definition of the parameters). The bottom part of the table reports the Schwarz Bayesian information criterion (SBC), the Akaike information criterion (AIC), the weighted Ljung-Box test statistic (WLB) provided by Fisher and Gallagher (2012) for the null of no serial correlation of order 1 in the standardized residuals and the corresponding p-value, the weighted Ljung-Box test statistic (WLB^2) and p-value using squared standardized residuals, the sign bias test statistic (SB) and p-value for the null of no leverage effects in the standardized residuals (i.e. positive and/or negative effects to shocks) following Engle and Ng (1993), and the adjusted version of Pearson's χ^2 goodness-of-fit test statistic ($APGof$) provided by Palm (1996) and p-value for the null that the empirical distribution of the standardized residuals matches the chosen theoretical density. The best model within each model class associated with the lowest value for the SBC is underlined and the best model across all models is reported in bold.

Table A.6: **GARCH models for sugar**

	GARCH					EGARCH					AP-GARCH					GJR-GARCH				
	$N(0,1)$	t_ν	$sN(0,1)_\kappa$	$st_{\nu,\kappa}$	GED_ν	$N(0,1)$	t_ν	$sN(0,1)_\kappa$	$st_{\nu,\kappa}$	GED_ν	$N(0,1)$	t_ν	$sN(0,1)_\kappa$	$st_{\nu,\kappa}$	GED_ν	$N(0,1)$	t_ν	$sN(0,1)_\kappa$	$st_{\nu,\kappa}$	GED_ν
ω	0.0259	0.0187	0.0189	0.0271	0.0132	**0.0075**	0.0104	0.0135	0.0256	0.0186	0.0187	0.0268	0.0132	0.0075	0.0103	0.0136	0.0172	0.0095	0.0129	0.0176
p-value	0.0001	0.0000	0.0000	0.0000	0.0004	**0.0000**	0.0000	0.0003	0.0001	0.0000	0.0000	0.0000	0.0004	0.0000	0.0000	0.0003	0.0001	0.0000	0.0000	0.0000
α	0.0354	-0.0080	0.0472	0.0312	0.0355	**-0.0010**	0.0464	0.0344	0.0352	-0.0079	0.0471	0.0310	0.0355	-0.0013	0.0464	0.0342	0.0352	-0.0033	0.0468	0.0330
p-value	0.0000	0.1435	0.0000	0.0000	0.0000	**0.8234**	0.0000	0.0000	0.0000	0.1417	0.0000	0.0000	0.0000	0.7744	0.0000	0.0000	0.0000	0.4681	0.0000	0.0000
β	0.9610	0.9914	0.9568	0.9598	0.9633	**0.9952**	0.9608	0.9630	0.9612	0.9914	0.9570	0.9599	0.9634	0.9952	0.9609	0.9629	0.9625	0.9940	0.9593	0.9619
p-value	0.0000	0.0000	0.0000	0.0000	0.0000	**0.0000**	0.0000	0.0000	0.0000	0.0000	0.0000	0.0000	0.0000	0.0000	0.0000	0.0000	0.0000	0.0000	0.0000	0.0000
γ		0.0909				**0.0889**				0.0907				0.0889				0.0897		
p-value		0.0000				**0.0000**				0.0000				0.0000				0.0000		
θ			0.0833				0.0051				0.0824				0.0084				0.0320	
p-value			0.1674				0.9213				0.1678				0.8715				0.5458	
δ			1.0565				0.9855				1.0553				0.9856				0.9963	
p-value			0.0000				0.0000				0.0000				0.0000				0.0000	
ϕ				0.0108				0.0027				0.0109				0.0033				0.0057
p-value				0.1030				0.6300				0.0976				0.5711				0.3224
ν					5.7009	**5.6715**	5.6483	5.7011					5.6962	5.6698	5.6459	5.7082	1.2965	1.3037	1.3024	1.2974
p-value					0.0000	**0.0000**	0.0000	0.0000					0.0000	0.0000	0.0000	0.0000	0.0000	0.0000	0.0000	0.0000
κ									1.0254	1.0270	1.0269	1.0260	1.0147	1.0156	1.0157	1.0151				
p-value									0.0000	0.0000	0.0000	0.0000	0.0000	0.0000	0.0000	0.0000				
SBC	4.4521	4.4442	4.4455	4.4522	4.3729	**4.3665**	4.3674	4.3737	4.4524	4.4444	4.4458	4.4525	4.3736	4.3672	4.3681	4.3744	4.3867	4.3808	4.3818	4.3873
AIC	4.4502	4.4416	4.4423	4.4496	4.3703	**4.3632**	4.3635	4.3705	4.4498	4.4412	4.4419	4.4493	4.3704	4.3633	4.3636	4.3705	4.3841	4.3776	4.3779	4.3841
WLB	2.0201	1.4487	1.4133	2.2333	2.0862	**1.3655**	1.2824	2.1401	2.0157	1.4447	1.4074	2.2319	2.0850	1.3685	1.2848	2.1517	2.0697	1.4021	1.3251	2.1833
p-value	0.1552	0.2287	0.2345	0.1351	0.1486	**0.2426**	0.2575	0.1435	0.1557	0.2294	0.2355	0.1352	0.1488	0.2421	0.2570	0.1424	0.1503	0.2364	0.2497	0.1395
WLB^2	1.7058	3.2316	3.1876	1.8460	1.5522	**2.9799**	3.1106	1.5721	1.7282	3.2499	3.2111	1.8761	1.5572	2.9989	3.1321	1.5721	1.5776	2.9648	3.0818	1.6332
p-value	0.1915	0.0722	0.0742	0.1743	0.2128	**0.0843**	0.0778	0.2099	0.1886	0.0714	0.0731	0.1708	0.2121	0.0833	0.0768	0.2099	0.2091	0.0851	0.0792	0.2013
SB	6.1219	4.6758	4.0385	5.3880	3.7216	**2.6952**	2.3635	3.5427	6.1409	4.6932	4.0625	5.4000	3.7315	2.6730	2.3417	3.5044	4.4267	3.1575	2.7219	4.0187
p-value	0.1058	0.1971	0.2573	0.1455	0.2931	**0.4410**	0.5005	0.3153	0.1050	0.1957	0.2548	0.1447	0.2920	0.4448	0.5046	0.3202	0.2189	0.3680	0.4365	0.2595
$APGof$	413.7141	412.1571	424.5350	411.9377	171.2654	**175.6532**	173.9759	169.8358	314.0750	317.9250	323.9901	317.2031	96.2123	96.5662	104.8040	98.6610	237.6277	247.2243	244.3298	233.1125
p-value	0.0000	0.0000	0.0000	0.0000	0.0000	**0.0000**	0.0000	0.0000	0.0000	0.0000	0.0000	0.0000	0.0000	0.0000	0.0000	0.0000	0.0000	0.0000	0.0000	0.0000

Note: The table reports coefficient estimates and goodness-of-fit statistics using several different GARCH models. We have used four different GARCH specifications: GARCH refers to Eq. (3), EGARCH to Eq. (4), AP-GARCH to Eq. (5) and GJR-GARCH to Eq. (6). For all these models we have considered five different distributional assumptions for ε_t: the standard normal (i.e. $N(0,1)$) and Student's t with shape ν (i.e. t_ν), the skew standard normal with skewness κ (i.e. $sN(0,1)_\kappa$), the skew t with shape ν and skewness κ (i.e. $t_{\nu,\kappa}$), and the generalized error distribution with shape ν (i.e. GED_ν). The upper part of the table provides all parameter estimates together with their p-values using robust standard errors according to White (1982) (see Eq. (3) to (6) for the definition of the parameters). The bottom part of the table reports the Schwarz Bayesian information criterion (SBC), the Akaike information criterion (AIC), the weighted Ljung-Box test statistic (WLB) provided by Fisher and Gallagher (2012) for the null of no serial correlation of order 1 in the standardized residuals and the corresponding p-value, the weighted Ljung-Box test statistic (WLB^2) and p-value using squared standardized residuals, the sign bias test statistic (SB) and p-value for the null of no leverage effects in the standardized residuals (i.e. positive and/or negative effects to shocks) following Engle and Ng (1993), and the adjusted version of Pearson's χ^2 goodness-of-fit test statistic ($APGof$) provided by Palm (1996) and p-value for the null that the empirical distribution of the standardized residuals matches the chosen theoretical density. The best model within each model class associated with the lowest value for the SBC is underlined and the best model across all models is reported in bold.

Table A.7: **GARCH models for wheat**

	GARCH					EGARCH					AP-GARCH					GJR-GARCH				
	$N(0,1)$	t_ν	$sN(0,1)_\kappa$	$st_{\nu,\kappa}$	GED_ν	$N(0,1)$	t_ν	$sN(0,1)_\kappa$	$st_{\nu,\kappa}$	GED_ν	$N(0,1)$	t_ν	$sN(0,1)_\kappa$	$st_{\nu,\kappa}$	GED_ν	$N(0,1)$	t_ν	$sN(0,1)_\kappa$	$st_{\nu,\kappa}$	GED_ν
ω	0.0395	0.0222	0.0271	0.0397	0.0187	0.0061	0.0124	0.0175	0.0399	0.0227	0.0277	0.0401	0.0184	**0.0061**	0.0123	0.0171	0.0263	0.0102	0.0179	0.0255
p-value	0.0012	0.0000	0.0000	0.0036	0.0000	0.0000	0.0000	0.0000	0.0015	0.0000	0.0000	0.0033	0.0000	**0.0000**	0.0000	0.0000	0.0000	0.0000	0.0000	0.0000
α	0.0371	0.0080	0.0573	0.0366	0.0379	0.0128	0.0542	0.0403	0.0369	0.0092	0.0572	0.0364	0.0373	**0.0121**	0.0536	0.0395	0.0367	0.0103	0.0552	0.0380
p-value	0.0000	0.3094	0.0000	0.0001	0.0000	0.0281	0.0000	0.0000	0.0000	0.2360	0.0000	0.0001	0.0000	**0.0359**	0.0000	0.0000	0.0000	0.1065	0.0000	0.0000
β	0.9505	0.9835	0.9397	0.9502	0.9565	0.9932	0.9512	0.9593	0.9505	0.9830	0.9394	0.9502	0.9571	**0.9933**	0.9518	0.9599	0.9549	0.9896	0.9469	0.9563
p-value	0.0000	0.0000	0.0000	0.0000	0.0000	0.0000	0.0000	0.0000	0.0000	0.0000	0.0000	0.0000	0.0000	**0.0000**	0.0000	0.0000	0.0000	0.0000	0.0000	0.0000
γ		0.1055				0.0952				0.1057				**0.0941**				0.0987		
p-value		0.0000				0.0000				0.0000				**0.0000**				0.0000		
θ			-0.1158				-0.1510				-0.1329				-0.1431				-0.1305	
p-value			0.2011				0.0194				0.1422				0.0266				0.0722	
δ			0.8420				0.8746				0.8415				0.8829				0.8509	
p-value			0.0000				0.0000				0.0000				0.0000				0.0000	
ϕ				0.0016				-0.0104				0.0016				-0.0098				-0.0054
p-value				0.8625				0.2392				0.8627				0.2584				0.5432
ν					6.1233	6.2966	6.3065	6.1150					6.2161	**6.3850**	6.3944	6.2086	1.3446	1.3561	1.3576	1.3440
p-value					0.0000	0.0000	0.0000	0.0000					0.0000	**0.0000**	0.0000	0.0000	0.0000	0.0000	0.0000	0.0000
κ									1.0633	1.0588	1.0609	1.0633	1.0756	**1.0746**	1.0739	1.0752				
p-value									0.0000	0.0000	0.0000	0.0000	0.0000	**0.0000**	0.0000	0.0000				
SBC	3.8889	3.8784	3.8784	3.8897	3.8058	3.7952	3.7958	3.8063	3.8869	3.8767	3.8765	3.8877	3.8039	**3.7935**	3.7941	3.8044	3.8281	3.8191	3.8195	3.8288
AIC	3.8870	3.8758	3.8752	3.8872	3.8032	3.7920	3.7920	3.8030	3.8843	3.8735	3.8727	3.8844	3.8007	**3.7896**	3.7896	3.8006	3.8255	3.8158	3.8156	3.8256
WLB	8.6068	8.6318	8.4834	8.6514	9.9387	10.1670	9.9231	9.6696	8.5755	8.5382	8.3739	8.6210	9.9393	**10.1866**	9.9371	9.6873	9.3536	9.4861	9.3001	9.2119
p-value	0.0033	0.0033	0.0036	0.0033	0.0016	0.0014	0.0016	0.0019	0.0034	0.0035	0.0038	0.0033	0.0016	**0.0014**	0.0016	0.0019	0.0022	0.0021	0.0023	0.0024
WLB^2	2.2003	1.6229	2.0096	2.1778	1.3065	1.8915	2.0574	1.5839	2.2434	1.5960	2.0081	2.2308	1.3850	**1.9779**	2.1291	1.6698	1.7454	1.7915	2.0727	1.8733
p-value	0.1380	0.2027	0.1563	0.1400	0.2530	0.1690	0.1515	0.2082	0.1342	0.2065	0.1565	0.1353	0.2393	**0.1596**	0.1445	0.1963	0.1865	0.1807	0.1500	0.1711
SB	20.2287	13.4518	11.9793	20.6182	14.7731	9.8818	9.1994	12.7630	20.4265	13.1396	11.5969	20.8402	14.9856	**10.1941**	9.5323	13.1046	17.2356	11.5145	10.5107	16.1036
p-value	0.0002	0.0038	0.0075	0.0001	0.0020	0.0196	0.0268	0.0052	0.0001	0.0043	0.0089	0.0001	0.0018	**0.0170**	0.0230	0.0044	0.0006	0.0092	0.0147	0.0011
$APGof$	358.3390	330.0408	326.1449	359.4923	170.5893	169.2602	170.2447	170.1885	246.2082	237.8959	230.0127	244.7736	72.7975	**63.4374**	66.4473	72.8397	267.4599	283.1350	287.0309	268.8664
p-value	0.0000	0.0000	0.0000	0.0000	0.0000	0.0000	0.0000	0.0000	0.0000	0.0000	0.0000	0.0000	0.0008	**0.0080**	0.0040	0.0008	0.0000	0.0000	0.0000	0.0000

Note: The table reports coefficient estimates and goodness-of-fit statistics using several different GARCH models. We have used four different GARCH specifications: GARCH refers to Eq. (3), EGARCH to Eq. (4), AP-GARCH to Eq. (5) and GJR-GARCH to Eq. (6). For all these models we have considered five different distributional assumptions for ε_t: the standard normal (i.e. $N(0,1)$) and Student's t with shape ν (i.e. t_ν), the skew standard normal with skewness κ (i.e. $sN(0,1)_\kappa$), the skew t with shape ν and skewness κ (i.e. $t_{\nu,\kappa}$), and the generalized error distribution with shape ν (i.e. GED_ν). The upper part of the table provides all parameter estimates together with their p-values using robust standard errors according to White (1982) (see Eq. (3) to (6) for the definition of the parameters). The bottom part of the table reports the Schwarz Bayesian information criterion (SBC), the Akaike information criterion (AIC), the weighted Ljung-Box test statistic (WLB) provided by Fisher and Gallagher (2012) for the null of no serial correlation of order 1 in the standardized residuals and the corresponding p-value, the weighted Ljung-Box test statistic (WLB^2) and p-value using squared standardized residuals, the sign bias test statistic (SB) and p-value for the null of no leverage effects in the standardized residuals (i.e. positive and/or negative effects to shocks) following Engle and Ng (1993), and the adjusted version of Pearson's χ^2 goodness-of-fit test statistic ($APGof$) provided by Palm (1996) and p-value for the null that the empirical distribution of the standardized residuals matches the chosen theoretical density. The best model within each model class associated with the lowest value for the SBC is underlined and the best model across all models is reported in bold.

A.4 Granger causality testing with forward expanding window

Figure A.3: **Time-varying Granger causality between agricultural futures volatility, trading volume and open interest**

The plots show the p-values for a forward expanding window version of the Granger causality test between the volatility of the returns of seven agricultural futures markets, their trading volume and their previous day open interest for a sample period running from January 3, 2000 to October 17, 2018. The test is applied with a forward expanding window starting with a sample period including the first 80 days (i.e. January 3, 2000 to April 26, 2000) and adding the next day in each step. The cyan areas highlight the US recession periods according to the classification of the National Bureau of Economic Research. The vertical axis covers values from 0 to 1 and the red dashed line represents the 10% significance level.

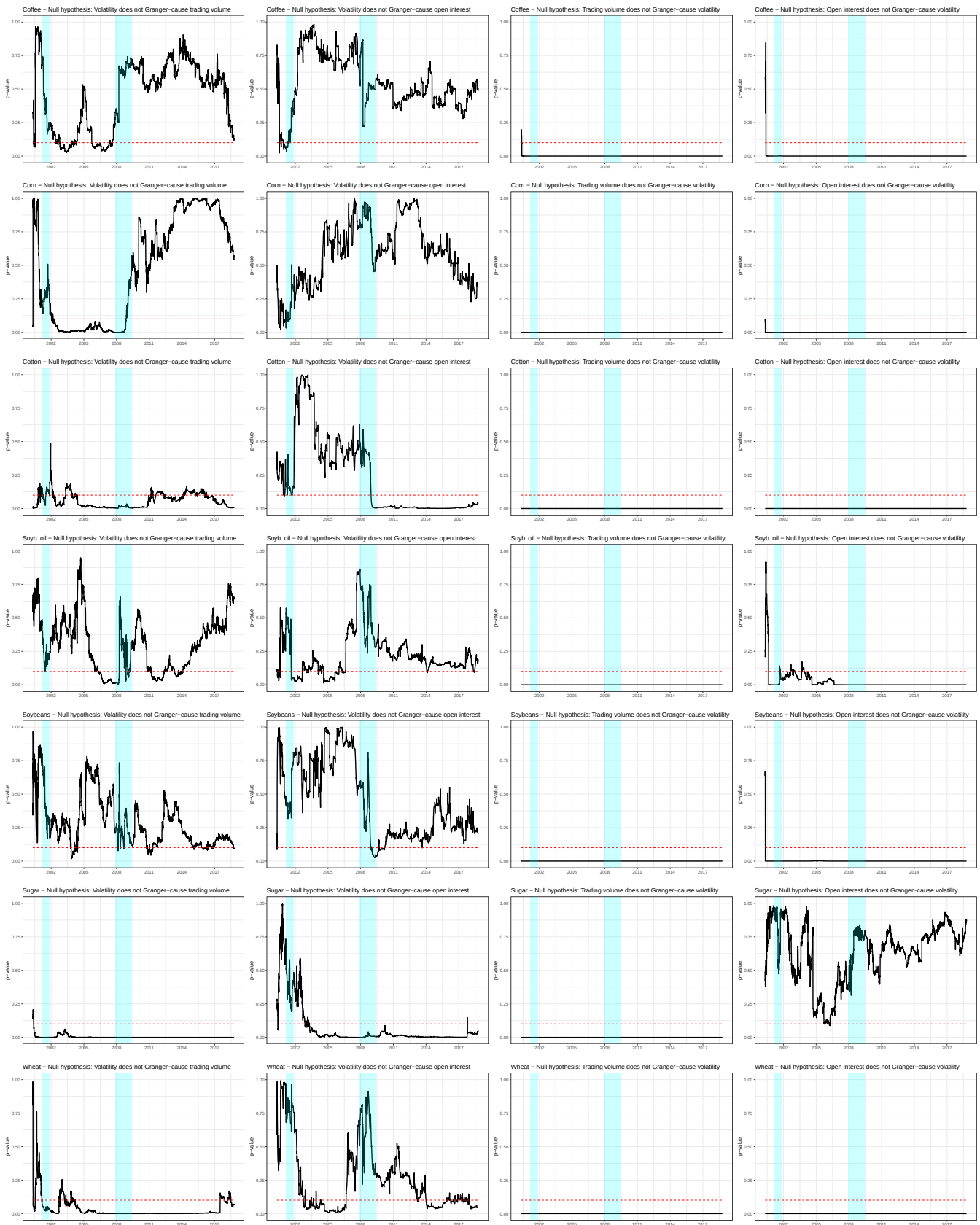

Figure A.4: **Time-varying autocorrelation functions for coffee**

The plots show the autocorrelation functions (ACF) of the Markov chains drawn for all parameters of the VAR model (3 equations x 3 variables x 2 lags + 3 intercepts = 21 coefficients; the ACFs for chains of the elements of the lower triangular matrix and the variances of the error terms are not shown to save space but these look very similar) for all time points in the sample period running from May 1, 2000 (the first 80 days starting from January 3, 2000 have been used as a training sample to initialize the coefficient priors) to October 17, 2018. The order of appearance is as follows: the first row starts with the intercept of the first equation (for open interest) followed by both lags of open interest, both lags of trading volume and both lags of volatility. Then all coefficients are provided for the second (trading volume) and third equation (volatility). The value of the ACF is provided on the vertical axis for the range from -1 to +1 and the ACF for lag 1 is shown as a black line, for lag 5 as a red line, for lag 10 as an orange line and for lag 20 as a yellow line. The cyan areas highlight the US recession periods according to the classification of the National Bureau of Economic Research.

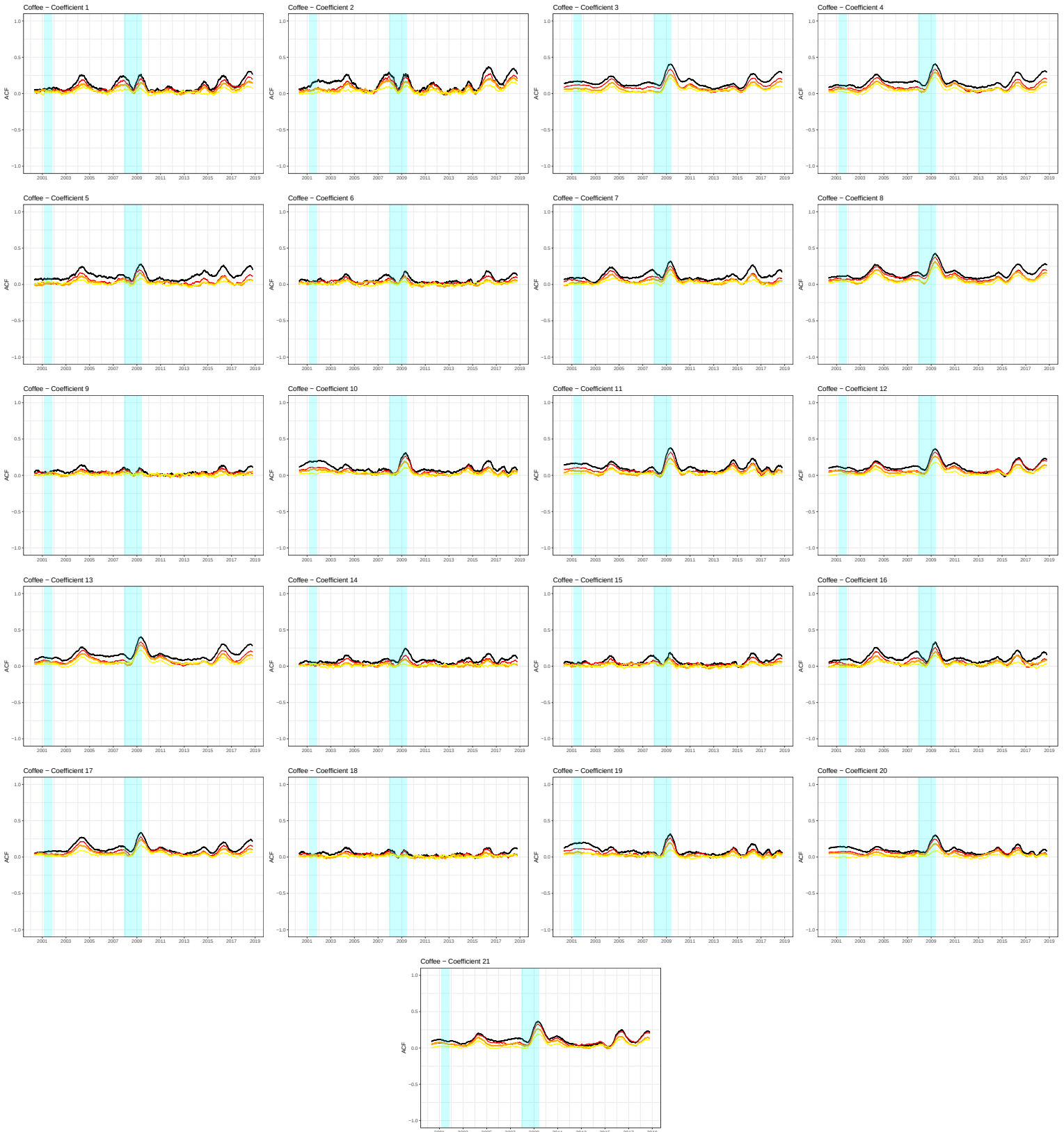

Figure A.5: **Time-varying autocorrelation functions for corn**

The plots show the autocorrelation functions (ACF) of the Markov chains drawn for all parameters of the VAR model (3 equations x 3 variables x 2 lags + 3 intercepts = 21 coefficients; the ACFs for chains of the elements of the lower triangular matrix and the variances of the error terms are not shown to save space but these look very similar) for all time points in the sample period running from May 1, 2000 (the first 80 days starting from January 3, 2000 have been used as a training sample to initialize the coefficient priors) to October 17, 2018. The order of appearance is as follows: the first row starts with the intercept of the first equation (for open interest) followed by both lags of open interest, both lags of trading volume and both lags of volatility. Then all coefficients are provided for the second (trading volume) and third equation (volatility). The value of the ACF is provided on the vertical axis for the range from -1 to +1 and the ACF for lag 1 is shown as a black line, for lag 5 as a red line, for lag 10 as an orange line and for lag 20 as a yellow line. The cyan areas highlight the US recession periods according to the classification of the National Bureau of Economic Research.

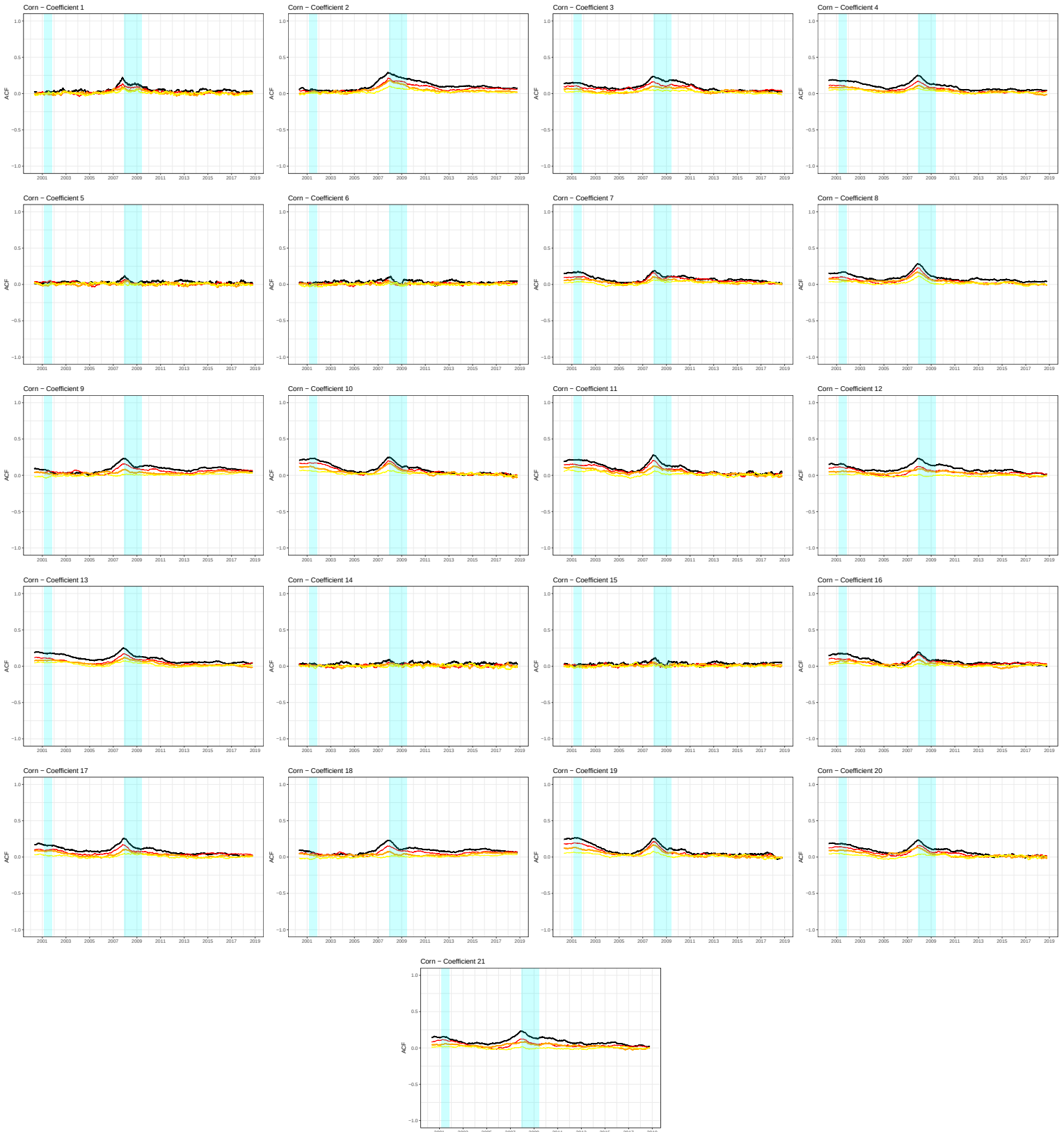

Figure A.6: **Time-varying autocorrelation functions for cotton**

The plots show the autocorrelation functions (ACF) of the Markov chains drawn for all parameters of the VAR model (3 equations x 3 variables x 2 lags + 3 intercepts = 21 coefficients; the ACFs for chains of the elements of the lower triangular matrix and the variances of the error terms are not shown to save space but these look very similar) for all time points in the sample period running from May 1, 2000 (the first 80 days starting from January 3, 2000 have been used as a training sample to initialize the coefficient priors) to October 17, 2018. The order of appearance is as follows: the first row starts with the intercept of the first equation (for open interest) followed by both lags of open interest, both lags of trading volume and both lags of volatility. Then all coefficients are provided for the second (trading volume) and third equation (volatility). The value of the ACF is provided on the vertical axis for the range from -1 to +1 and the ACF for lag 1 is shown as a black line, for lag 5 as a red line, for lag 10 as an orange line and for lag 20 as a yellow line. The cyan areas highlight the US recession periods according to the classification of the National Bureau of Economic Research.

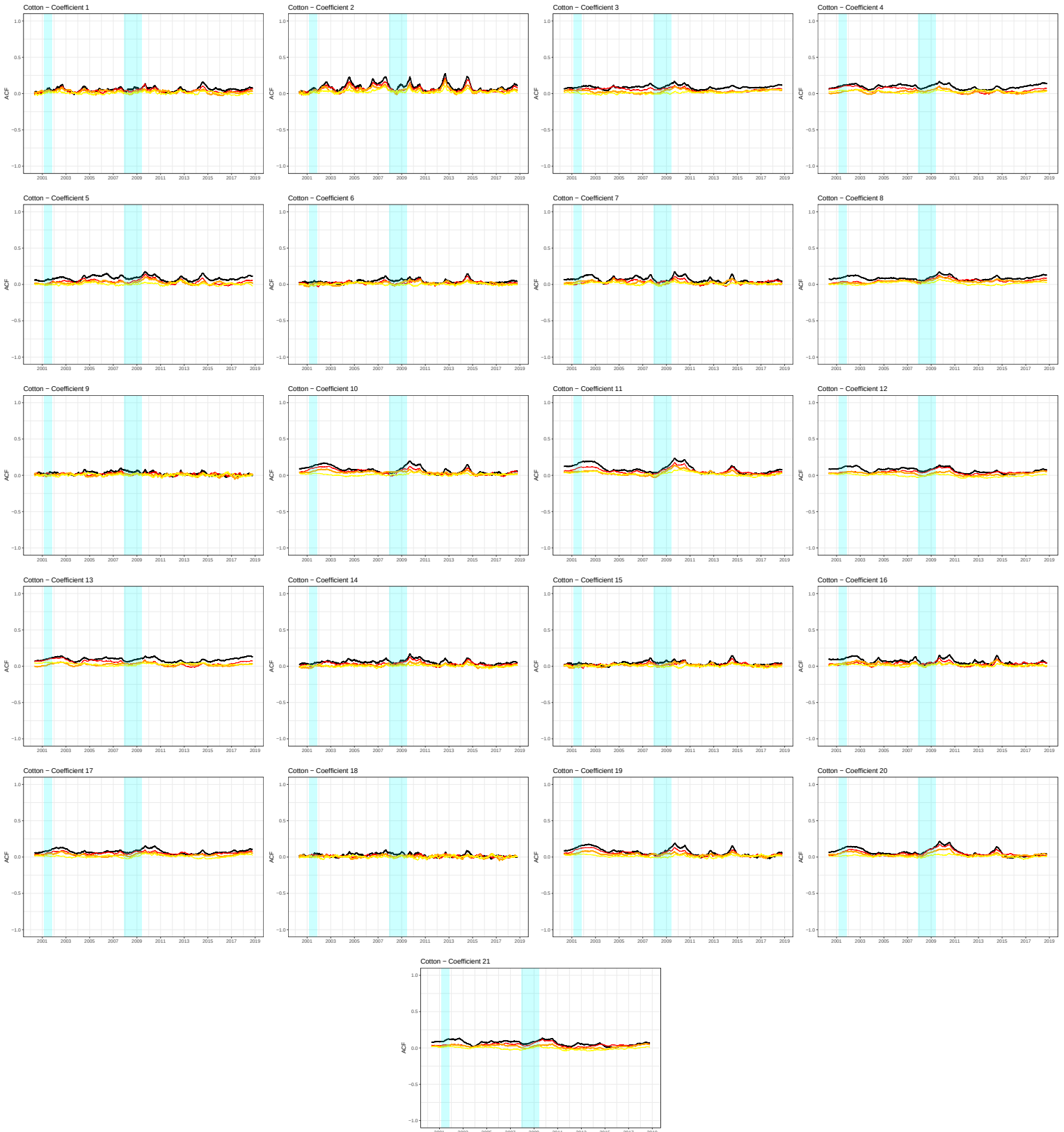

Figure A.7: **Time-varying autocorrelation functions for soybean oil**

The plots show the autocorrelation functions (ACF) of the Markov chains drawn for all parameters of the VAR model (3 equations x 3 variables x 2 lags + 3 intercepts = 21 coefficients; the ACFs for chains of the elements of the lower triangular matrix and the variances of the error terms are not shown to save space but these look very similar) for all time points in the sample period running from May 1, 2000 (the first 80 days starting from January 3, 2000 have been used as a training sample to initialize the coefficient priors) to October 17, 2018. The order of appearance is as follows: the first row starts with the intercept of the first equation (for open interest) followed by both lags of open interest, both lags of trading volume and both lags of volatility. Then all coefficients are provided for the second (trading volume) and third equation (volatility). The value of the ACF is provided on the vertical axis for the range from -1 to +1 and the ACF for lag 1 is shown as a black line, for lag 5 as a red line, for lag 10 as an orange line and for lag 20 as a yellow line. The cyan areas highlight the US recession periods according to the classification of the National Bureau of Economic Research.

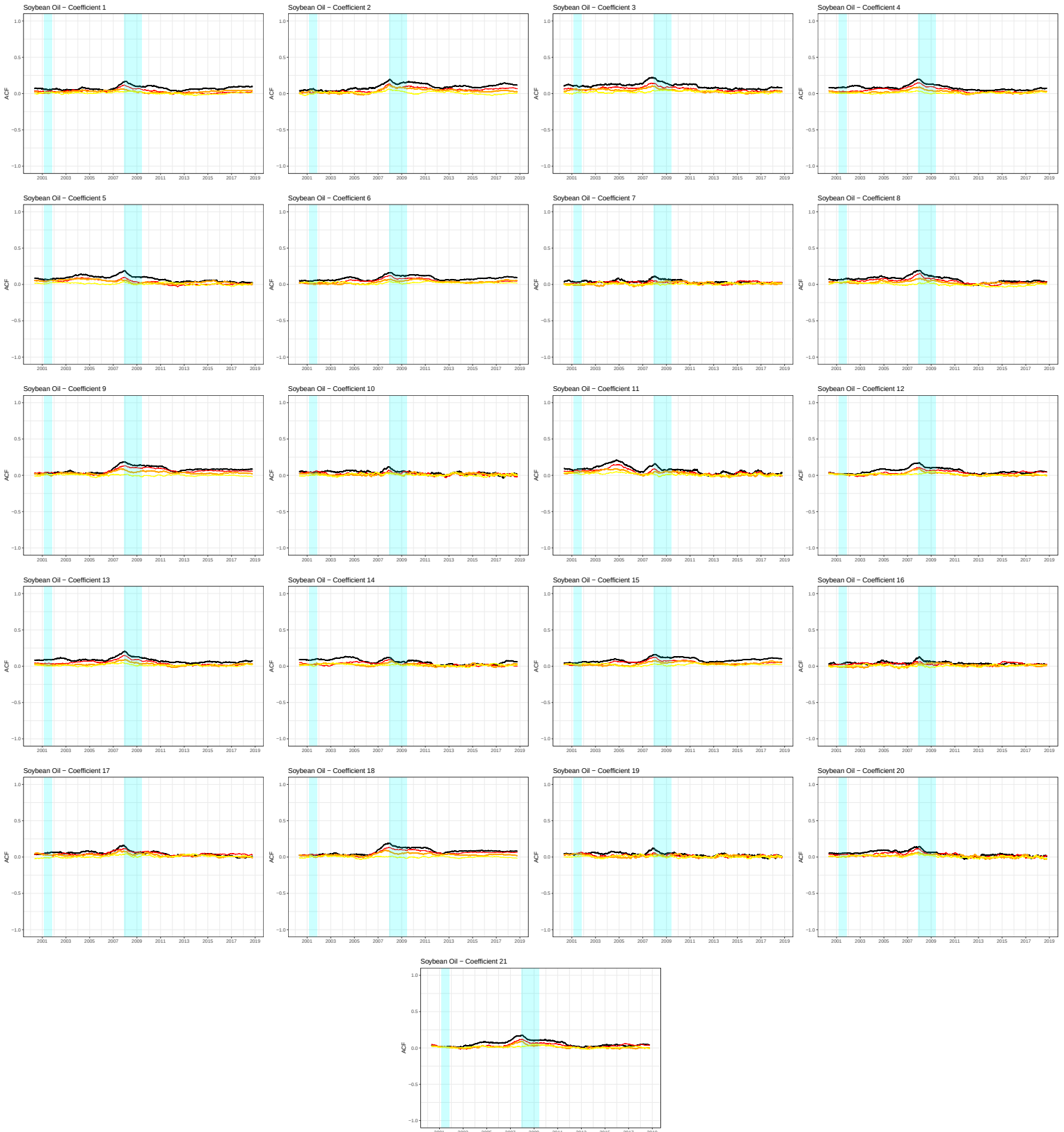

Figure A.8: **Time-varying autocorrelation functions for soybeans**

The plots show the autocorrelation functions (ACF) of the Markov chains drawn for all parameters of the VAR model (3 equations x 3 variables x 2 lags + 3 intercepts = 21 coefficients; the ACFs for chains of the elements of the lower triangular matrix and the variances of the error terms are not shown to save space but these look very similar) for all time points in the sample period running from May 1, 2000 (the first 80 days starting from January 3, 2000 have been used as a training sample to initialize the coefficient priors) to October 17, 2018. The order of appearance is as follows: the first row starts with the intercept of the first equation (for open interest) followed by both lags of open interest, both lags of trading volume and both lags of volatility. Then all coefficients are provided for the second (trading volume) and third equation (volatility). The value of the ACF is provided on the vertical axis for the range from -1 to +1 and the ACF for lag 1 is shown as a black line, for lag 5 as a red line, for lag 10 as an orange line and for lag 20 as a yellow line. The cyan areas highlight the US recession periods according to the classification of the National Bureau of Economic Research.

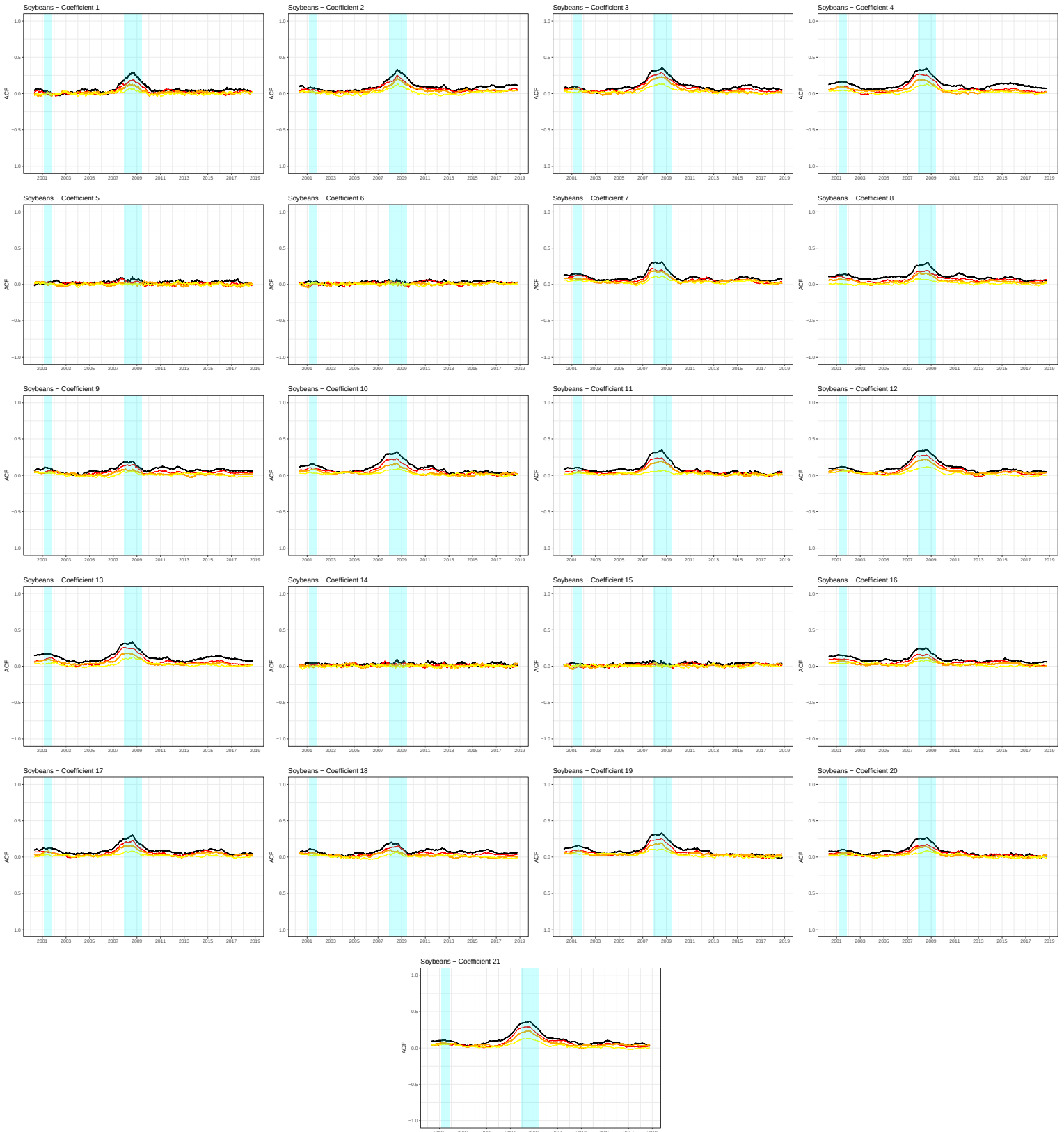

Figure A.9: **Time-varying autocorrelation functions for sugar**

The plots show the autocorrelation functions (ACF) of the Markov chains drawn for all parameters of the VAR model (3 equations x 3 variables x 2 lags + 3 intercepts = 21 coefficients; the ACFs for chains of the elements of the lower triangular matrix and the variances of the error terms are not shown to save space but these look very similar) for all time points in the sample period running from May 1, 2000 (the first 80 days starting from January 3, 2000 have been used as a training sample to initialize the coefficient priors) to October 17, 2018. The order of appearance is as follows: the first row starts with the intercept of the first equation (for open interest) followed by both lags of open interest, both lags of trading volume and both lags of volatility. Then all coefficients are provided for the second (trading volume) and third equation (volatility). The value of the ACF is provided on the vertical axis for the range from -1 to +1 and the ACF for lag 1 is shown as a black line, for lag 5 as a red line, for lag 10 as an orange line and for lag 20 as a yellow line. The cyan areas highlight the US recession periods according to the classification of the National Bureau of Economic Research.

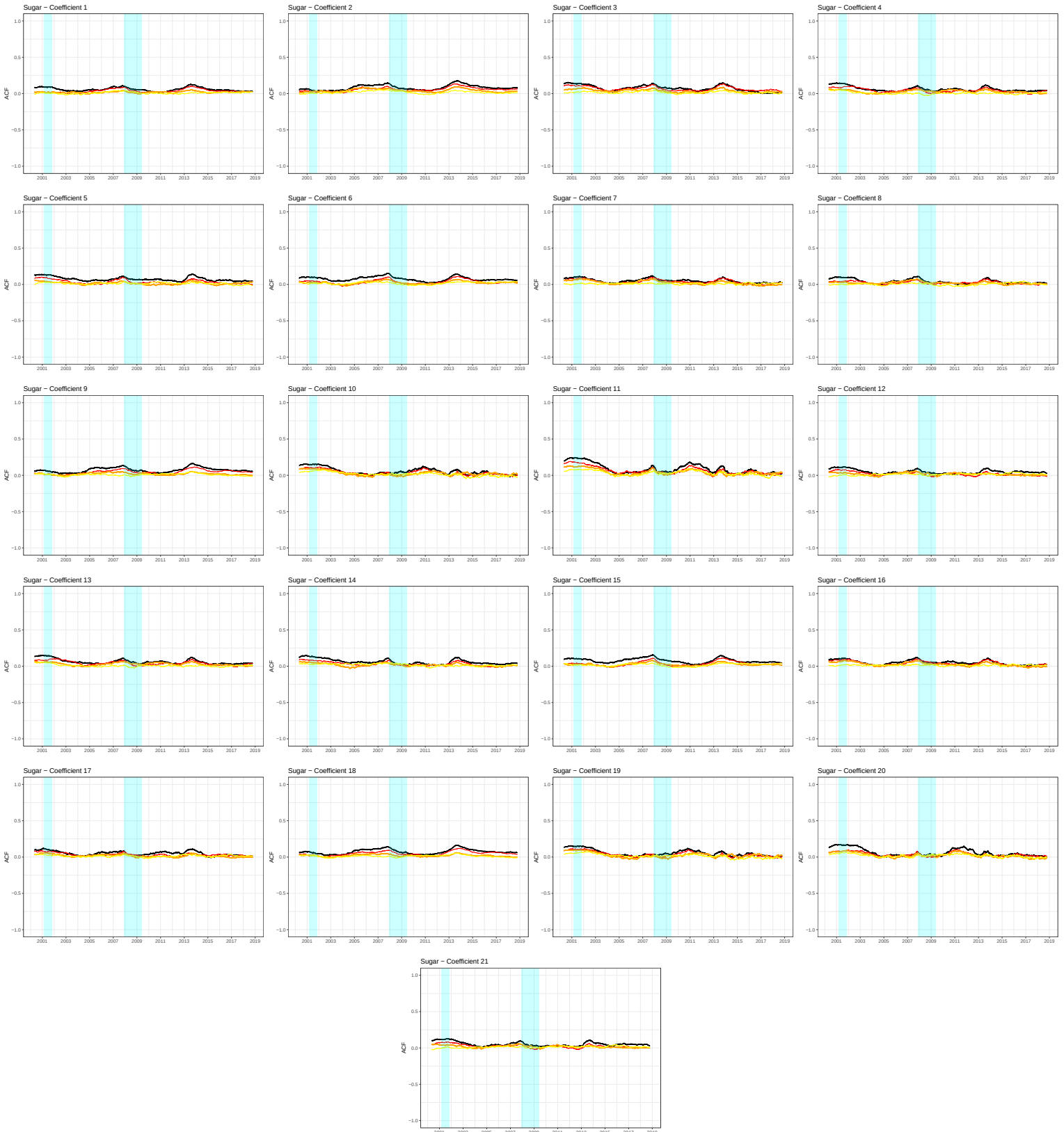

Figure A.10: **Time-varying autocorrelation functions for wheat**

The plots show the autocorrelation functions (ACF) of the Markov chains drawn for all parameters of the VAR model (3 equations x 3 variables x 2 lags + 3 intercepts = 21 coefficients; the ACFs for chains of the elements of the lower triangular matrix and the variances of the error terms are not shown to save space but these look very similar) for all time points in the sample period running from May 1, 2000 (the first 80 days starting from January 3, 2000 have been used as a training sample to initialize the coefficient priors) to October 17, 2018. The order of appearance is as follows: the first row starts with the intercept of the first equation (for open interest) followed by both lags of open interest, both lags of trading volume and both lags of volatility. Then all coefficients are provided for the second (trading volume) and third equation (volatility). The value of the ACF is provided on the vertical axis for the range from -1 to +1 and the ACF for lag 1 is shown as a black line, for lag 5 as a red line, for lag 10 as an orange line and for lag 20 as a yellow line. The cyan areas highlight the US recession periods according to the classification of the National Bureau of Economic Research.

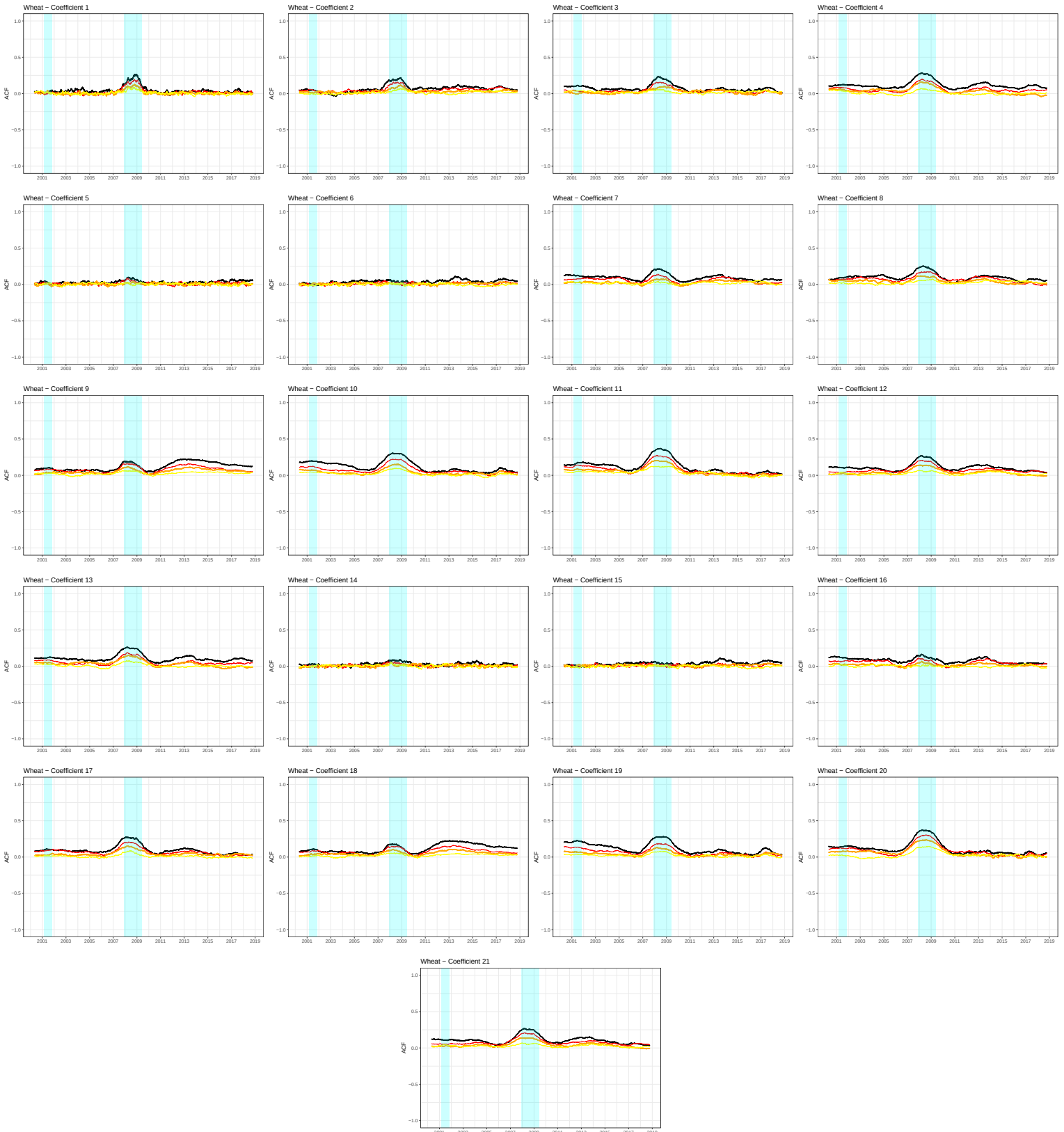

Figure A.11: **Time-varying Geweke diagnostic for coffee**

The plots show the p-values for the Geweke diagnostic (Geweke (1992)) of the Markov chains drawn for all parameters of the VAR model (3 equations x 3 variables x 2 lags + 3 intercepts = 21 coefficients; statistics for chains of the elements of the lower triangular matrix and the variances of the error terms are not shown to save space but these look very similar) for all time points in the sample period running from May 1, 2000 (the first 80 days starting from January 3, 2000 have been used as a training sample to initialize the coefficient priors) to October 17, 2018. The order of appearance is as follows: the first row starts with the intercept of the first equation (for open interest) followed by both lags of open interest, both lags of trading volume and both lags of volatility. Then all coefficients are provided for the second (trading volume) and third equation (volatility). p-values for the Geweke diagnostic are provided on the vertical axis for the range from 0 to 1 and are computed for testing the null hypothesis of equal means in the first 10% and the last 50% of the Markov chain to examine if the two parts of the chain are from the same distribution. The red dashed line marks the 5% significance level. The cyan areas highlight the US recession periods according to the classification of the National Bureau of Economic Research.

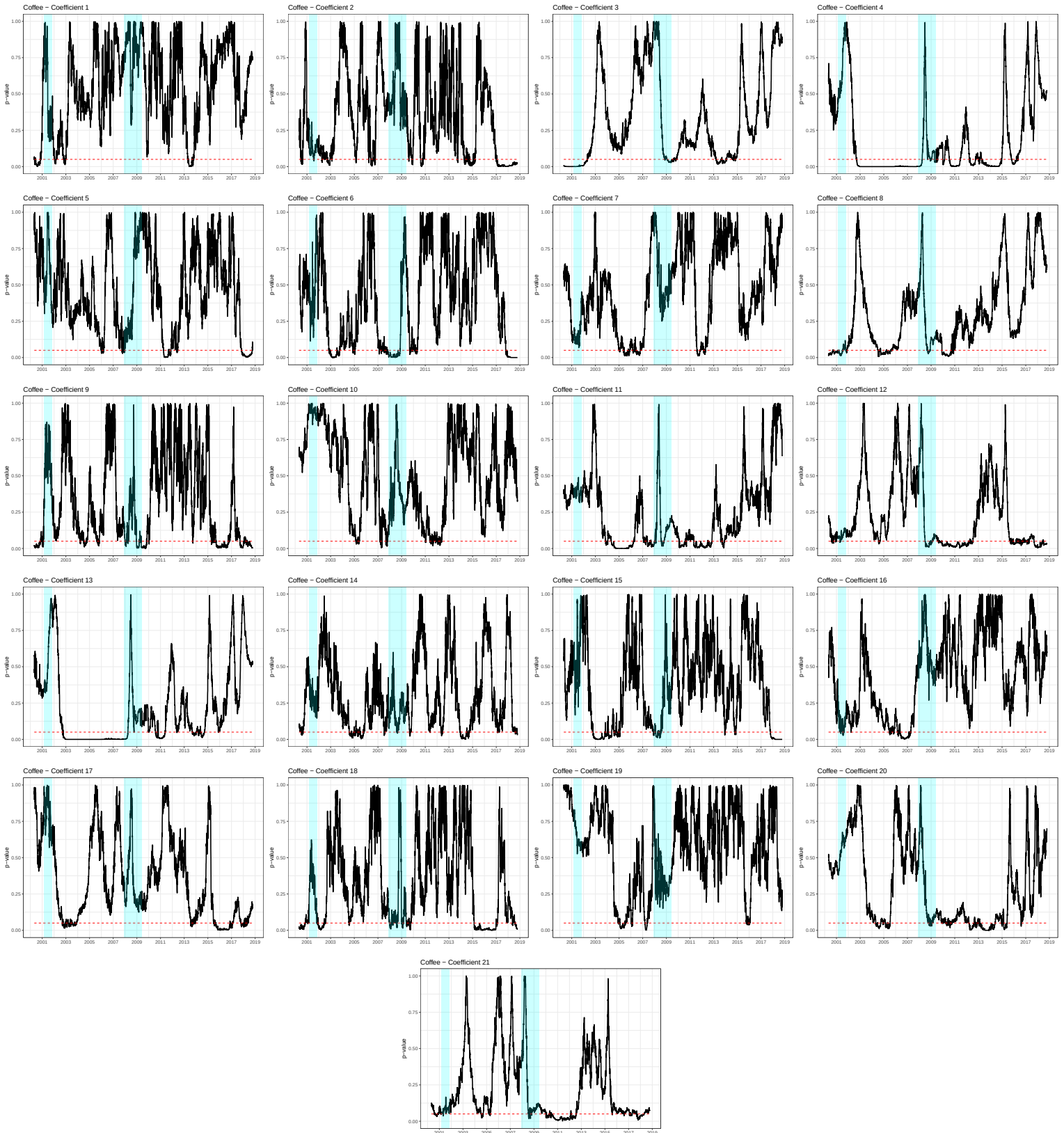

Figure A.12: **Time-varying Geweke diagnostic for corn**

The plots show the p-values for the Geweke diagnostic (Geweke (1992)) of the Markov chains drawn for all parameters of the VAR model (3 equations x 3 variables x 2 lags + 3 intercepts = 21 coefficients; statistics for chains of the elements of the lower triangular matrix and the variances of the error terms are not shown to save space but these look very similar) for all time points in the sample period running from May 1, 2000 (the first 80 days starting from January 3, 2000 have been used as a training sample to initialize the coefficient priors) to October 17, 2018. The order of appearance is as follows: the first row starts with the intercept of the first equation (for open interest) followed by both lags of open interest, both lags of trading volume and both lags of volatility. Then all coefficients are provided for the second (trading volume) and third equation (volatility). p-values for the Geweke diagnostic are provided on the vertical axis for the range from 0 to 1 and are computed for testing the null hypothesis of equal means in the first 10% and the last 50% of the Markov chain to examine if the two parts of the chain are from the same distribution. The red dashed line marks the 5% significance level. The cyan areas highlight the US recession periods according to the classification of the National Bureau of Economic Research.

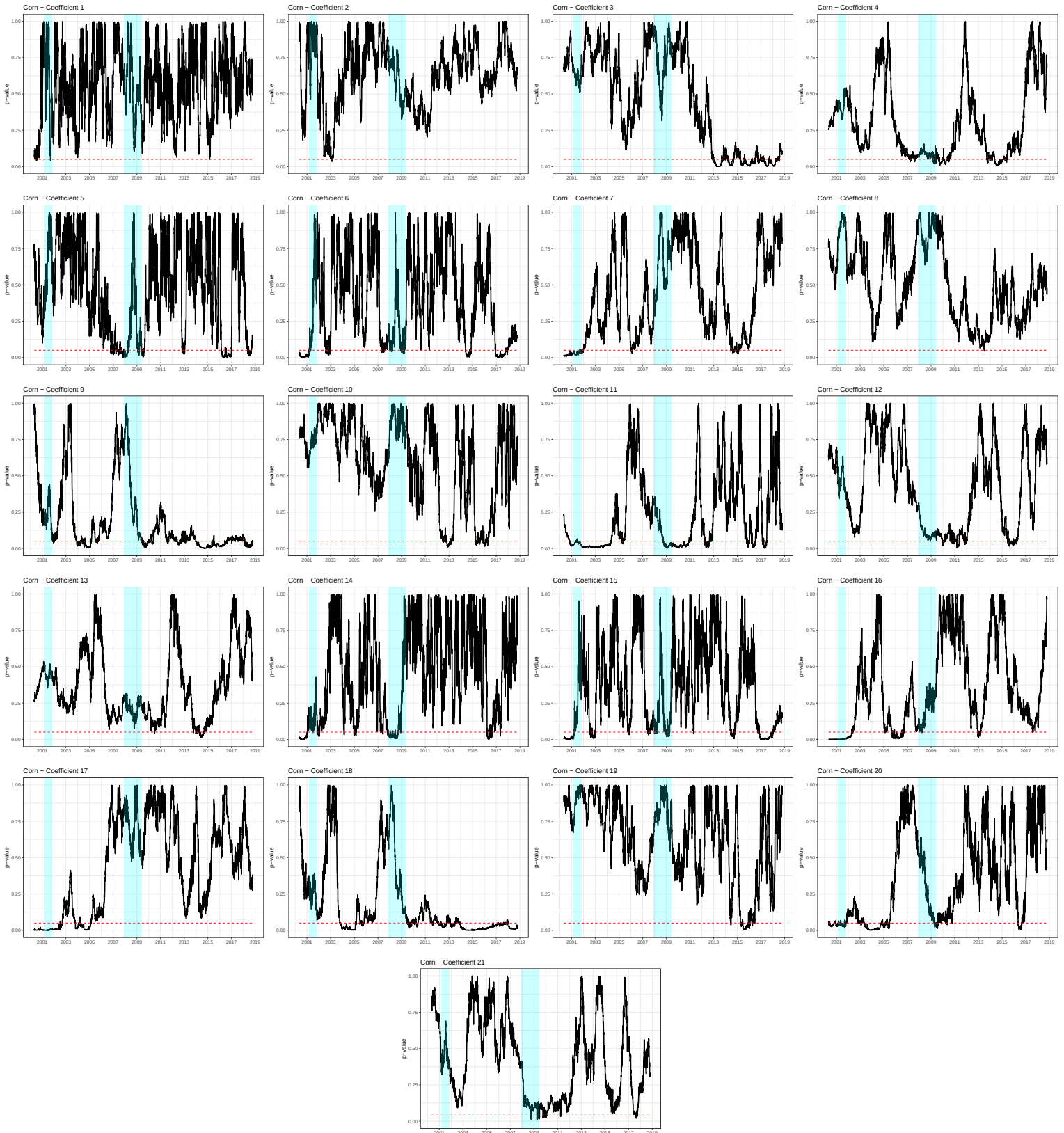

Figure A.13: **Time-varying Geweke diagnostic for cotton**

The plots show the p-values for the Geweke diagnostic (Geweke (1992)) of the Markov chains drawn for all parameters of the VAR model (3 equations x 3 variables x 2 lags + 3 intercepts = 21 coefficients; statistics for chains of the elements of the lower triangular matrix and the variances of the error terms are not shown to save space but these look very similar) for all time points in the sample period running from May 1, 2000 (the first 80 days starting from January 3, 2000 have been used as a training sample to initialize the coefficient priors) to October 17, 2018. The order of appearance is as follows: the first row starts with the intercept of the first equation (for open interest) followed by both lags of open interest, both lags of trading volume and both lags of volatility. Then all coefficients are provided for the second (trading volume) and third equation (volatility). p-values for the Geweke diagnostic are provided on the vertical axis for the range from 0 to 1 and are computed for testing the null hypothesis of equal means in the first 10% and the last 50% of the Markov chain to examine if the two parts of the chain are from the same distribution. The red dashed line marks the 5% significance level. The cyan areas highlight the US recession periods according to the classification of the National Bureau of Economic Research.

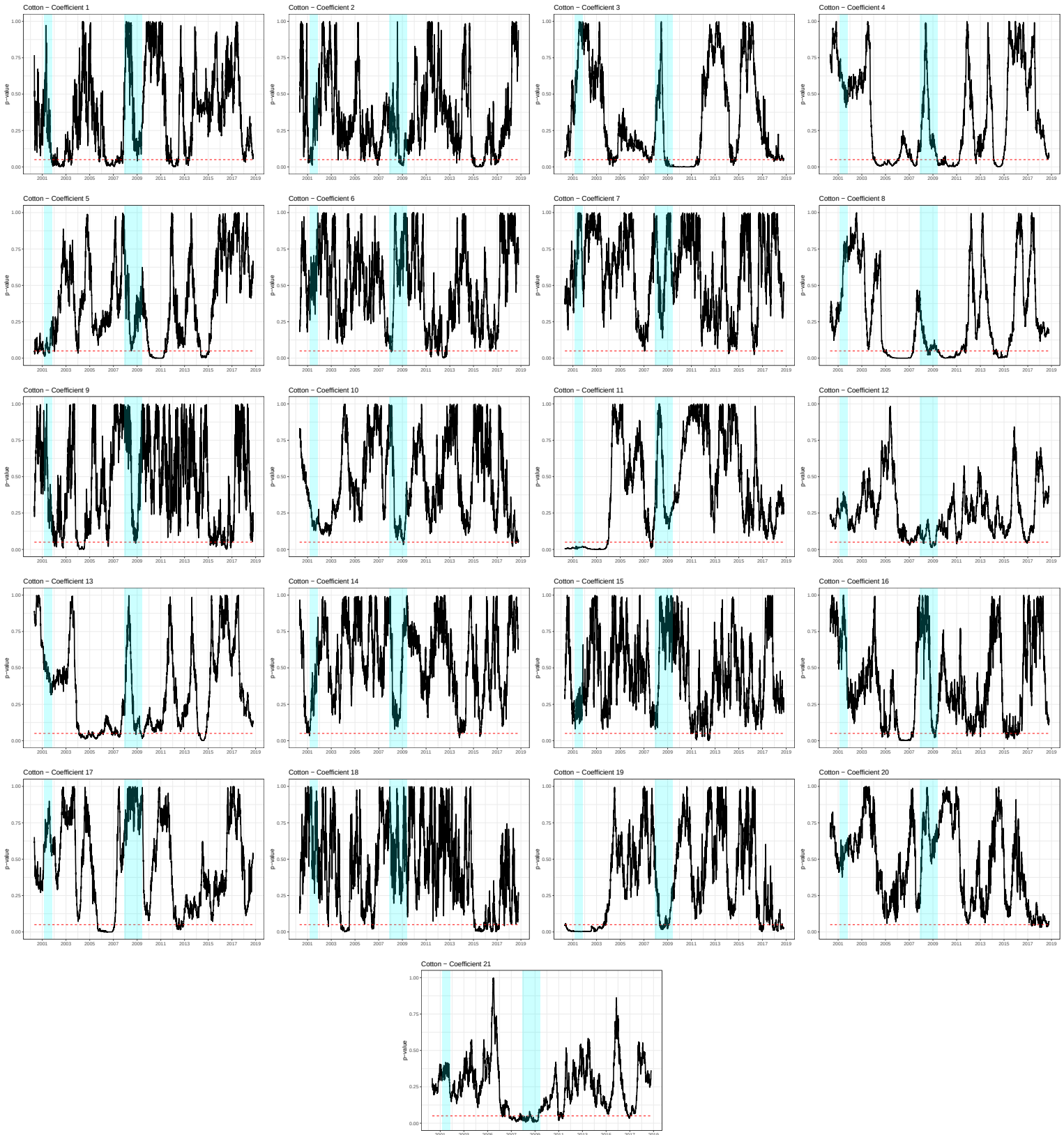

Figure A.14: **Time-varying Geweke diagnostic for soybean oil**

The plots show the p-values for the Geweke diagnostic (Geweke (1992)) of the Markov chains drawn for all parameters of the VAR model (3 equations x 3 variables x 2 lags + 3 intercepts = 21 coefficients; statistics for chains of the elements of the lower triangular matrix and the variances of the error terms are not shown to save space but these look very similar) for all time points in the sample period running from May 1, 2000 (the first 80 days starting from January 3, 2000 have been used as a training sample to initialize the coefficient priors) to October 17, 2018. The order of appearance is as follows: the first row starts with the intercept of the first equation (for open interest) followed by both lags of open interest, both lags of trading volume and both lags of volatility. Then all coefficients are provided for the second (trading volume) and third equation (volatility). p-values for the Geweke diagnostic are provided on the vertical axis for the range from 0 to 1 and are computed for testing the null hypothesis of equal means in the first 10% and the last 50% of the Markov chain to examine if the two parts of the chain are from the same distribution. The red dashed line marks the 5% significance level. The cyan areas highlight the US recession periods according to the classification of the National Bureau of Economic Research.

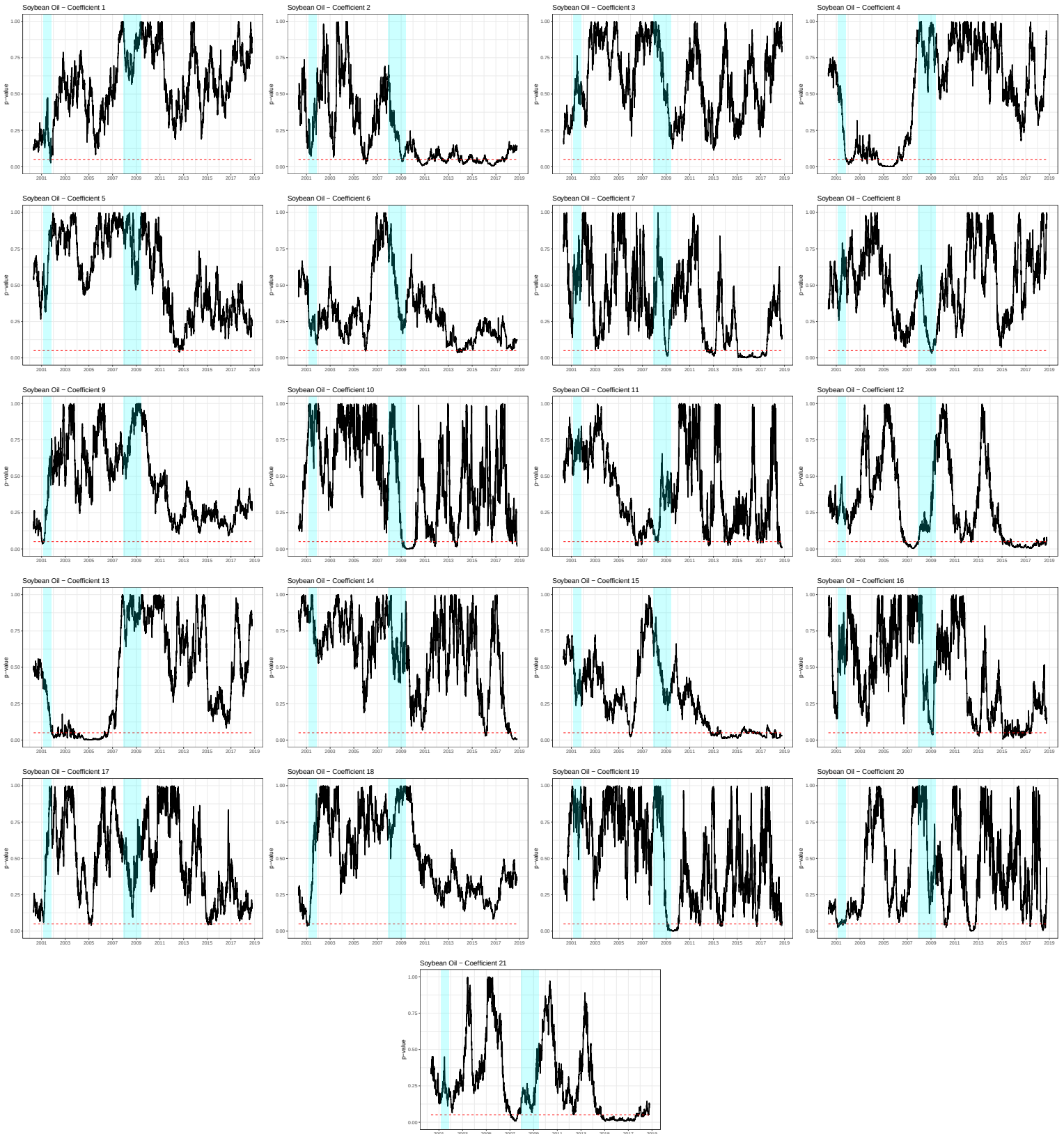

Figure A.15: **Time-varying Geweke diagnostic for soybeans**

The plots show the p-values for the Geweke diagnostic (Geweke (1992)) of the Markov chains drawn for all parameters of the VAR model (3 equations x 3 variables x 2 lags + 3 intercepts = 21 coefficients; statistics for chains of the elements of the lower triangular matrix and the variances of the error terms are not shown to save space but these look very similar) for all time points in the sample period running from May 1, 2000 (the first 80 days starting from January 3, 2000 have been used as a training sample to initialize the coefficient priors) to October 17, 2018. The order of appearance is as follows: the first row starts with the intercept of the first equation (for open interest) followed by both lags of open interest, both lags of trading volume and both lags of volatility. Then all coefficients are provided for the second (trading volume) and third equation (volatility). p-values for the Geweke diagnostic are provided on the vertical axis for the range from 0 to 1 and are computed for testing the null hypothesis of equal means in the first 10% and the last 50% of the Markov chain to examine if the two parts of the chain are from the same distribution. The red dashed line marks the 5% significance level. The cyan areas highlight the US recession periods according to the classification of the National Bureau of Economic Research.

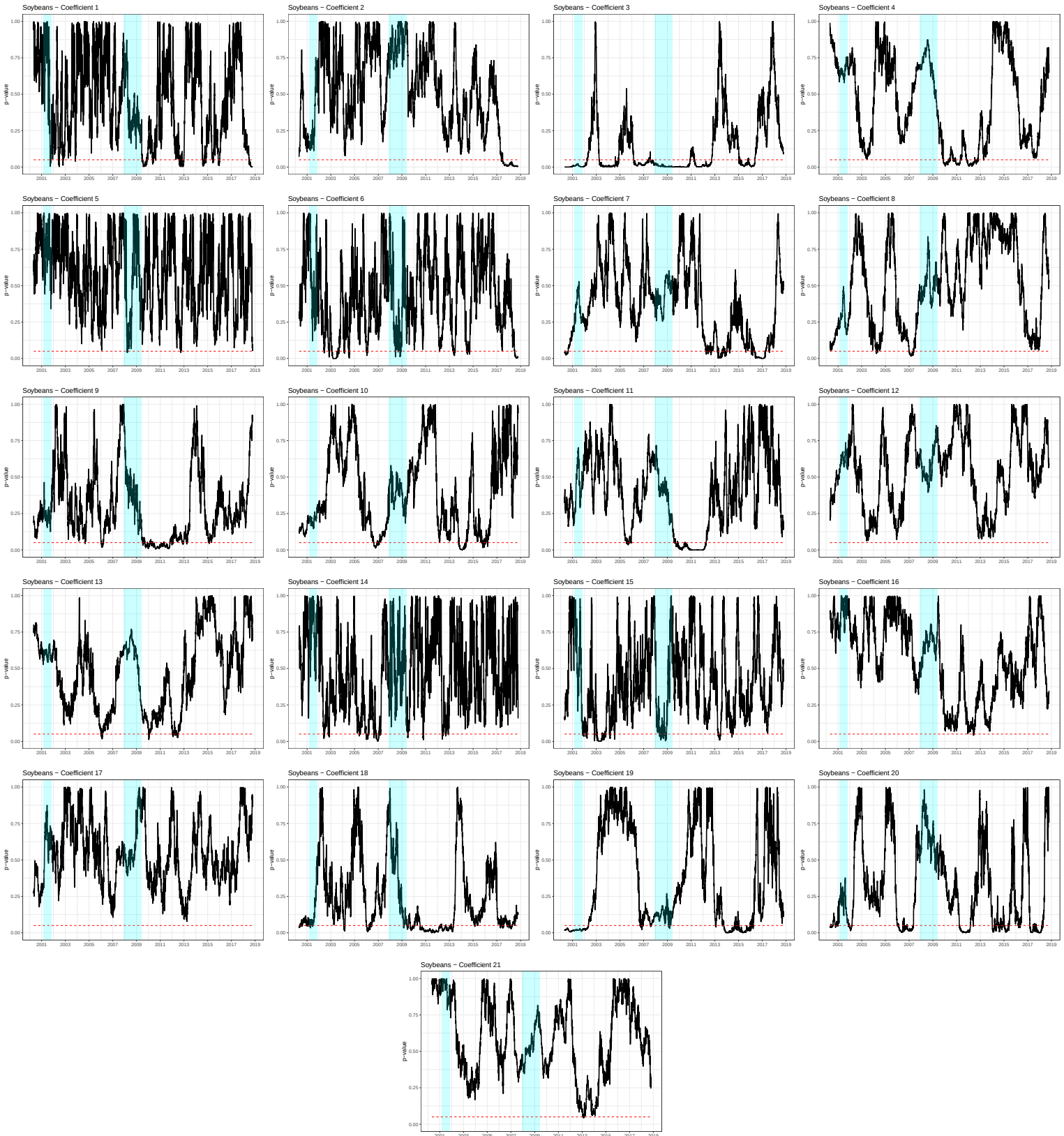

Figure A.16: **Time-varying Geweke diagnostic for sugar**

The plots show the p-values for the Geweke diagnostic (Geweke (1992)) of the Markov chains drawn for all parameters of the VAR model (3 equations x 3 variables x 2 lags + 3 intercepts = 21 coefficients; statistics for chains of the elements of the lower triangular matrix and the variances of the error terms are not shown to save space but these look very similar) for all time points in the sample period running from May 1, 2000 (the first 80 days starting from January 3, 2000 have been used as a training sample to initialize the coefficient priors) to October 17, 2018. The order of appearance is as follows: the first row starts with the intercept of the first equation (for open interest) followed by both lags of open interest, both lags of trading volume and both lags of volatility. Then all coefficients are provided for the second (trading volume) and third equation (volatility). p-values for the Geweke diagnostic are provided on the vertical axis for the range from 0 to 1 and are computed for testing the null hypothesis of equal means in the first 10% and the last 50% of the Markov chain to examine if the two parts of the chain are from the same distribution. The red dashed line marks the 5% significance level. The cyan areas highlight the US recession periods according to the classification of the National Bureau of Economic Research.

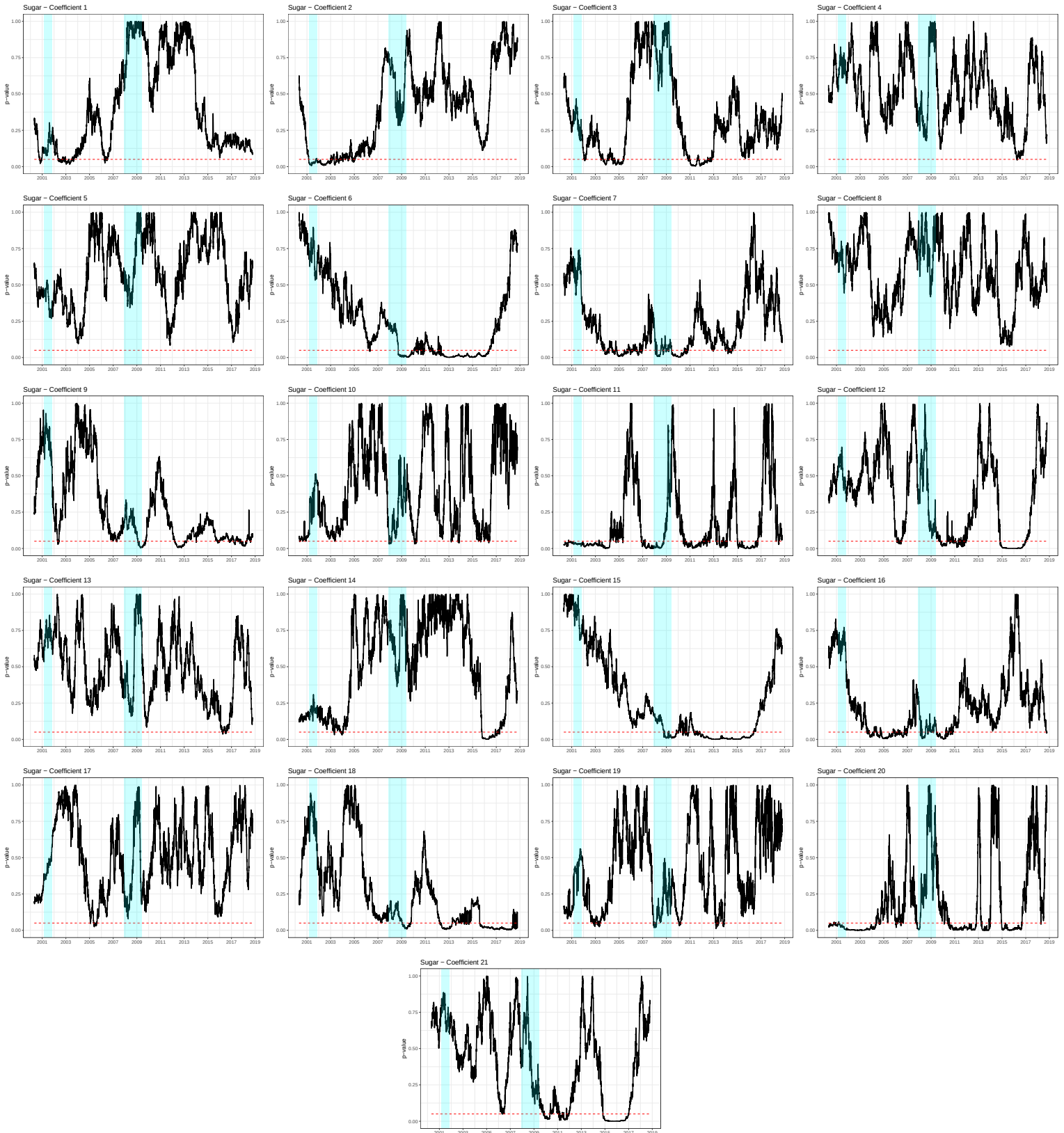

Figure A.17: **Time-varying Geweke diagnostic for wheat**

The plots show the p-values for the Geweke diagnostic (Geweke (1992)) of the Markov chains drawn for all parameters of the VAR model (3 equations x 3 variables x 2 lags + 3 intercepts = 21 coefficients; statistics for chains of the elements of the lower triangular matrix and the variances of the error terms are not shown to save space but these look very similar) for all time points in the sample period running from May 1, 2000 (the first 80 days starting from January 3, 2000 have been used as a training sample to initialize the coefficient priors) to October 17, 2018. The order of appearance is as follows: the first row starts with the intercept of the first equation (for open interest) followed by both lags of open interest, both lags of trading volume and both lags of volatility. Then all coefficients are provided for the second (trading volume) and third equation (volatility). p-values for the Geweke diagnostic are provided on the vertical axis for the range from 0 to 1 and are computed for testing the null hypothesis of equal means in the first 10% and the last 50% of the Markov chain to examine if the two parts of the chain are from the same distribution. The red dashed line marks the 5% significance level. The cyan areas highlight the US recession periods according to the classification of the National Bureau of Economic Research.

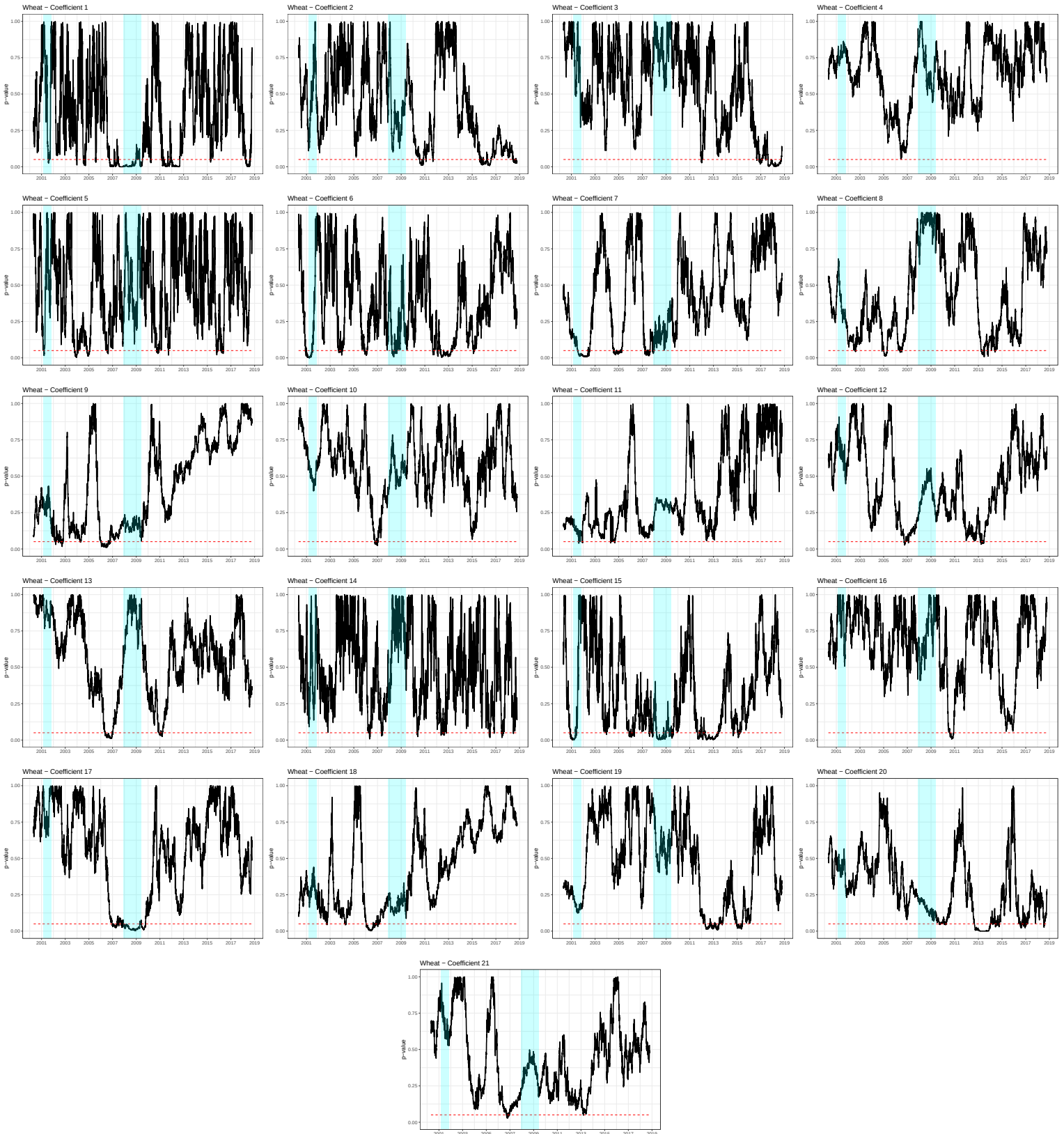

A.7 Rotated impulse responses

Figure A.18: **Rotated time-varying impulse responses for coffee**

The plots show the time-varying reactions of one unit shocks between the volatility of returns, the trading volume and the previous day open interest. The corresponding reactions have been calculated for a sample period running from January 3, 2000 to October 17, 2018 on a daily basis while data for the first 80 days (until April 26, 2000) has been used as a training sample to initialize the coefficient priors.

Response of trading volume to a shock in volatility

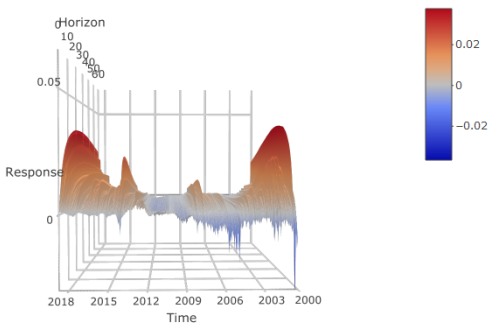

Response of open interest to a shock in volatility

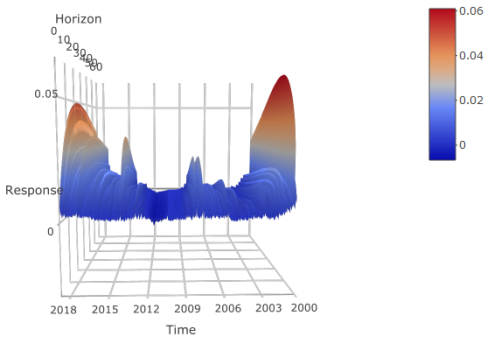

Response of volatility to a shock in trading volume

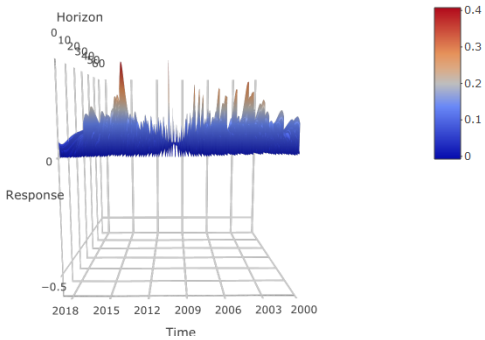

Response of volatility to a shock in open interest

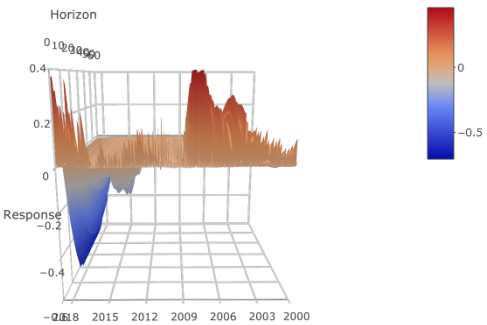

Figure A.19: **Rotated time-varying impulse responses for corn**

The plots show the time-varying reactions of one unit shocks between the volatility of returns, the trading volume and the previous day open interest. The corresponding reactions have been calculated for a sample period running from January 3, 2000 to October 17, 2018 on a daily basis while data for the first 80 days (until April 26, 2000) has been used as a training sample to initialize the coefficient priors.

Response of trading volume to a shock in volatility

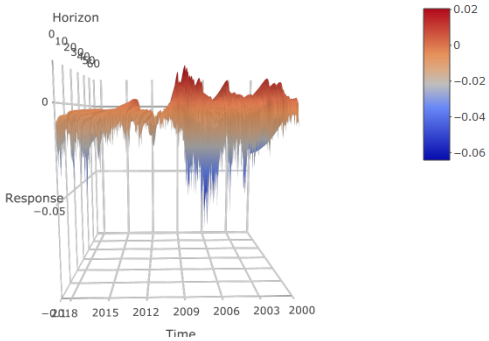

Response of open interest to a shock in volatility

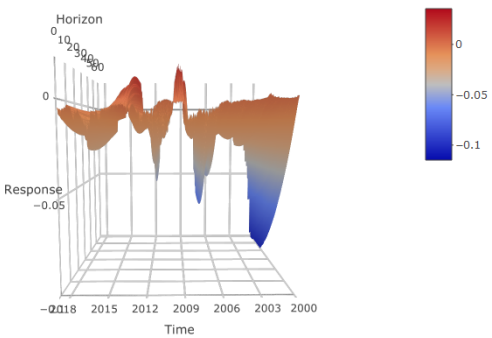

Response of volatility to a shock in trading volume

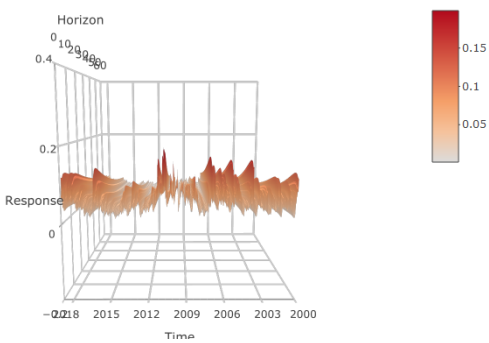

Response of volatility to a shock in open interest

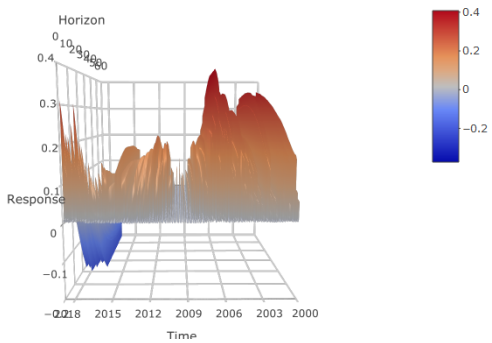

Figure A.20: **Rotated time-varying impulse responses for cotton**

The plots show the time-varying reactions of one unit shocks between the volatility of returns, the trading volume and the previous day open interest. The corresponding reactions have been calculated for a sample period running from January 3, 2000 to October 17, 2018 on a daily basis while data for the first 80 days (until April 26, 2000) has been used as a training sample to initialize the coefficient priors.

Response of trading volume to a shock in volatility

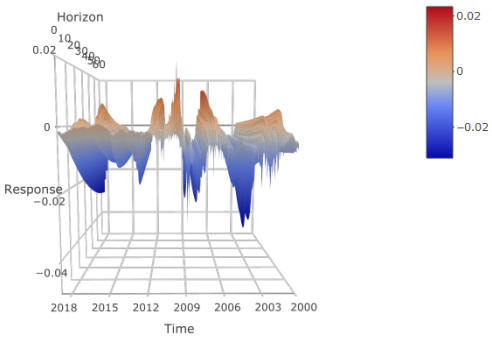

Response of open interest to a shock in volatility

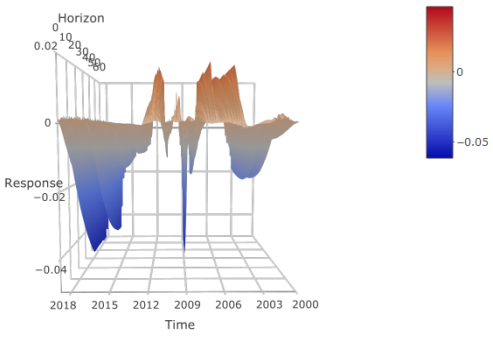

Response of volatility to a shock in trading volume

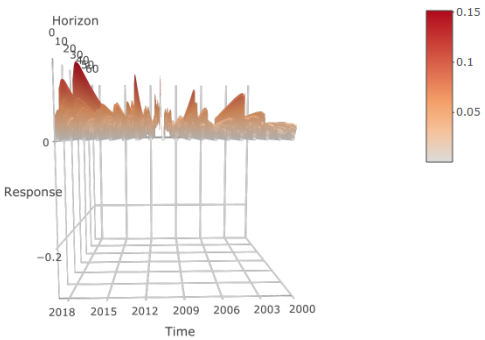

Response of volatility to a shock in open interest

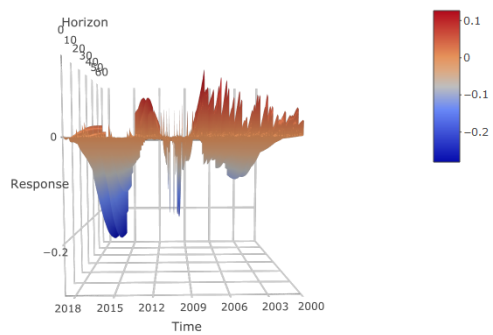

Figure A.21: **Rotated time-varying impulse responses for soybean oil**

The plots show the time-varying reactions of one unit shocks between the volatility of returns, the trading volume and the previous day open interest. The corresponding reactions have been calculated for a sample period running from January 3, 2000 to October 17, 2018 on a daily basis while data for the first 80 days (until April 26, 2000) has been used as a training sample to initialize the coefficient priors.

Response of trading volume to a shock in volatility

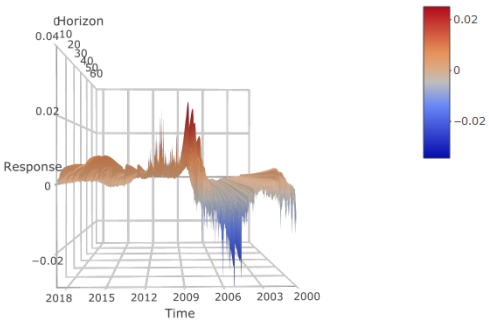

Response of open interest to a shock in volatility

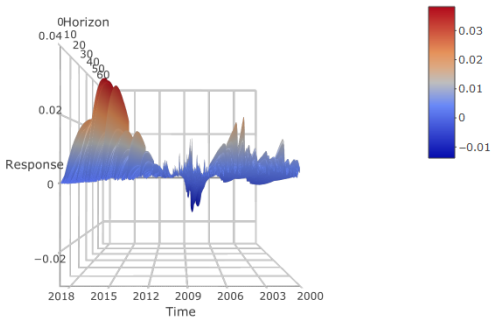

Response of volatility to a shock in trading volume

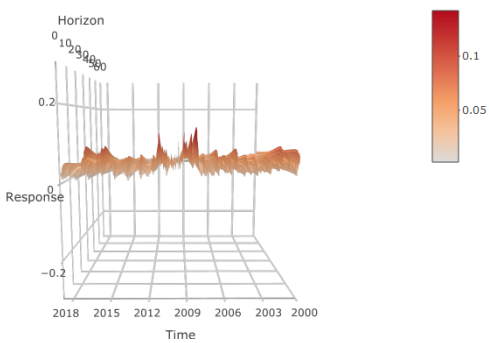

Response of volatility to a shock in open interest

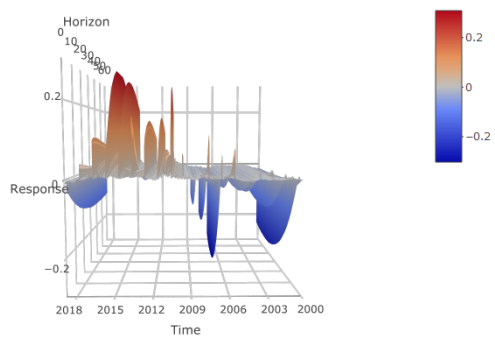

Figure A.22: **Rotated time-varying impulse responses for soybeans**

The plots show the time-varying reactions of one unit shocks between the volatility of returns, the trading volume and the previous day open interest. The corresponding reactions have been calculated for a sample period running from January 3, 2000 to October 17, 2018 on a daily basis while data for the first 80 days (until April 26, 2000) has been used as a training sample to initialize the coefficient priors.

Response of trading volume to a shock in volatility

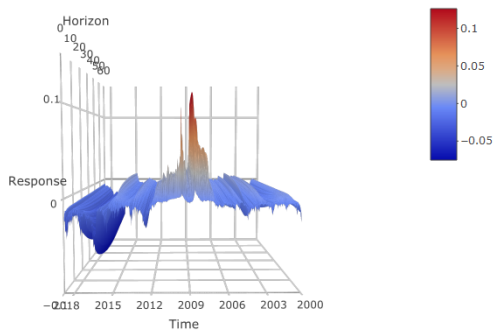

Response of open interest to a shock in volatility

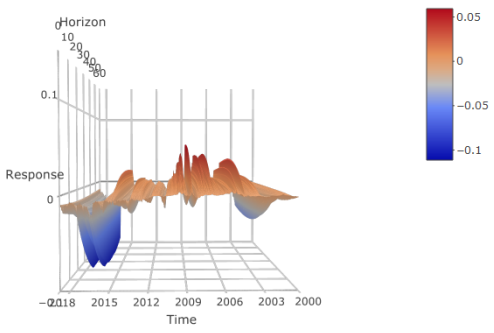

Response of volatility to a shock in trading volume

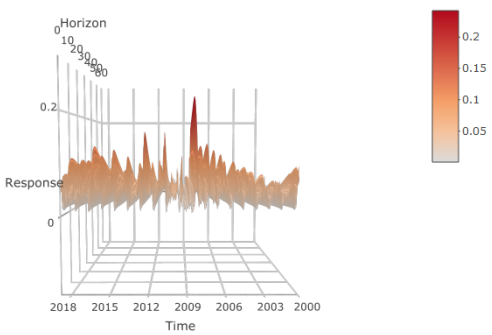

Response of volatility to a shock in open interest

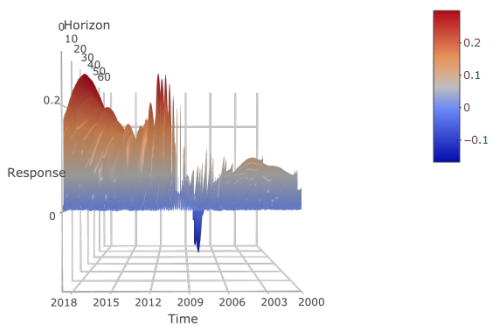

Figure A.23: **Rotated time-varying impulse responses for sugar**

The plots show the time-varying reactions of one unit shocks between the volatility of returns, the trading volume and the previous day open interest. The corresponding reactions have been calculated for a sample period running from January 3, 2000 to October 17, 2018 on a daily basis while data for the first 80 days (until April 26, 2000) has been used as a training sample to initialize the coefficient priors.

Response of trading volume to a shock in volatility

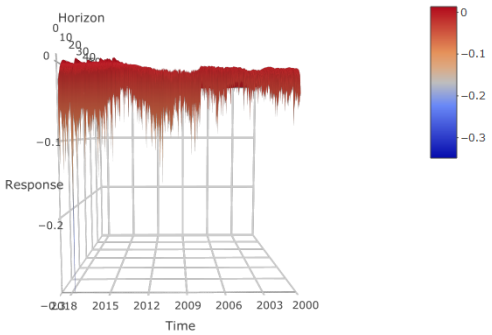

Response of open interest to a shock in volatility

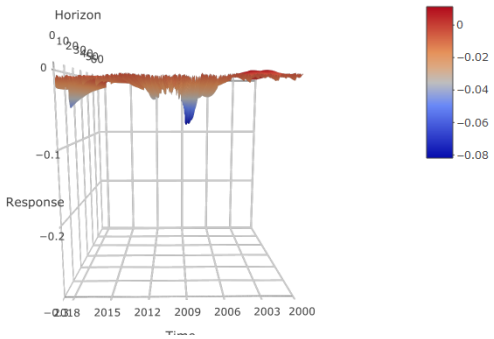

Response of volatility to a shock in trading volume

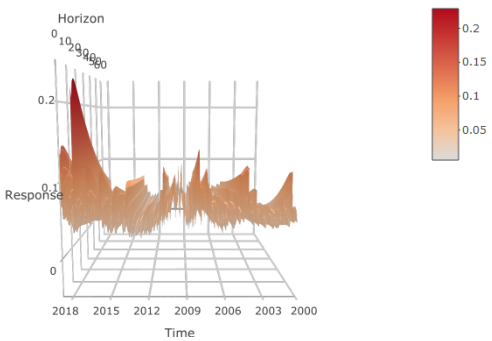

Response of volatility to a shock in open interest

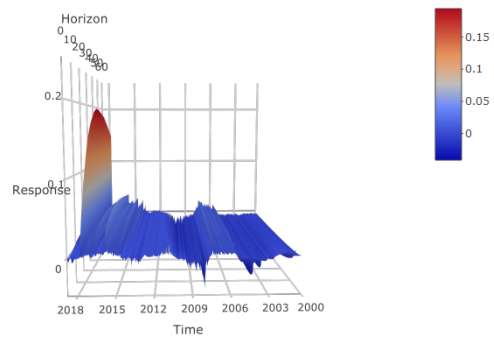

Figure A.24: **Rotated time-varying impulse responses for wheat**

The plots show the time-varying reactions of one unit shocks between the volatility of returns, the trading volume and the previous day open interest. The corresponding reactions have been calculated for a sample period running from January 3, 2000 to October 17, 2018 on a daily basis while data for the first 80 days (until April 26, 2000) has been used as a training sample to initialize the coefficient priors.

Response of trading volume to a shock in volatility

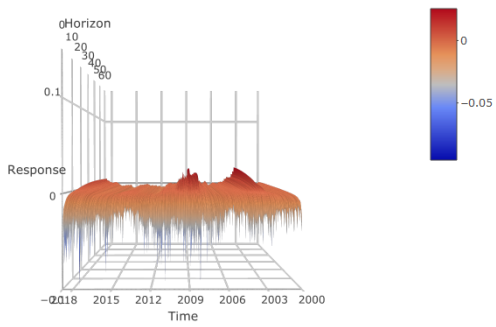

Response of open interest to a shock in volatility

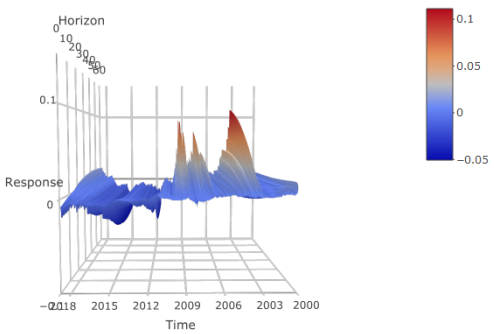

Response of volatility to a shock in trading volume

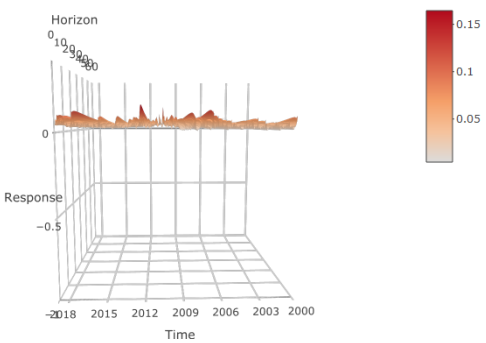

Response of volatility to a shock in open interest

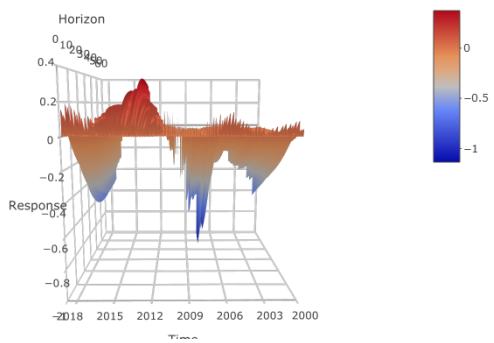

A.8 Contour plots of impulse responses

Figure A.25: **Contour plots of time-varying impulse responses for coffee**

The plots show the time-varying reactions of one unit shocks between the volatility of returns, the trading volume and the previous day open interest. The corresponding reactions have been calculated for a sample period running from January 3, 2000 to October 17, 2018 on a daily basis while data for the first 80 days (until April 26, 2000) has been used as a training sample to initialize the coefficient priors.

Response of trading volume to a shock in volatility

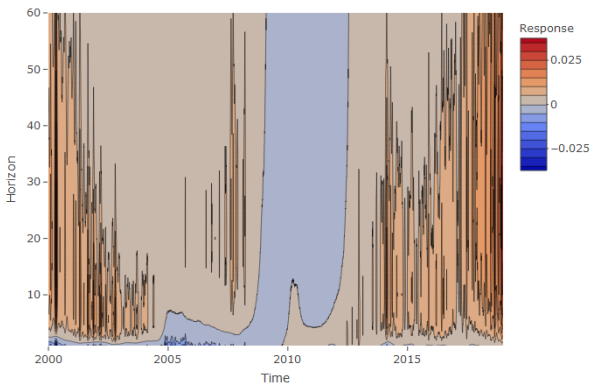

Response of open interest to a shock in volatility

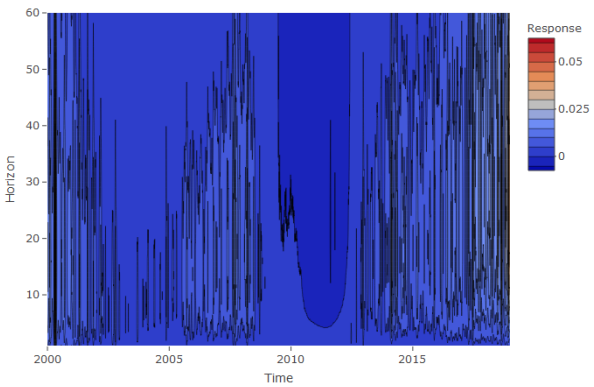

Response of volatility to a shock in trading volume

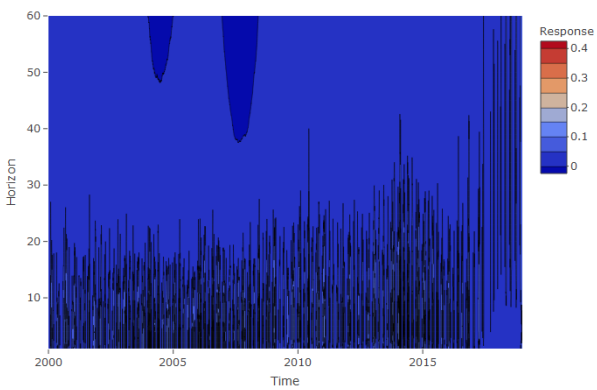

Response of volatility to a shock in open interest

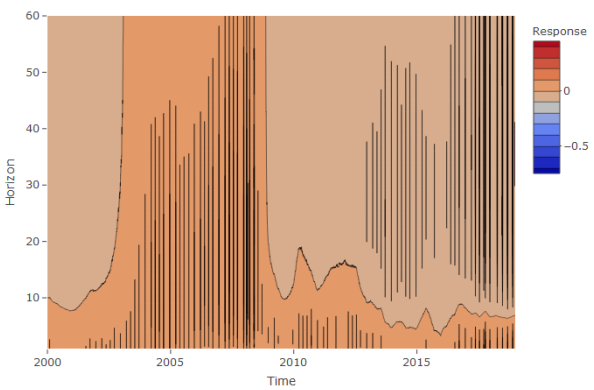

Figure A.26: **Contour plots of time-varying impulse responses for corn**

The plots show the time-varying reactions of one unit shocks between the volatility of returns, the trading volume and the previous day open interest. The corresponding reactions have been calculated for a sample period running from January 3, 2000 to October 17, 2018 on a daily basis while data for the first 80 days (until April 26, 2000) has been used as a training sample to initialize the coefficient priors.

Response of trading volume to a shock in volatility

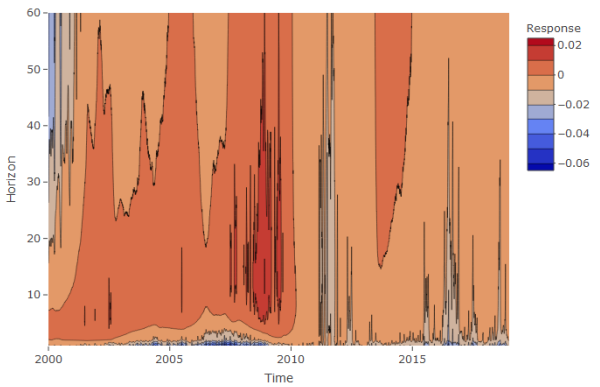

Response of open interest to a shock in volatility

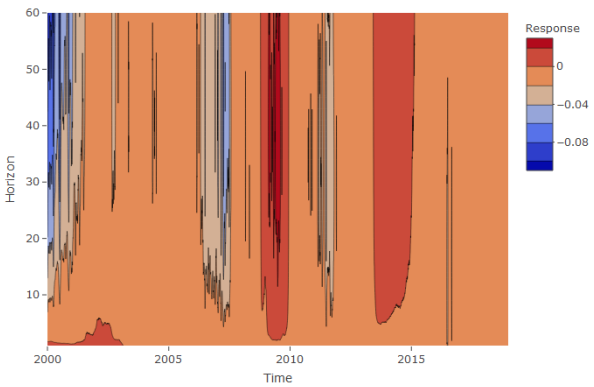

Response of volatility to a shock in trading volume

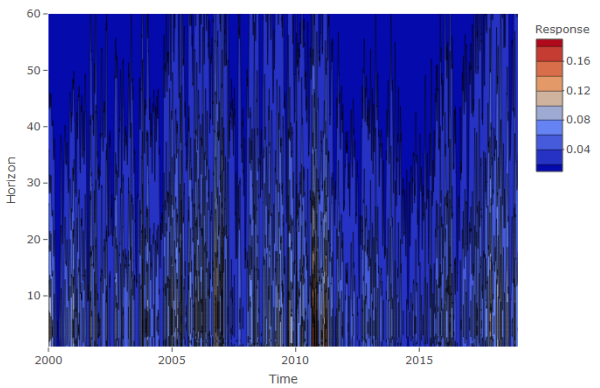

Response of volatility to a shock in open interest

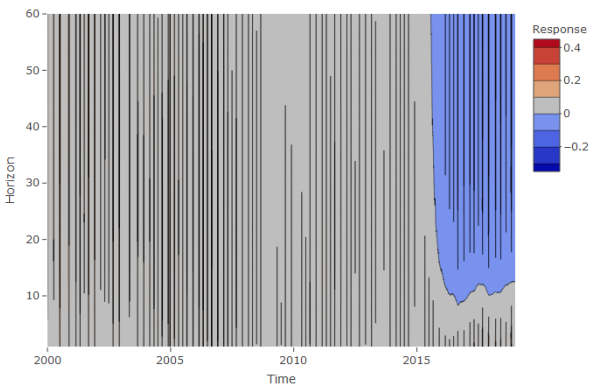

Figure A.27: **Contour plots of time-varying impulse responses for cotton**

The plots show the time-varying reactions of one unit shocks between the volatility of returns, the trading volume and the previous day open interest. The corresponding reactions have been calculated for a sample period running from January 3, 2000 to October 17, 2018 on a daily basis while data for the first 80 days (until April 26, 2000) has been used as a training sample to initialize the coefficient priors.

Response of trading volume to a shock in volatility

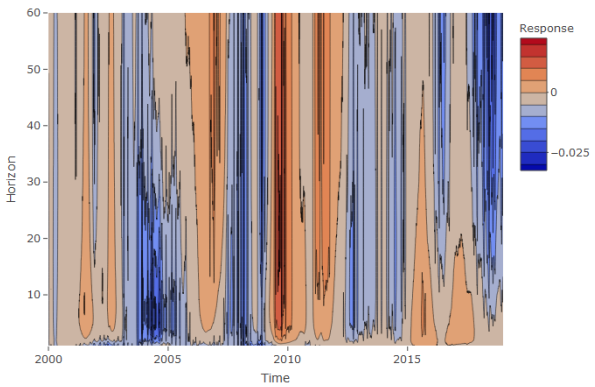

Response of open interest to a shock in volatility

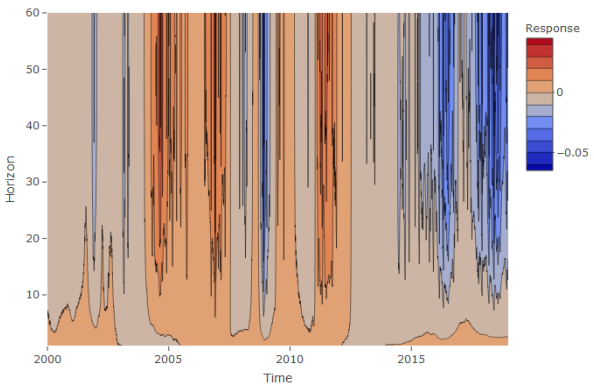

Response of volatility to a shock in trading volume

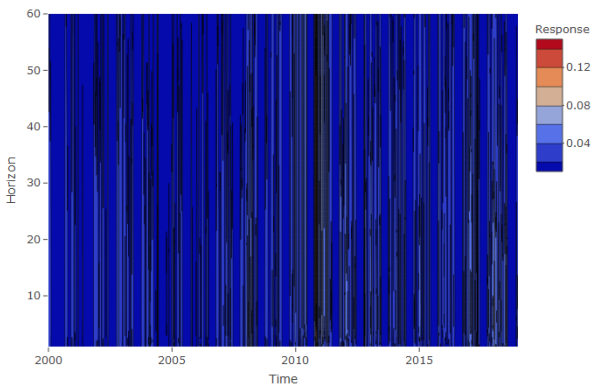

Response of volatility to a shock in open interest

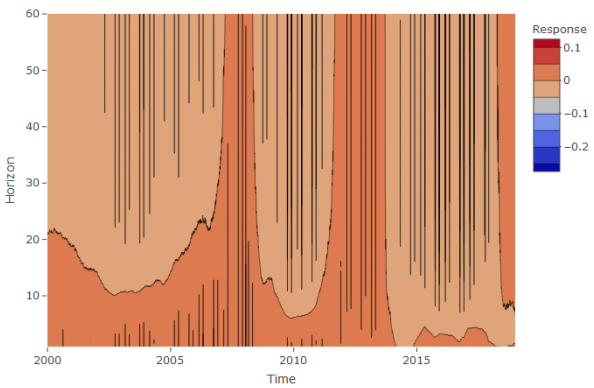

Figure A.28: **Contour plots of time-varying impulse responses for soybean oil**

The plots show the time-varying reactions of one unit shocks between the volatility of returns, the trading volume and the previous day open interest. The corresponding reactions have been calculated for a sample period running from January 3, 2000 to October 17, 2018 on a daily basis while data for the first 80 days (until April 26, 2000) has been used as a training sample to initialize the coefficient priors.

Response of trading volume to a shock in volatility

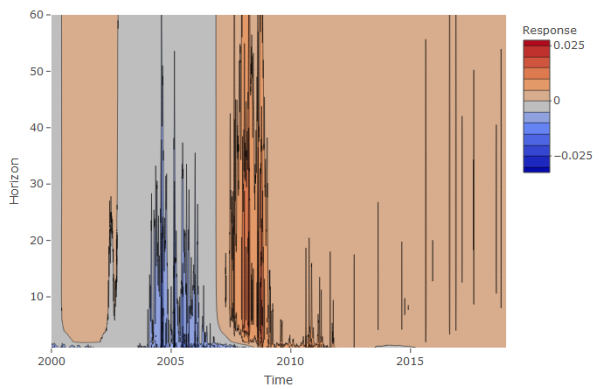

Response of open interest to a shock in volatility

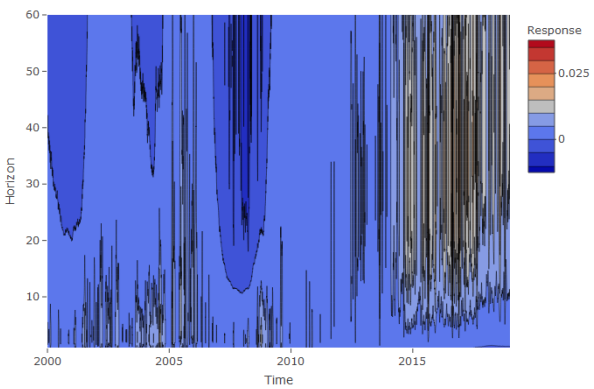

Response of volatility to a shock in trading volume

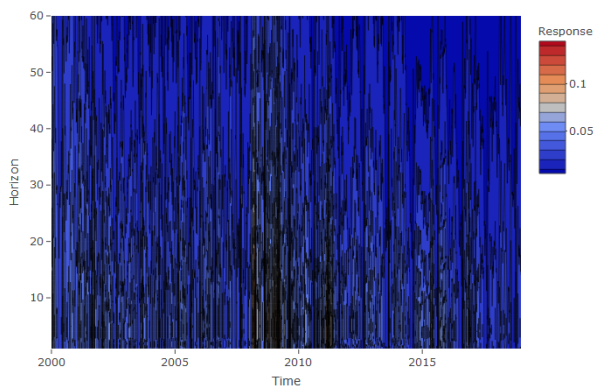

Response of volatility to a shock in open interest

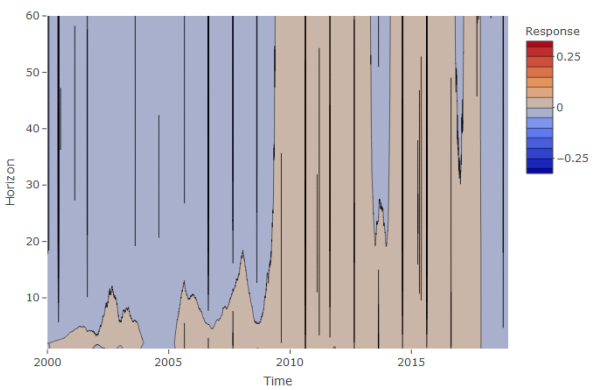

Figure A.29: **Contour plots of time-varying impulse responses for soybeans**

The plots show the time-varying reactions of one unit shocks between the volatility of returns, the trading volume and the previous day open interest. The corresponding reactions have been calculated for a sample period running from January 3, 2000 to October 17, 2018 on a daily basis while data for the first 80 days (until April 26, 2000) has been used as a training sample to initialize the coefficient priors.

Response of trading volume to a shock in volatility

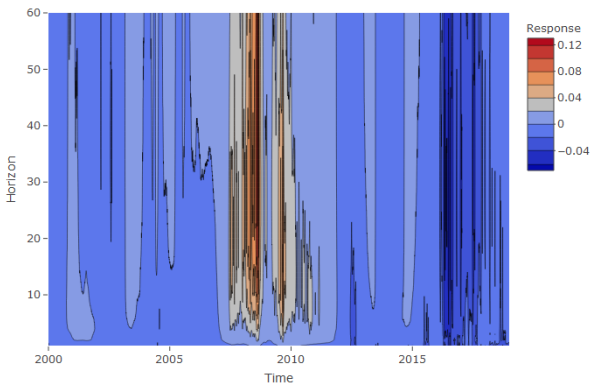

Response of open interest to a shock in volatility

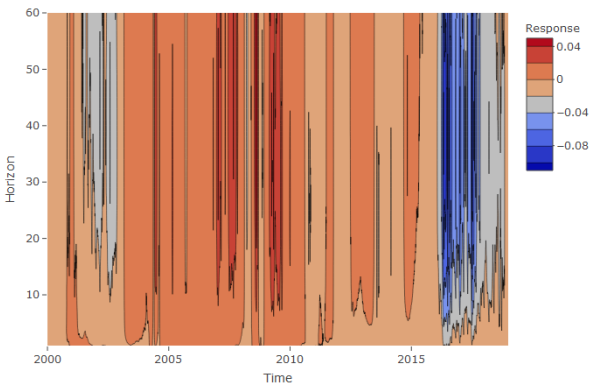

Response of volatility to a shock in trading volume

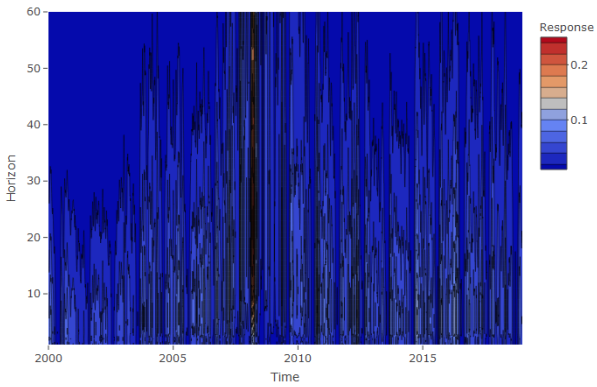

Response of volatility to a shock in open interest

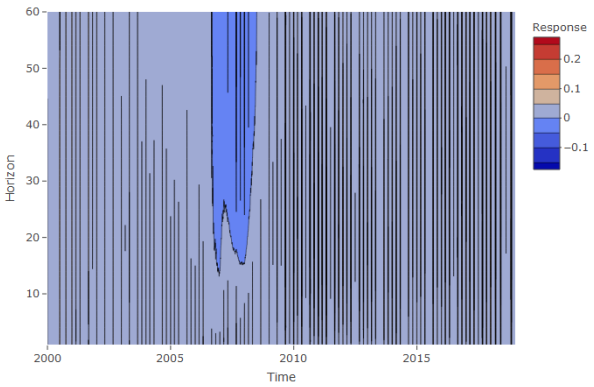

Figure A.30: **Contour plots of time-varying impulse responses for sugar**

The plots show the time-varying reactions of one unit shocks between the volatility of returns, the trading volume and the previous day open interest. The corresponding reactions have been calculated for a sample period running from January 3, 2000 to October 17, 2018 on a daily basis while data for the first 80 days (until April 26, 2000) has been used as a training sample to initialize the coefficient priors.

Response of trading volume to a shock in volatility

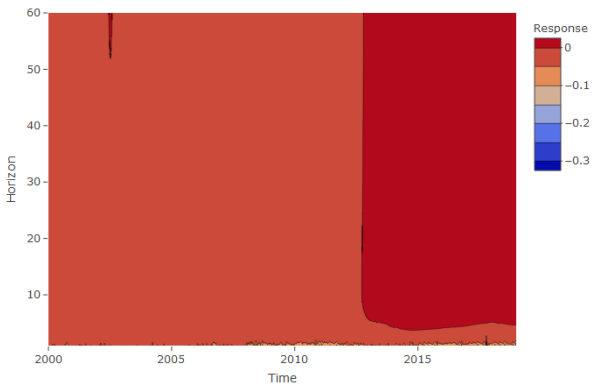

Response of open interest to a shock in volatility

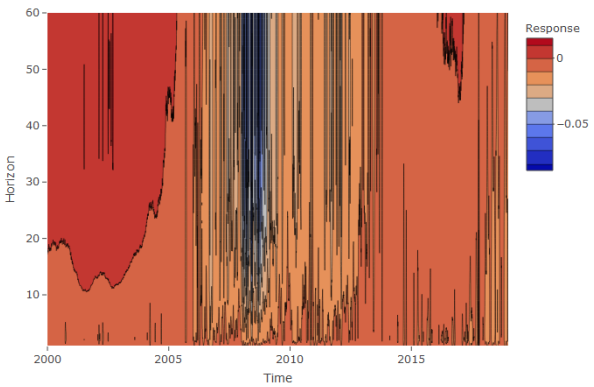

Response of volatility to a shock in trading volume

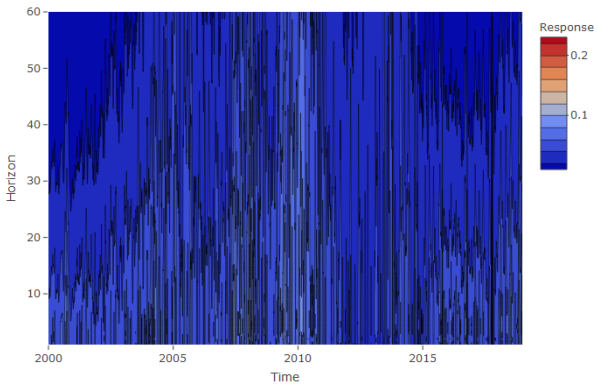

Response of volatility to a shock in open interest

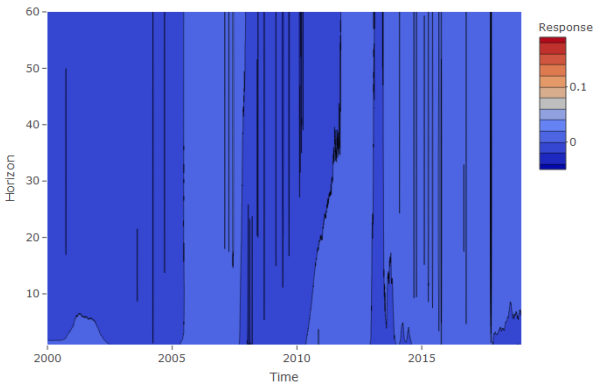

Figure A.31: **Contour plots of time-varying impulse responses for wheat**

The plots show the time-varying reactions of one unit shocks between the volatility of returns, the trading volume and the previous day open interest. The corresponding reactions have been calculated for a sample period running from January 3, 2000 to October 17, 2018 on a daily basis while data for the first 80 days (until April 26, 2000) has been used as a training sample to initialize the coefficient priors.

Response of trading volume to a shock in volatility

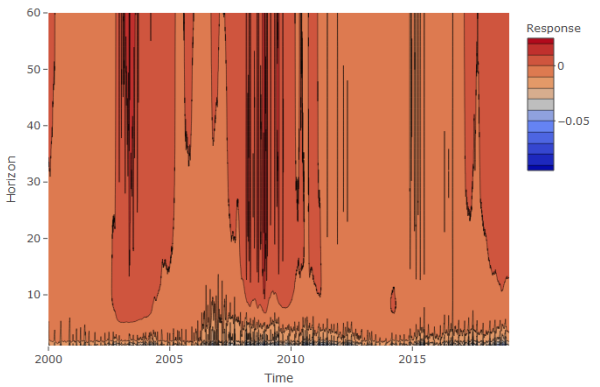

Response of open interest to a shock in volatility

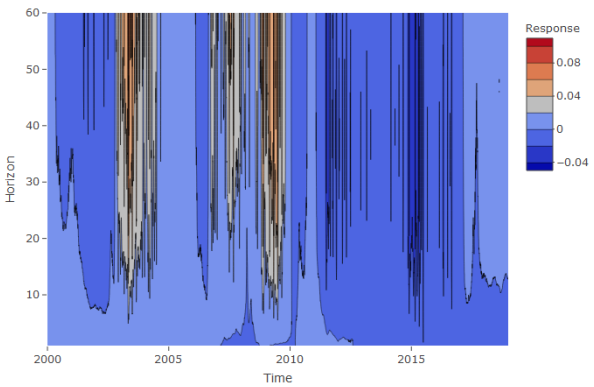

Response of volatility to a shock in trading volume

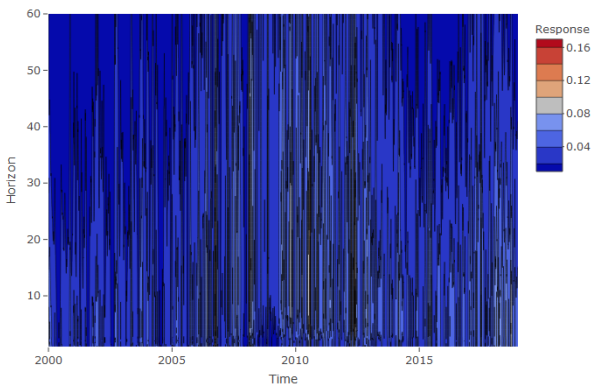

Response of volatility to a shock in open interest

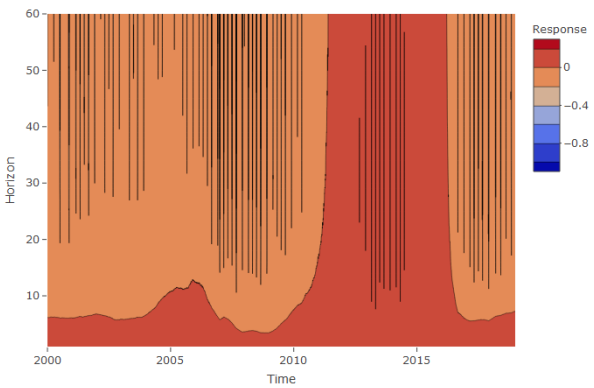

Figure A.32: **Impulse responses for coffee**

The plots show the time-varying reactions of one unit shocks between the volatility of returns, the trading volume and the previous day open interest. The corresponding reactions are shown for three different points in time: 2000-05-01, 2008-09-15 and 2018-10-17. The reaction is represented by the solid red line and the corresponding confidence bands by blue shadings (the 95% level in light blue and the 68% in dark blue). The dashed black line displays the zero line.

Panel (a): Response of trading volume to a shock in volatility

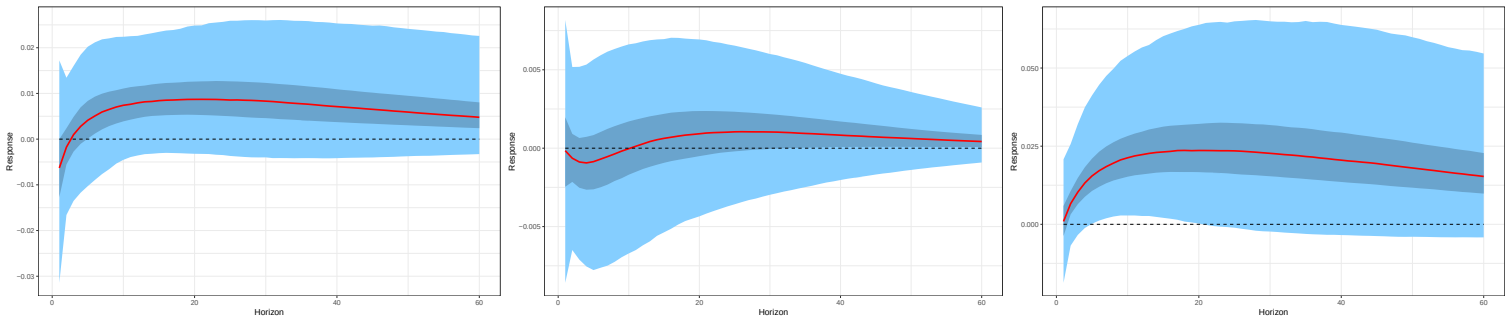

Panel (b): Response of open interest to a shock in volatility

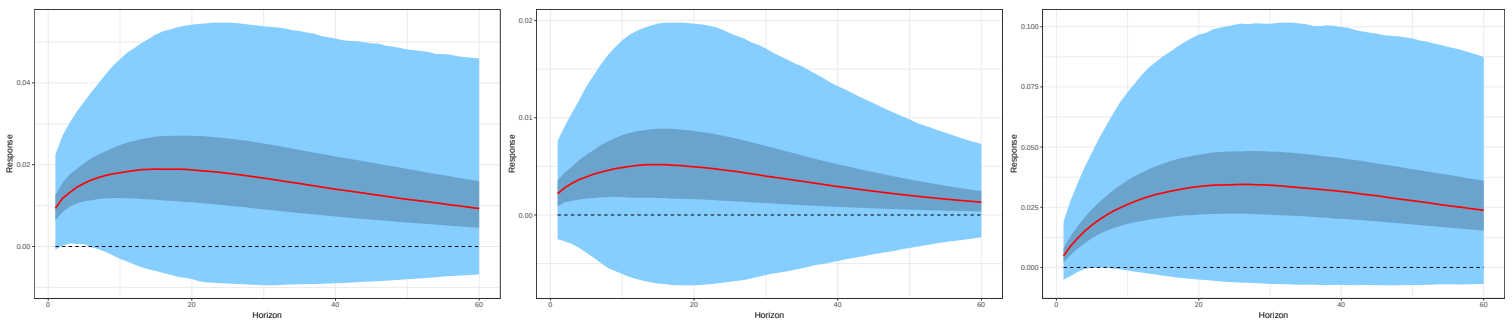

Panel (c): Response of volatility to a shock in trading volume

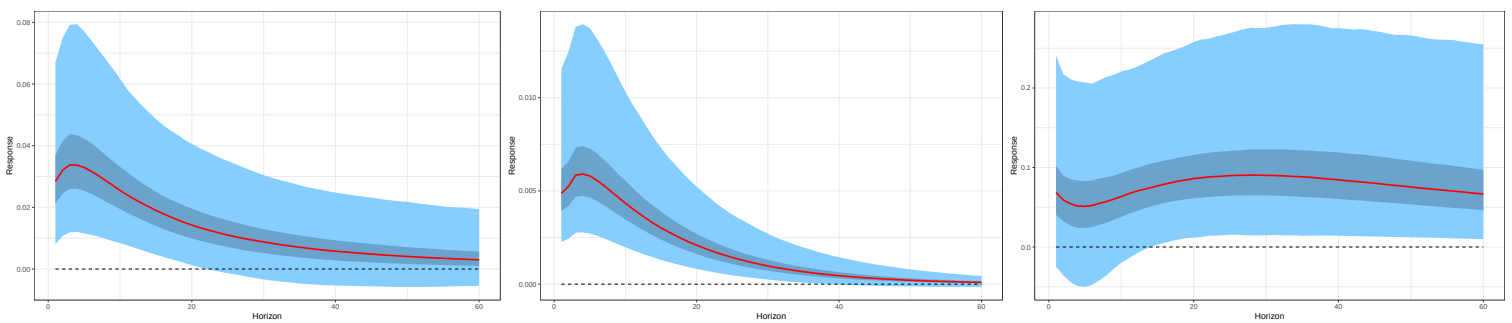

Panel (d): Response of volatility to a shock in open interest

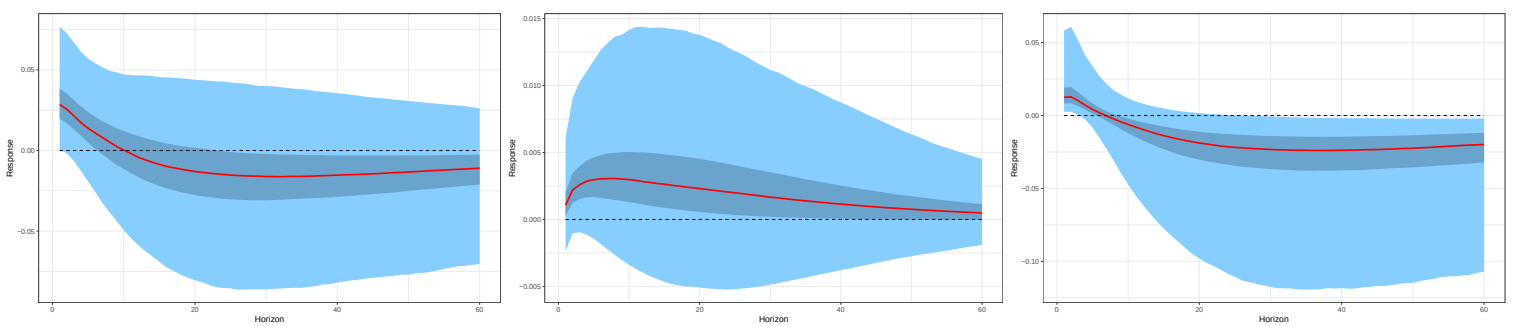

Figure A.33: **Impulse responses for corn**

The plots show the time-varying reactions of one unit shocks between the volatility of returns, the trading volume and the previous day open interest. The corresponding reactions are shown for three different points in time: 2000-05-01, 2008-09-15 and 2018-10-17. The reaction is represented by the solid red line and the corresponding confidence bands by blue shadings (the 95% level in light blue and the 68% in dark blue). The dashed black line displays the zero line.

Panel (a): Response of trading volume to a shock in volatility

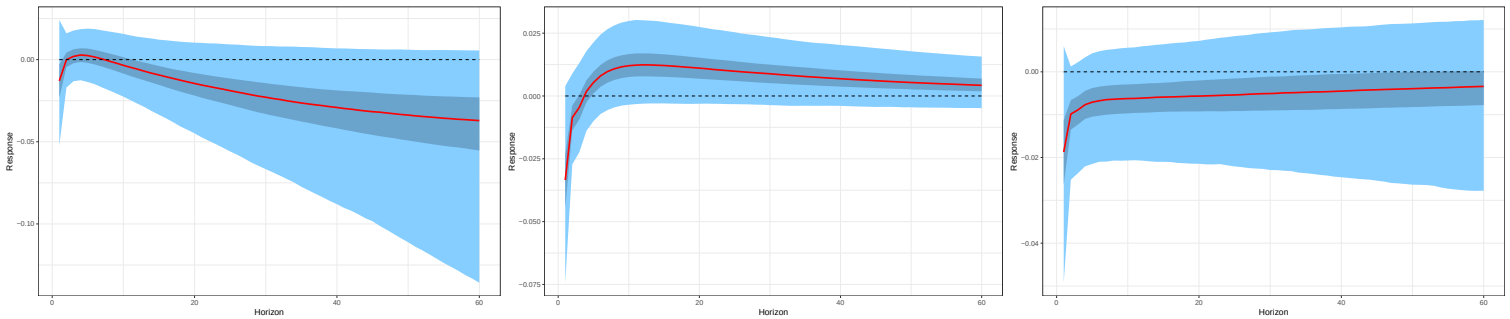

Panel (b): Response of open interest to a shock in volatility

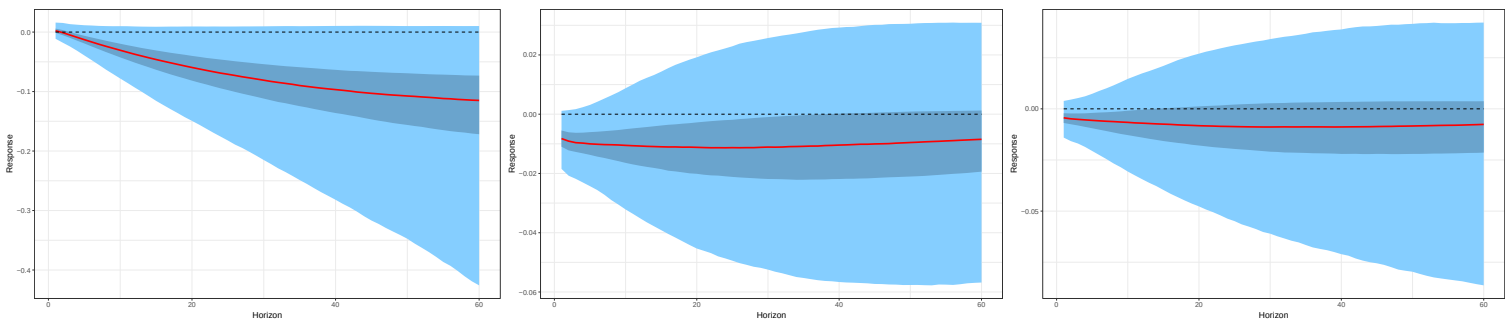

Panel (c): Response of volatility to a shock in trading volume

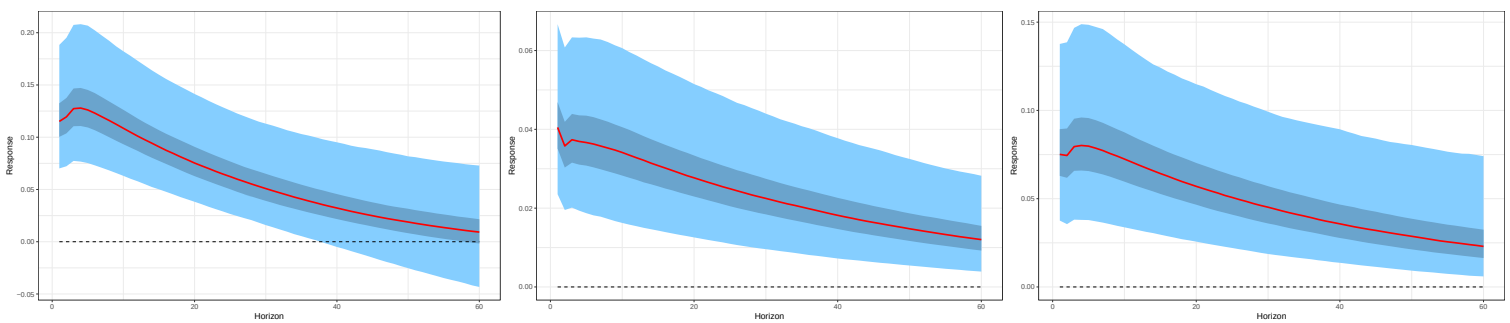

Panel (d): Response of volatility to a shock in open interest

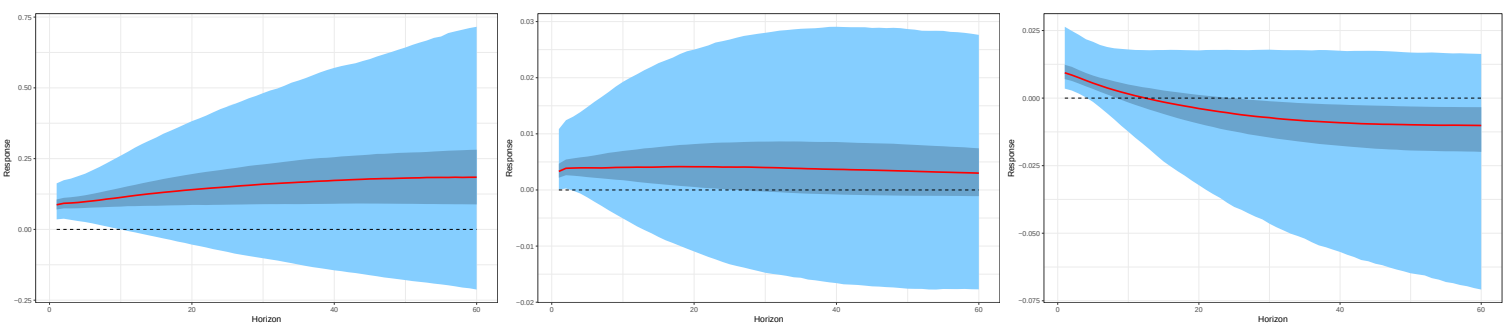

Figure A.34: **Impulse responses for cotton**

The plots show the time-varying reactions of one unit shocks between the volatility of returns, the trading volume and the previous day open interest. The corresponding reactions are shown for three different points in time: 2000-05-01, 2008-09-15 and 2018-10-17. The reaction is represented by the solid red line and the corresponding confidence bands by blue shadings (the 95% level in light blue and the 68% in dark blue). The dashed black line displays the zero line.

Panel (a): Response of trading volume to a shock in volatility

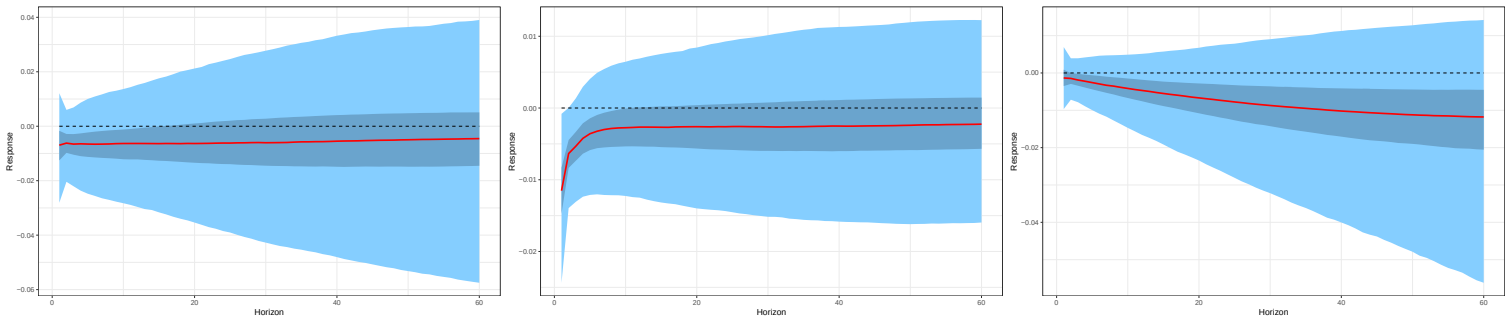

Panel (b): Response of open interest to a shock in volatility

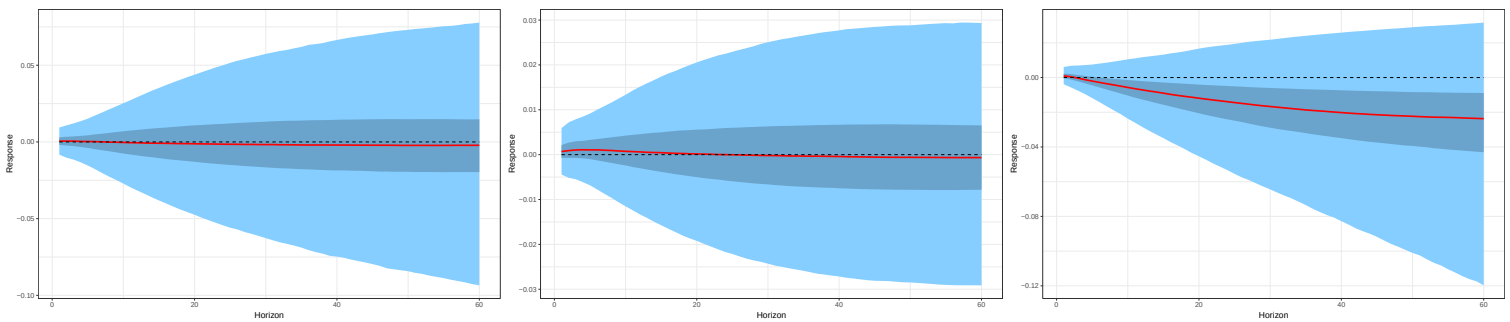

Panel (c): Response of volatility to a shock in trading volume

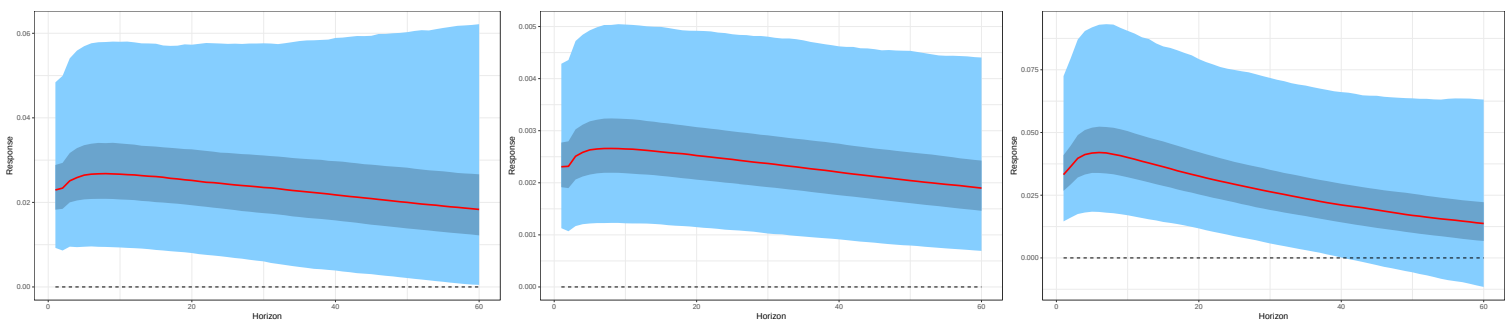

Panel (d): Response of volatility to a shock in open interest

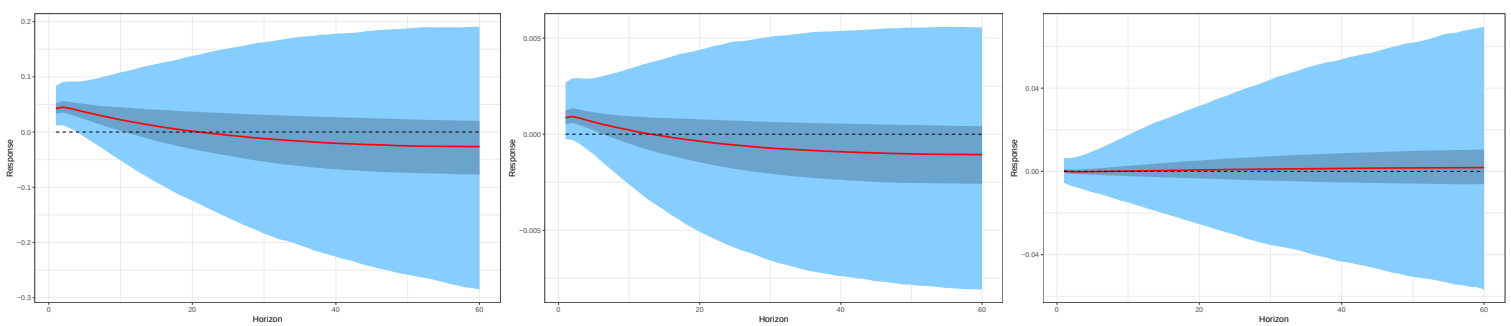

Figure A.35: **Impulse responses for soybean oil**

The plots show the time-varying reactions of one unit shocks between the volatility of returns, the trading volume and the previous day open interest. The corresponding reactions are shown for three different points in time: 2000-05-01, 2008-09-15 and 2018-10-17. The reaction is represented by the solid red line and the corresponding confidence bands by blue shadings (the 95% level in light blue and the 68% in dark blue). The dashed black line displays the zero line.

Panel (a): Response of trading volume to a shock in volatility

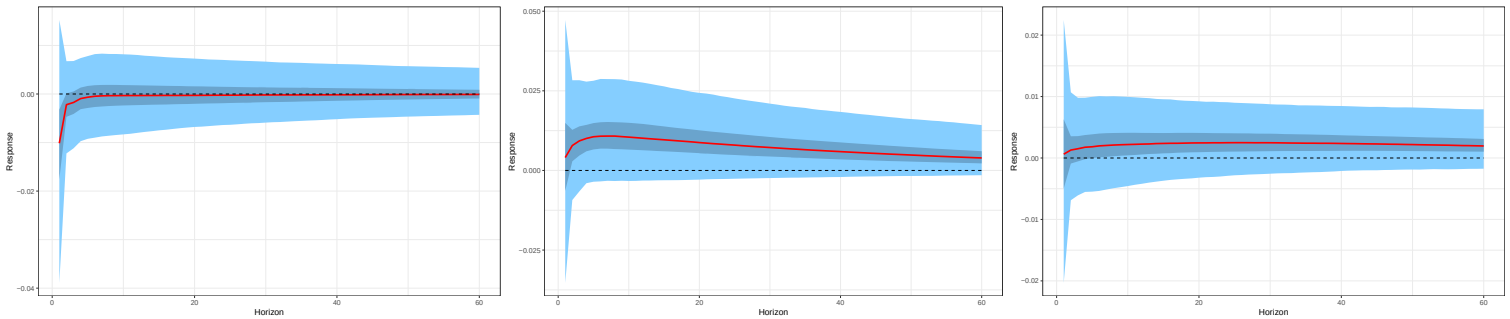

Panel (b): Response of open interest to a shock in volatility

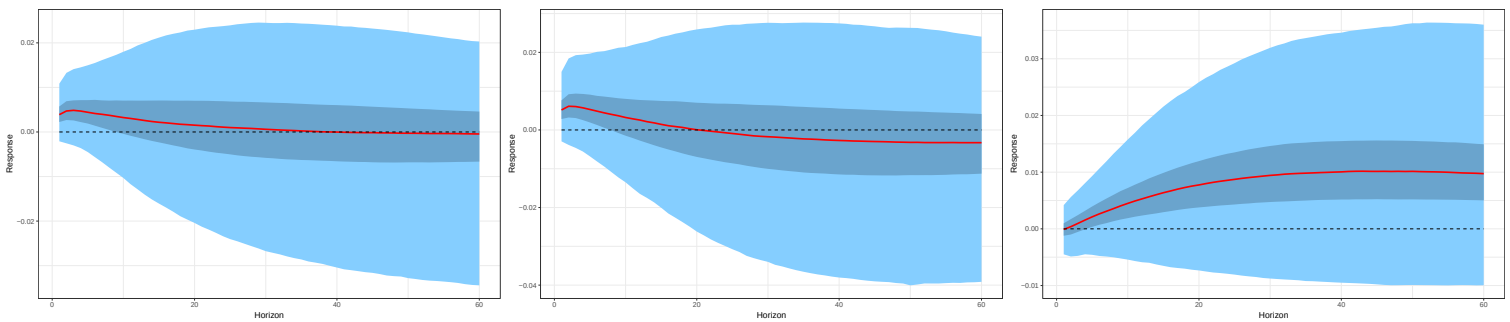

Panel (c): Response of volatility to a shock in trading volume

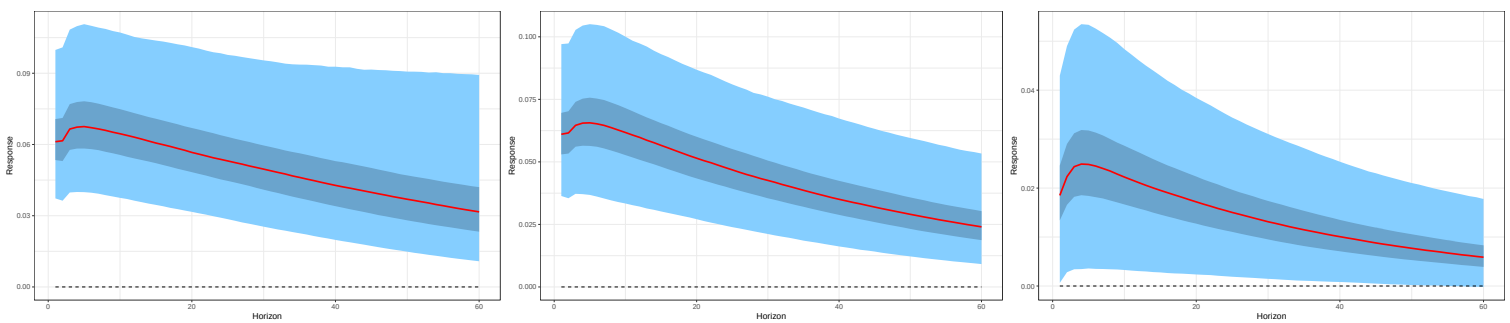

Panel (d): Response of volatility to a shock in open interest

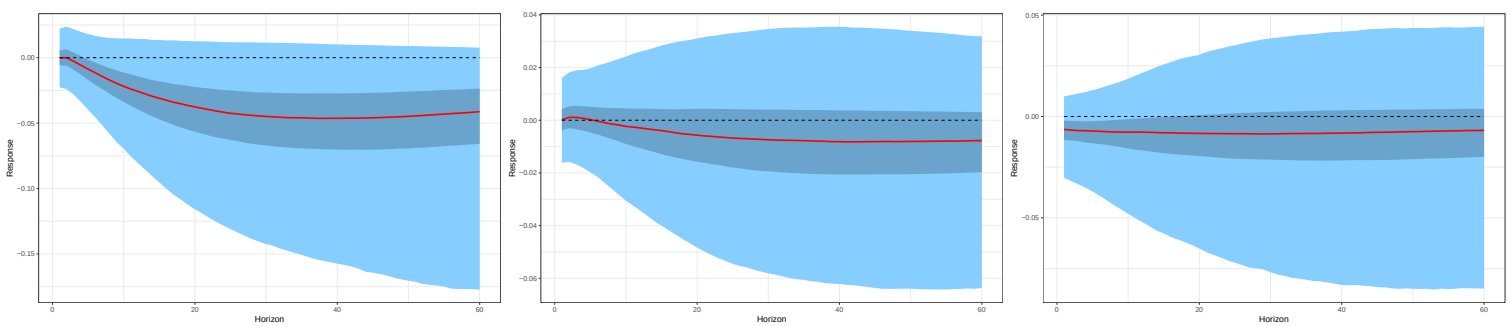

Figure A.36: **Impulse responses for soybeans**

The plots show the time-varying reactions of one unit shocks between the volatility of returns, the trading volume and the previous day open interest. The corresponding reactions are shown for three different points in time: 2000-05-01, 2008-09-15 and 2018-10-17. The reaction is represented by the solid red line and the corresponding confidence bands by blue shadings (the 95% level in light blue and the 68% in dark blue). The dashed black line displays the zero line.

Panel (a): Response of trading volume to a shock in volatility

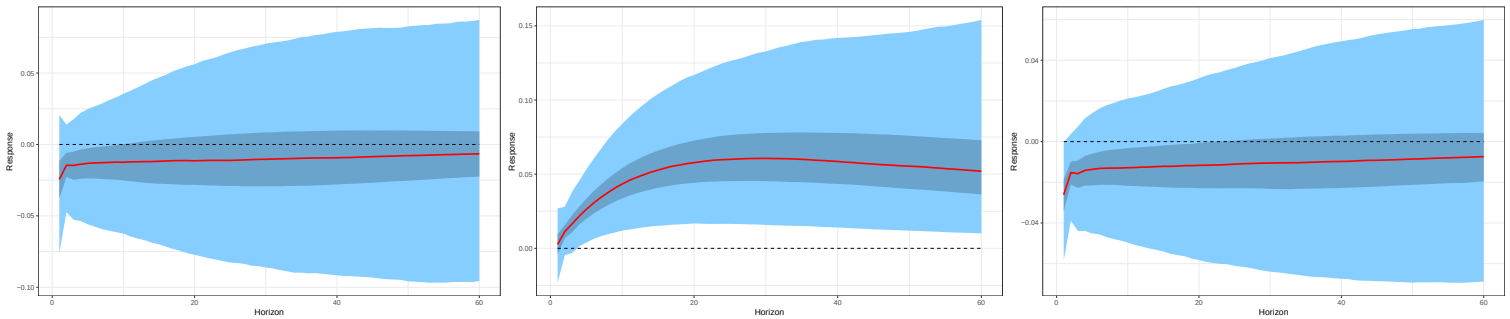

Panel (b): Response of open interest to a shock in volatility

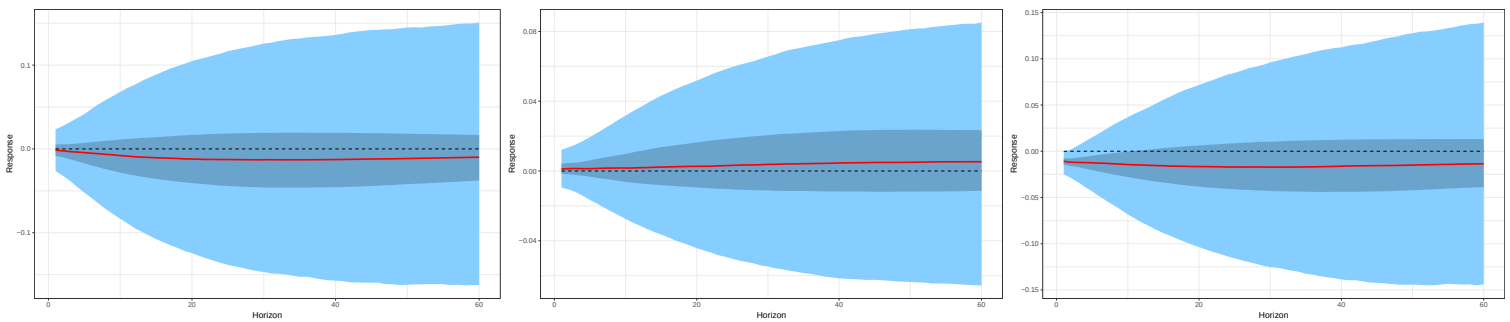

Panel (c): Response of volatility to a shock in trading volume

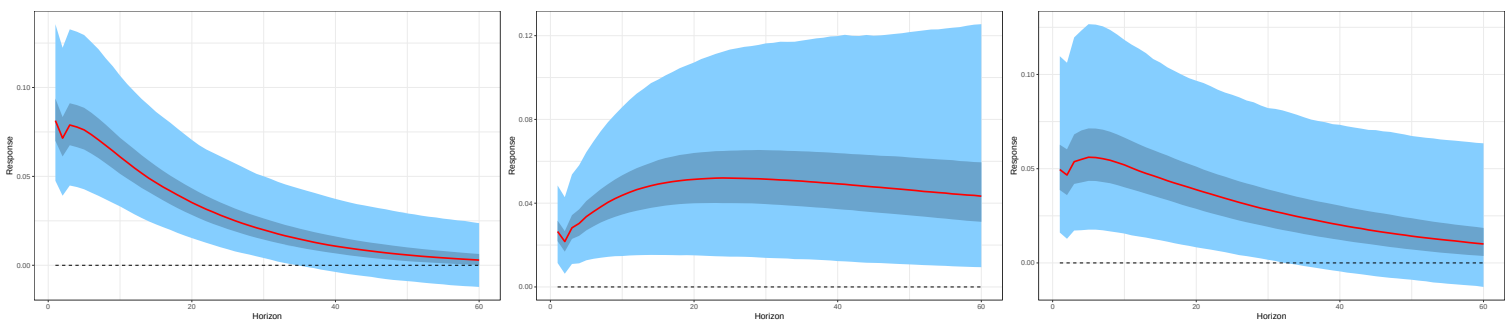

Panel (d): Response of volatility to a shock in open interest

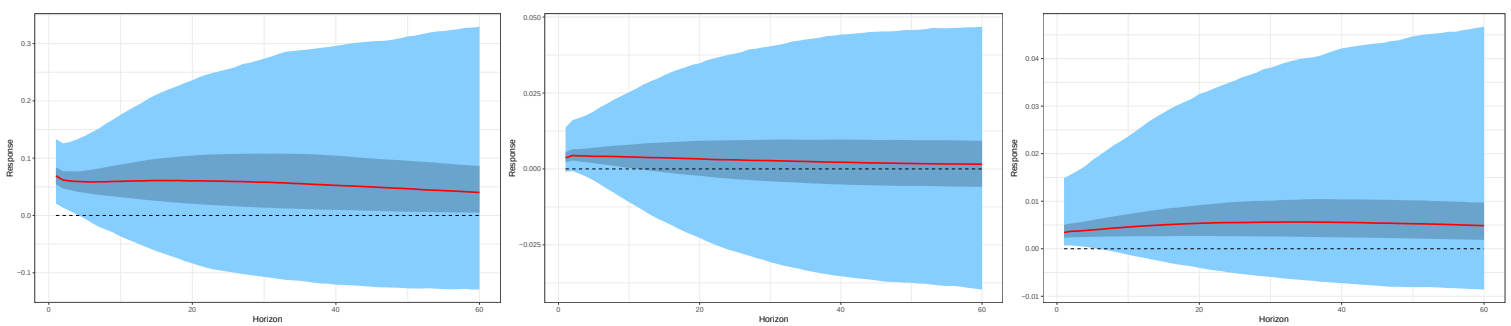

Figure A.37: **Impulse responses for sugar**

The plots show the time-varying reactions of one unit shocks between the volatility of returns, the trading volume and the previous day open interest. The corresponding reactions are shown for three different points in time: 2000-05-01, 2008-09-15 and 2018-10-17. The reaction is represented by the solid red line and the corresponding confidence bands by blue shadings (the 95% level in light blue and the 68% in dark blue). The dashed black line displays the zero line.

Panel (a): Response of trading volume to a shock in volatility

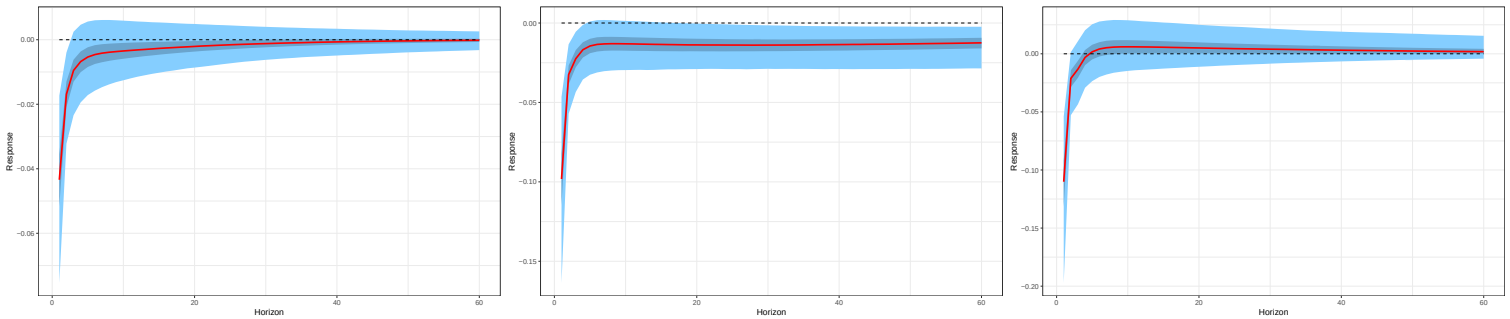

Panel (b): Response of open interest to a shock in volatility

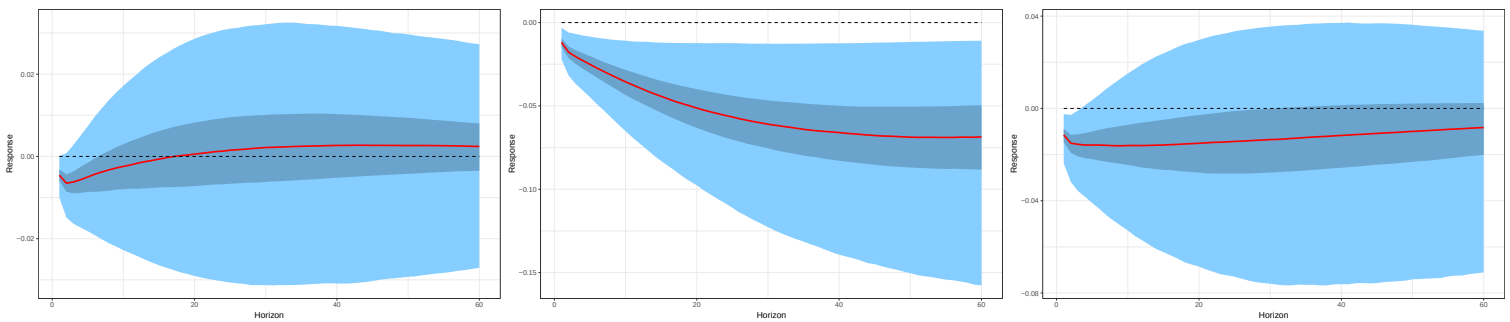

Panel (c): Response of volatility to a shock in trading volume

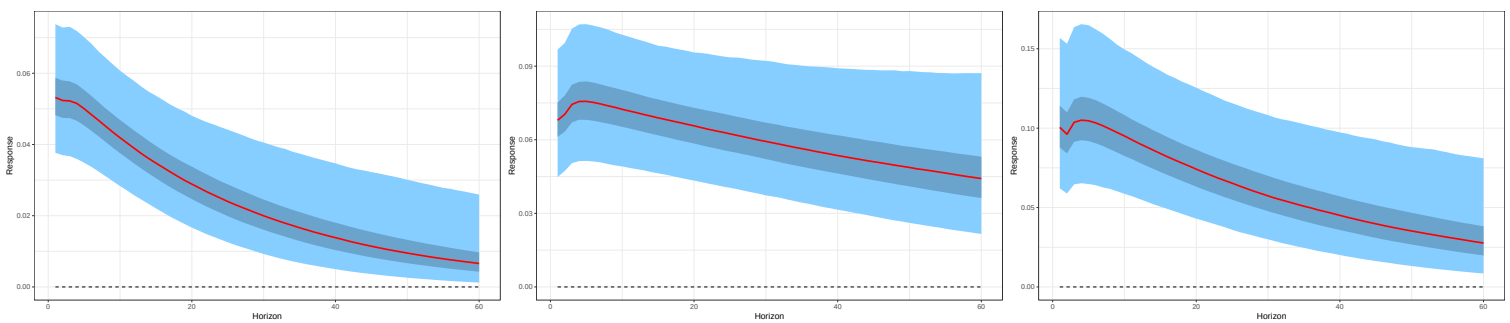

Panel (d): Response of volatility to a shock in open interest

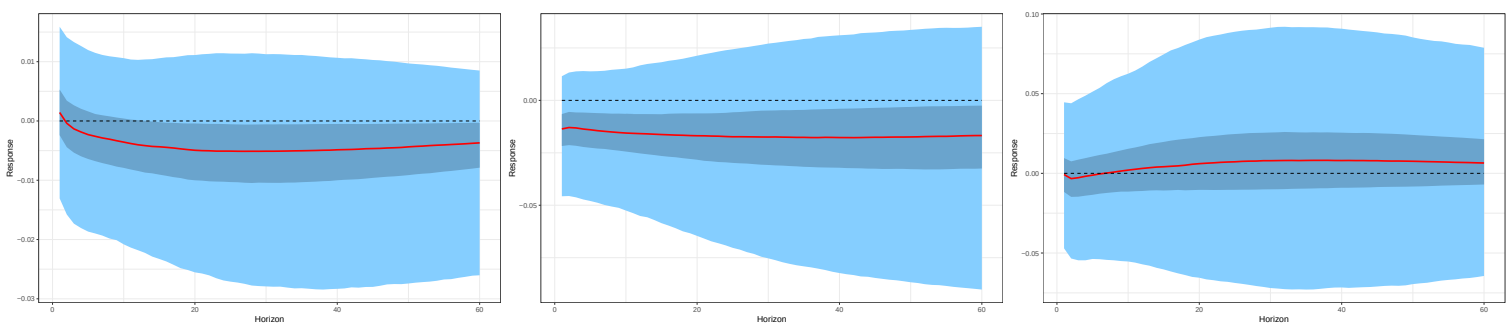

Figure A.38: **Impulse responses for wheat**

The plots show the time-varying reactions of one unit shocks between the volatility of returns, the trading volume and the previous day open interest. The corresponding reactions are shown for three different points in time: 2000-05-01, 2008-09-15 and 2018-10-17. The reaction is represented by the solid red line and the corresponding confidence bands by blue shadings (the 95% level in light blue and the 68% in dark blue). The dashed black line displays the zero line.

Panel (a): Response of trading volume to a shock in volatility

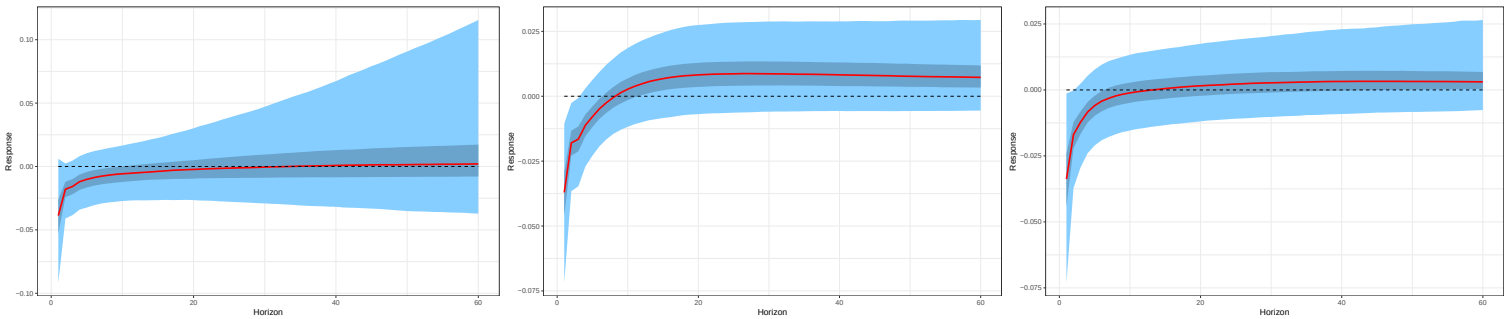

Panel (b): Response of open interest to a shock in volatility

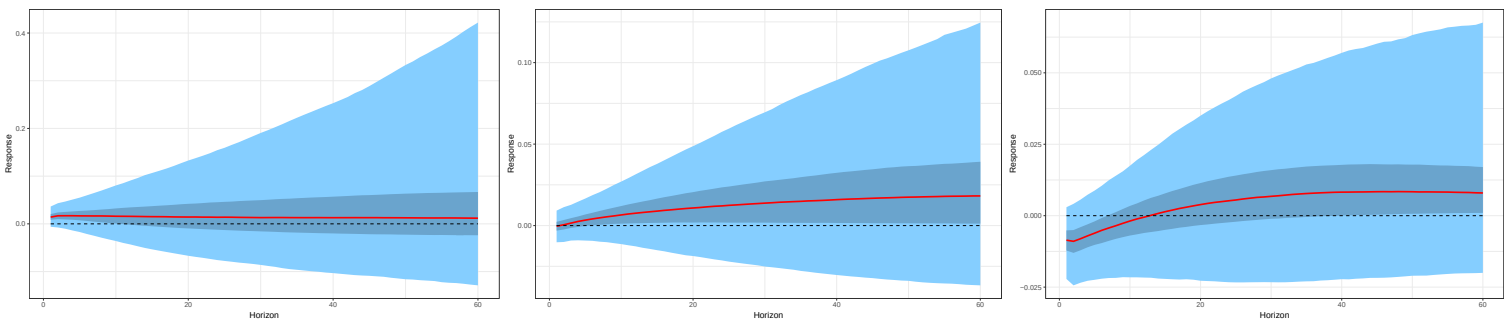

Panel (c): Response of volatility to a shock in trading volume

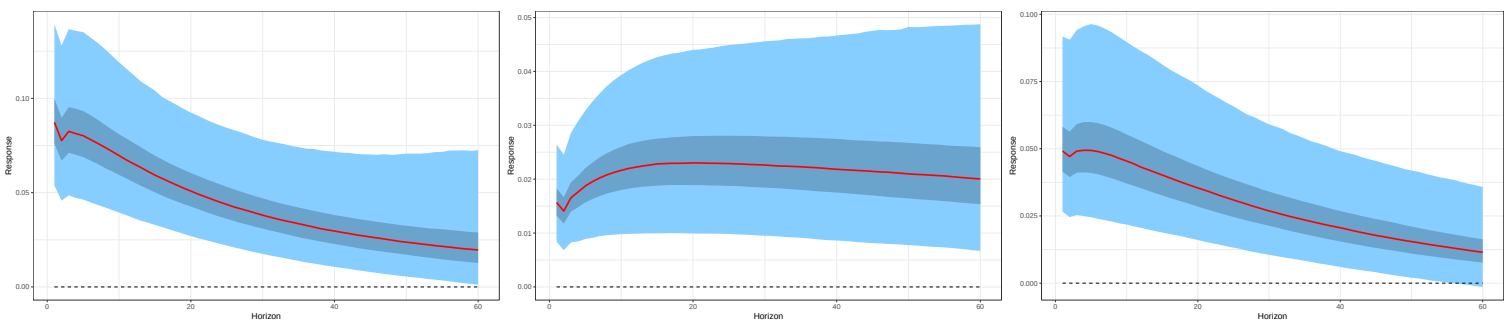

Panel (d): Response of volatility to a shock in open interest